DM

Preliminary Studies on the Use of Exosomes as Dendrimer Carriers

MASTER DISSERTATION

José Filipe Sousa de Olim
MASTER IN APPLIED BIOCHEMISTRY

UNIVERSIDADE da MADEIRA
A Nossa Universidade
www.uma.pt

November | 2017

Preliminary Studies on the Use of Exosomes as Dendrimer Carriers

MASTER DISSERTATION

José Filipe Sousa de Olim
MASTER IN APPLIED BIOCHEMISTRY

ORIENTADORA
Helena Maria Pires Gaspar Tomás

CO-ORIENTADOR
João Manuel Cunha Rodrigues

Preliminary studies on the use of exosomes as dendrimer carriers

Dissertation submitted to the University of Madeira in fulfilment of the requirements for the degree of Master in Applied Biochemistry

By José Filipe Sousa de Olim

Work developed under the supervision of

Professor Dr. Helena Maria Pires Gaspar Tomás and

Co-supervised by Professor Dr. João Manuel Cunha Rodrigues

Faculdade de Ciências Exatas e de Engenharia,

Centro de Química da Madeira,

Campus Universitário da Penteada,

Funchal – Portugal

November 2017

Acknowledgments

First, I would like to thank the person who contributed the most to the success of this body of work, my supervisor Prof. Helena Tomás, for her advice, her words of support, her help and patience through the making of this thesis. Also, for being one of the best people I've met, personally and professionally. I would also like to thank my co-supervisor Prof. João Rodrigues and other professors who contributed to my academic development.

Thank you the LBCC members who contributed to the elaboration of this Master Thesis, specially to Ana Olival and Carla Alves, for the support, help and guidance in some experiments.

A special thank you to my colleague and good friend Débora Reis, for the help, the laughs, the irreplaceable friendship and all the support given throughout these years. I also want to thank all my CQM colleagues who became my dearest friends and who I will forever cherish: Ana Rute, Bruna Pereira, Carla Miguel, Catarina Silva, Gonçalo Martins, Mariana Vieira, Núria Fernandes, Rosa Perestrelo, Sonia Medina and Vítor Spínola.

I'm also deeply thankful to the laboratory technician Paula Andrade, for her support, her disponibility in providing the necessary tools for the elaboration of this work, and also for her friendship.

I'm extremely grateful for the support and love given by my family, specially my mother, for all the efforts and sacrifices she had to make to give me a better education and providing me with the tools for me to build a better future.

Last but not least, I'd like to thank my amazing boyfriend Alex Faria, for his endless love, support and for providing me with the best moments in my life. He inspires me to become a better person each and every day. Without him, things would be for sure, harder to overcome. I love you.

Finally, I want to thank CQM for providing me the tools and support in the development of this Master Project.

Thank you.

This work was supported by *FCT-Fundação para a Ciência e a Tecnologia* (project Pest-OE/QUI/UI0674/2013, CQM, Portuguese Government funds), and *Associação Regional para o Desenvolvimento da Investigação Tecnologia e Inovação* (ARDITI) through the project M1420-01-0145-FEDER-000005 - Centro de Química da Madeira - CQM+ (Madeira 14-20).

Preliminary notes

This Master Thesis was the first research work at CQM (Centro de Química da Madeira) exploring the use of extracellular vesicles as nanocarriers. Although many questions remain to be answered due to the complexity of this field and the limited time available for the experimental work, this work allowed the gain of experience in the isolation and characterization of extracellular vesicles and, certainly, will serve as a basis for the development of future studies in CQM. For the student, it was an opportunity to learn how to access and discuss scientific data, design a research project, interpret experimental results and communicate in a scientific manner. Regarding the laboratory skills, it was also a chance for him to learn basic animal cell culture techniques, how to label dendrimers with fluorescent dyes, and how to characterize nanomaterials with techniques such as NMR, FTIR-ATR, UV/Vis, DLS and fluorescence spectroscopy. The student also gained experience using microscopy techniques, such as fluorescence microscopy and TEM, as well as using biological/biochemical techniques, like cell viability evaluation, organelle staining, and enzyme activity determination.

Presentations in scientific meetings in the scope of this master project:

1) Filipe Olim, João Rodrigues, Helena Tomás. Nanomaterials inclusion in exosomes for drug delivery. Oral presentation in the 4th CQM Annual Meeting. 3-4 February 2017; Funchal, Madeira (Portugal).

Courses done in the scope of this master project:

1) *Basics of Extracellular Vesicles* online course provided by University of California, Irvine, and coordinated by Cecilia Lässer, Researcher at Krefting Research Center, University of Gothenburg. Approved with a final classification of 98.9 %. The respective certificate is in Annex C.

Abstract

Eukaryotic and prokaryotic cells can release vesicles into the biological fluids that differ in size and mechanism of biogenesis. In recent years, particular attention has been paid to exosomes which are naturally occurring nanoparticles (50 – 150 nm) that have been found in various biological fluids and are recognized as having an important role in intercellular communication and other biological processes. Human mesenchymal stem cells (hMSCs) are multipotent cells that can be found in different tissues in the adult. hMSCs have a large capacity for *ex vivo* expansion and show immunosuppressive properties, making them the ideal source of exosomes for biomedical applications.

Dendrimers are nanoscale molecules that have promising properties as drug/gene delivery vehicles and, as such, their inclusion inside hMSCs exosomes may be a way for their easier spreading and target reaching in the body. The present work was focused on the hypothesis that exosomes can be loaded before their isolation from cells by simple cell exposure to dendrimers. First, dendrimers were labelled with rhodamine and then characterized by ^{1}H NMR, FTIR, UV/Vis spectroscopy, and fluorescence spectroscopy. Then, the effect of the pH in the stability of the fluorescence emission of these conjugates was study, as well as their cytotoxicity behavior and kinetics of cellular internalization. After, a protocol for exosome isolation was established using a precipitation-based approach and the isolated exosomes were characterized by DLS, TEM and acetylcholinesterase activity. hMSCs were then exposed to a solution containing the labelled dendrimers and the released exosomes were collected to evaluate the presence of the dendrimers inside. Contrary to what was expected, the dendrimers were not excreted inside exosomes and, instead, were accumulated in the cellular perinuclear zone. By fluorescence microscopy and using specific biochemical markers, it was possible to co-localize the conjugated dendrimers with the Golgi complex and the endoplasmic reticulum.

Keywords: Extracellular vesicles; Exosomes; Mesenchymal stem cells; PAMAM dendrimers

Resumo

As células eucariotas e procarióticas podem libertar vesículas nos fluidos biológicos que diferem no tamanho e mecanismo de biogénese. Os exossomas, nanopartículas de ocorrência natural (50 - 150 nm), podem ser encontrados em diversos fluidos biológicos e possuem um papel importante na comunicação intercelular e noutros processos biológicos. As células estaminais mesenquimais humanas (hMSCs) são células multipotentes que podem ser encontradas em diferentes tecidos adultos, que possuem uma larga expansão *ex vivo* e propriedades imunossupressoras.

Os dendrímeros são moléculas com tamanhos nanométricos que possuem propriedades promissoras para a entrega de fármacos/genes e, como tal, a sua inclusão dentro de exossomas derivados de hMSC poderá representar uma maneira de facilitar a sua circulação no corpo de modo a atingirem os alvos biológicos. O presente trabalho focou-se na hipótese de que os exossomas podem ser carregados por simples exposição das células às soluções de dendrímero. Primeiro, os dendrímeros foram marcados com rodamina e caracterizados utilizando ^{1}H RMN, *FTIR*, espectroscopia *UV/Vis* e espectroscopia de fluorescência. Depois, estudou-se o efeito do pH na estabilidade da emissão de fluorescência desses conjugados, bem como o seu comportamento de citotoxicidade e cinética de internalização celular. Seguidamente, os exossomas foram isolados por precipitação através da utilização de um reagente comercial e caracterizados por *DLS*, *TEM* e pela atividade da acetilcolinesterase. As hMSCs foram então expostas a uma solução contendo os dendrímeros e os exossomas libertados foram colhidos e avaliados de maneira a determinar a presença de dendrímeros no seu interior. Ao contrário do que era esperado, os dendrímeros não foram excretados dentro dos exossomas e, em vez disso, ficaram acumulados na região perinuclear das células. Por microscopia de fluorescência e utilizando marcadores bioquímicos específicos, foi possível co-localizar os dendrímeros conjugados com o complexo de Golgi e o retículo endoplasmático.

Palavras-chave: Vesículas extracelulares; Exossomas Células Estaminais Mesenquimais; PAMAM-RITC

Index

Figures index

Tables index

Abbreviations

AA Antibiotic-Antimycotic
AChE Acetylcholinesterase
ADP Adenosine diphosphate
AFM Atomic force microscopy
ARF6 ADP-ribosylation factor 6
ATPase Adenylpyrophosphatase
BSA Bovine serum albumin
C3b complement component 3
c-Met Tyrosine-protein kinase Met
CT Computed tomography
DAPI 4',6-diamidino-2-phenylindole
DLS Dynamic light scattering
DMEM Dulbecco's modified eagle medium
DMSO Dimethyl sulfoxide
DNA Deoxyribonucleic acid
EDA Ethylenediamine
EDS Energy dispersive spectroscopy
EDTA Ethylenediaminetetraacetic acid
EF-1 Elongation factor 1
ELISA Enzyme-linked immunosorbent assay
EM Electron microscopy
ESCRT Endosomal sorting complexes required for transport
EVs Extracellular vesicles
FBS Fetal bovine serum
FITC Fluorescein isothiocyanate
FTIR-ATR Attenuated total reflectance Fourier-transform infrared spectroscopy
GTP Guanosine triphosphate
HDL High density lipoprotein
hMSCs Human mesenchymal stem cells
HPA *Helix pomatia* agglutinin
HPLC High-performance liquid chromatography
Hsp70 Heat shock protein 70
ILVs Intraluminal vesicles
iRNA Interference RNA

ISEV International Society for Extracellular Vesicles
KRAS Kirsten rat sarcoma viral oncogene homolog
LAMP2 Lysosome-associated membrane protein 2
LDL Low density lipoprotein
MEM Minimum essential medium
MFG-E8 Milk fat globule-EGF factor 8 protein
MHC Major histocompatibility complex
miRNA MicroRNA
MRI Magnetic resonance imaging
mRNA Messenger RNA
MSCs Mesenchymal stem cells
MVBs Multivesicular bodies
MWCO Molecular weight cut-off
NMR Nuclear magnetic resonance
NTA Nanoparticle tracking analysis
PAMAM Poly(amidoamine)
PBS Phosphate buffered saline
PdI Polydispersity index
PEG Polyethylene glycol
PET Positron-emission tomography
PLGA Poly(lactic-co-glycolic acid)
PVDF Polyninylidene difluoride
RFU Relative fluorescence units
RIPA Radioimmunoprecipitation assay
RITC Rhodamine B isothiocyanate
RNA Ribonucleic acid
RSD Relative standard deviation
SDS-PAGE Sodium dodecyl sulfate polyacrylamide gel electrophoresis
SEM Scanning electron microscopy
siRNA Small interfering RNA
T-cell T lymphocyte
TEM Transmission electron microscopy
TRPS Tunable resistive pulse sensing
TSG101 Tumor susceptibility gene 101 protein
VAMP3 Vesicle-associated membrane protein 3
VPS4 Vacuolar protein sorting-associated protein 4

Part 1. Introduction

Contents

1. Introduction

1.1. Extracellular vesicles (EVs)

Intercellular communication is a crucial and important aspect in multicellular organisms. Communication among cells can occur by direct contact, through adhesion molecules and gap junctions, or by mediation of soluble factors, such as cytokines, growth factors and hormones [1]. In the last two decades, a third mechanism is being elucidated, consisting of the intercellular transfer of extracellular vesicles (EVs), at short and long distances [2,3]. These membrane-based structures serve as vehicles to carry different types of cellular cargo to recipient cells, like lipids, proteins and nucleic acids [4].

The term “extracellular vesicle” was recently introduced and is being used for the description of any type of membrane vesicle secreted into the extracellular milieu, independently of their biogenesis and composition. All cells produce EVs, including those of prokaryotic organisms [5]. EVs have been traditionally classified based on their cell or tissue of origin. For example, prostasomes are derived from prostate cells and oncosomes from tumour cells [1]. These EVs can be distinguished based on their size, mechanism of biogenesis, buoyant density, and so on. A recent classification of EVs based on their biogenesis pathway or intracellular origin led to three different subsets of these structures: apoptotic bodies, ectosomes (or microvesicles) and exosomes [6], which are represented in Figure 1.

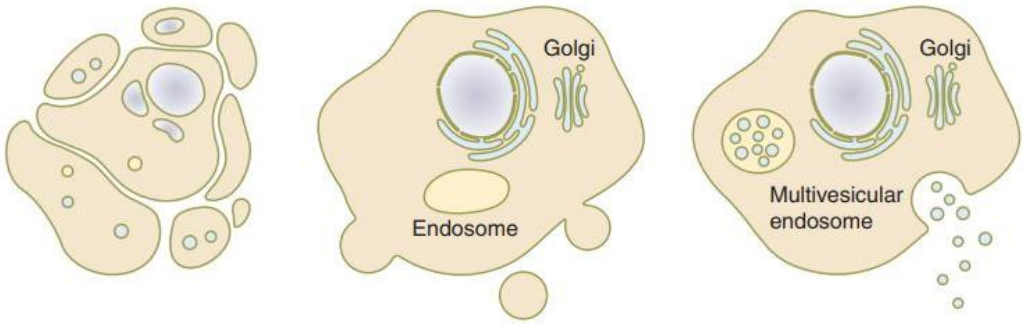

Figure 1 – Origin of the different types of EVs. Apoptotic bodies are formed in the late stage of programmed cell death (apoptosis). Ectosomes (or microvesicles) are formed through the outward shedding of the plasma membrane. Exosomes are released upon the fusion of multivesicular bodies with the cell membrane. Figure from reference [7].

1.1.1. Apoptotic bodies

Apoptosis is the process of cell death and may occur in both normal and cancer cells. This mechanism has different stages, starting by nuclear chromatin condensation, followed by membrane blebbing and finishing in the incorporation of cellular content into membrane vesicles called apoptotic bodies or apoptosomes [8]. Apoptotic bodies are generally the biggest EVs, with sizes around 500 – 4000 nm, and are characterized by having organelles inside. However, smaller vesicles (50 – 500 nm) can be released in this process too [9].

Normally, most of the apoptotic bodies are phagocytosed by macrophages and locally cleared upon their formation (Figure 2). This process is mediated by the establishment of specific interactions between receptors in the phagocyte membrane and ligands at the apoptotic body membrane. One of the best characterized events in the apoptosis mechanism is the translocation of phosphatidylserine to the outer part of the lipid membrane. When phosphatidylserines are translocated, they can bind to Annexin V, and therefore be recognized by phagocytes [10]. Other well characterized change in the apoptotic process is the oxidation of proteins localized at the membrane surface. These oxidation sites can bind to thrombospondin and C3b, and thus be equally recognized by phagocytes [11]

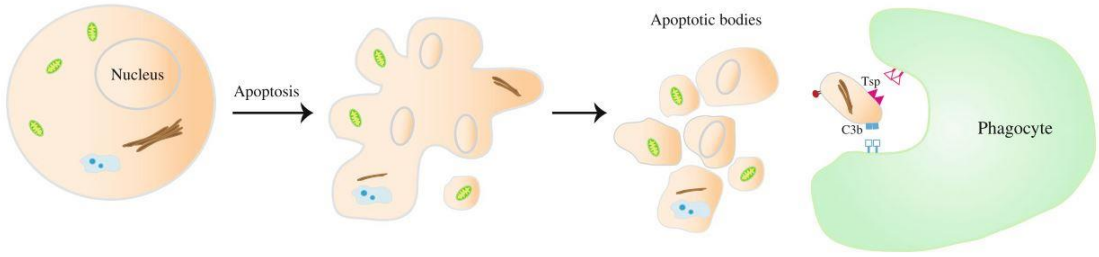

Figure 2 – The formation of apoptotic bodies during programmed cell death (apoptosis) and their phagocythosis. Tsp: Trombospondin; C3b: Large element formed by the cleavage of complement component 3. Figure adapted from reference [12].

1.1.2. Ectosomes or microvesicles

Microvesicles, also known as ectosomes, result from direct shedding of the cell membrane (13). Relative to exosomes, microvesicles normally have a bigger size, around 50-2000 nm. Although there is an overlap between the size range of these two types of EVs, their main difference is the underlying biogenesis mechanism.[13].

The formation process of microvesicles results from different factors, such as cytoskeletal protein contraction and phospholipid redistribution. The cell membrane has a heterogenous distribution of proteins and phospholipids, forming micro-domains. This heterogeneity is regulated by the aminophospholipid translocase. This enzyme, also known as flippase, is responsible for the transportation of phospholipids from the outer to the inner side of the cell membrane, whereas floppases transfer phospholipids from the inner to the outer side of the cell membrane. It is reported that membrane shedding/microvesicle formation is induced by the translocation of phosphatidylserine to the outer side of the cell membrane [14] and that the shedding process is completed through contractions of cytoskeletal structures resulting from actin-myosin interactions [15].

The content of microvesicles seems to be enriched in a set of proteins. For example, these melanoma microvesicles were enriched in B1 integrin receptors and other membrane proteins, such as the vesicle-associated membrane protein 3 (VAMP3) [15]. However, the transferrin receptors, highly present in exosomes, do not seem to appear in microvesicles [16].

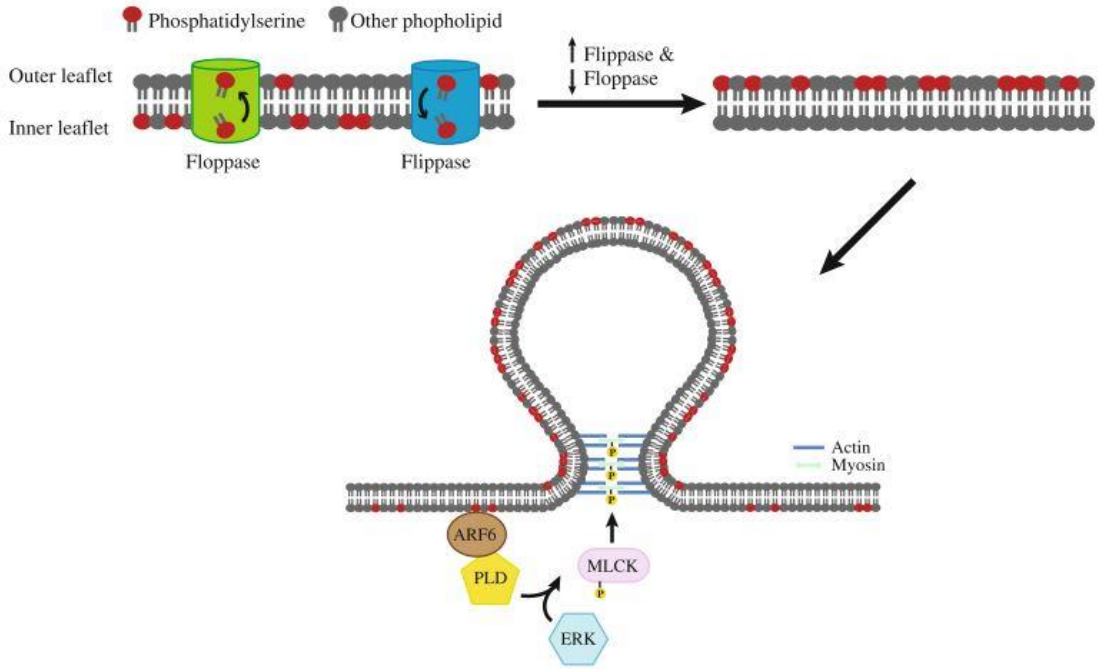

Figure 3 – The process of microvesicle/ectosome biogenesis. In a melanoma model, the overexpression of the Guanosine triphosphate (GTP)-binding protein Adenosine diphosphate (ADP)-ribosylation factor 6 (ARF6), a Rho family member, resulted in microvesicle secretion increase. The activated ARF6 starts a signal cascade, first with phospholipase D (PLD) activation and finishing by phosphorylation and activation of the myosin light chain, like showed in Figure 3. These signalling cascade events do not alter the formation and secretion of smaller vesicles, like exosomes, which supports the fact that the biogenesis of microvesicles is distinct from that of exosomes; ERK: Extracellular signal-regulated signal; MLCK: Myosin light-chain kinase. Figure adapted from reference [12].

1.1.3. Exosomes

In 1983, Harding *et al* followed the cell uptake of gold-labelled transferrin through a clathrin-mediated endocytosis process in rat reticulocytes. They reported that the gold-labelled transferrin accumulated inside vesicles which existed inside non-lysosomal endosomes referred as multivesicular bodies. These multivesicular bodies then fused with the plasma membrane and released their inner vesicles by exocytosis [17]. The term exosome was introduced by Johnstone *et al* in 1987, to refer to these released vesicles [18]. They observed that during the process of reticulocyte maturation, there were large sacs inside the cells containing small vesicles (exosomes). Then, they also labelled the transferrin receptor with gold nanoparticles, and observed the fusion of the large sacs with the cell membrane and subsequent release of the small vesicles into the extracellular environment [19].

1.1.3.1. Origin and molecular composition of exosomes

Exosomes have been discovered in a variety of supernatants from different cell lines in culture, and are present in all the human fluids, which suggests that all cells have the potential to produce them [20]. Exosomes are nano-sized vesicles with a diameter of 50-150 nm, formed by the endocytic cellular pathway which can be separated into three stages: (i) the first stage corresponds to plasma membrane invagination to form the endocytic vesicles; (ii) in the second stage, the inward budding of endosomal membrane starts giving rise to multivesicular bodies (MVBs); (iii) in the last and third stage, MVBs fuse with the plasma membrane and release their vesicular content (exosomes) [21]. These steps are shown in Figure 4.

As mentioned before, endocytic vesicles are created from the invagination of the plasma membrane, creating what are called “endosomes”, which mature and become late endosomes. Then, through the inward budding of these late endosomes, vesicles are accumulated in the endosomal lumen. The accumulation of these vesicles inside late endosomes leads to the formation of multivesicular bodies (MVBs). The MVBs can either fuse with lysosomes for degradation of their content or fuse with the plasma membrane, releasing their intraluminal vesicles (ILVs) in the extracellular space, where they become known as exosomes The main difference between these pathways relies on the action of protein sorting complexes known as endosomal sorting complexes required for transport (ESCRT) [22].

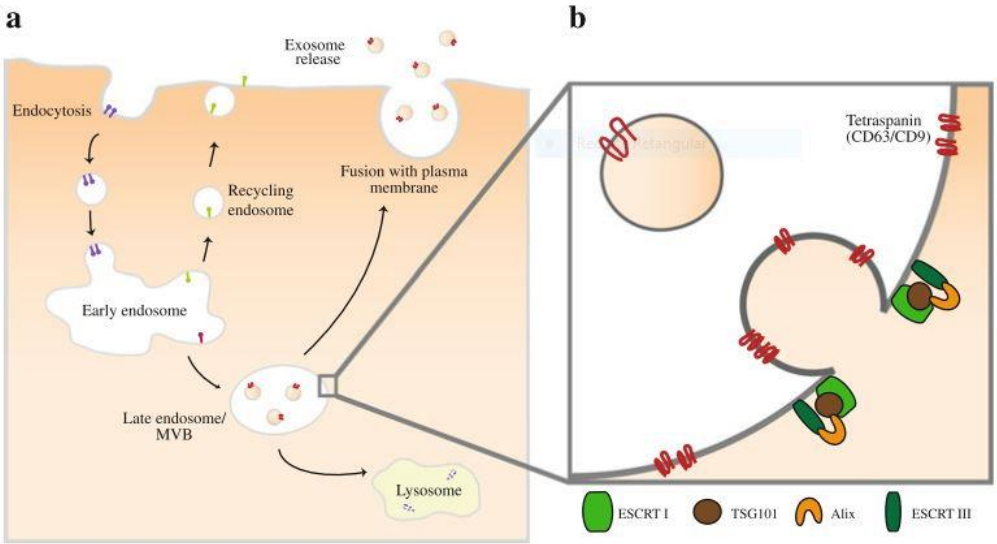

Figure 4 – Biogenesis of exosomes. Figure adapted from reference [12]

The ESCRT machinery consists of four multi-protein complexes, namely ESCRT-0, ESCRT-I, ESCRT-II and ESCRT-III. These complexes are recruited to sort a set of specific proteins into ILVs. The process is known to require ubiquitination of the cytosolic tail of endocytosed receptors [23]. These cargos constitute proteins that will be incorporated into ILVs and later become part of the exosomes released. For example, the protein codified by the tumour susceptibility gene 101 (TSG101), a component of ESCRT-I, forms a complex with the ubiquitinated cargo protein, and helps in the activation of ESCRT-II, inducing endosomal membrane budding. This complex is then involved in the sequestration of MVB proteins and the recruitment of the deubiquitination enzyme to remove ubiquitin from the cargo proteins before sorting them into the ILVs. Then, at last, the ESCRT-III is disassembled by the vacuolar protein sorting-associated protein 4 (VPS4) adenosine triphosphatase (VPS4 is an ATPase) [24].

The nano-spherical membrane of exosomes is formed by a bilayer of lipids. The membrane contains a set of diverse types of lipids and proteins (Figure 5), which are related to the parent cells from which exosomes are released. According to *ExoCarta*, an exosome database, there are currently 8000 proteins and 194 lipids known to be associated with exosomes [25].

Since exosomes are originated from endosomes, they contain multiple families of proteins, such as tetraspanins (CD63, CD81, CD9), heat shock proteins (Hsp70), lysosomal proteins (Lamp2b), and fusion proteins (CD9, flotillin, Annexin), as shown in Figure 5. Tetraspanins have received a high attention, because of the use of the trinity CD63, CD81 and CD9 as exosome markers. However, as mentioned before, the existence of a single exosome-specific protein remains to be disclosed [26]. Besides proteins and lipids, exosomes also contain biologically active nucleic acids, especially ribonucleic acid (RNA), demonstrating their ability to mediate the horizontal transfer of genetic material. The existence of two types of RNA inside exosomes, specifically messenger RNA (mRNA) and micro RNA (miRNA), has also been demonstrated [27].

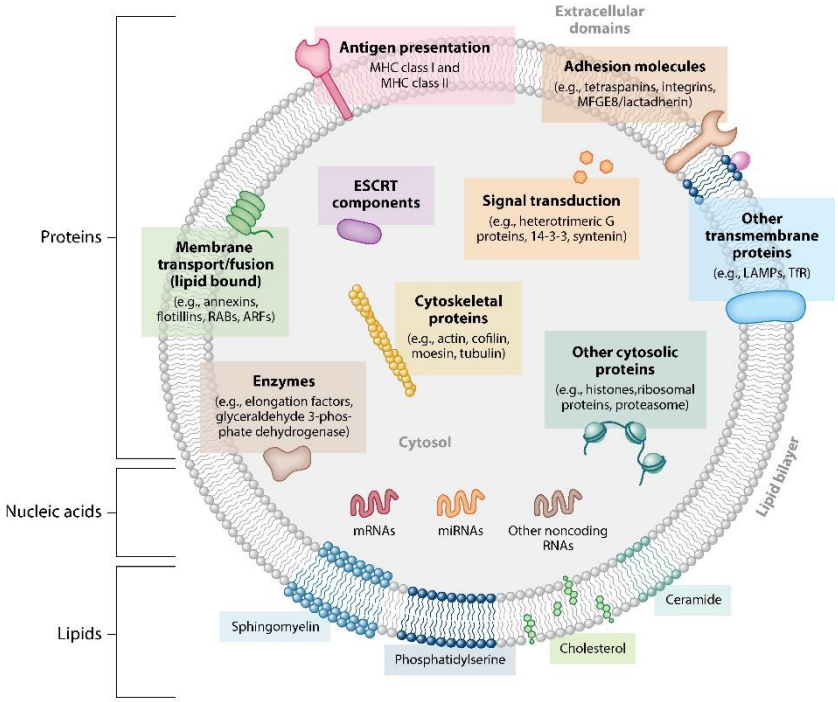

Figure 5 – Biochemical composition of exosomes. Figure adapted from reference [28].

1.1.3.2. Biological functions of exosomes

Exosomes circulate in the body through different biofluids, such as saliva, serum, urine, blood, synovial fluid and breast milk, which suggests that these EVs play an important role in the intercellular communication and biological responses. There are some examples of the biological roles that exosomes can play in the body, like the removal of unnecessary proteins from cell maturation processes. One factor that affects the biological response of exosomes is their cellular origin. Some studies demonstrated that exosomes secreted from antigen presenting cells can have the ability to express, and have at their surface, both the major histocompatibility complex (MHC) I and II. These complexes help in the activation of $CD8^+$ and $CD4^+$ T-cells to trigger specific immune responses [29]. Besides the delivery and exchange of proteins and lipids among different cells, exosomes can transport some types of nucleic acids, as mentioned before. For example, there are studies reporting the secretion of mRNA and small RNA by mast cells in exosomes, which were then translated in the recipient cells [30].

Besides their role in normal biological responses and processes, exosomes seem to be involved in many diseases. For example, in cancer, it seems that exosomes can induce or facilitate the development of a tumoral microenvironment with the transfer of mRNA and some proteins to distant cells. One example is the mutant Kirsten rat sarcoma

(kRAS) viral oncogene protein and the c-Met oncoprotein that promote tumour cell proliferation, thrombosis and angiogenesis [31,32].

Like it was mentioned before, exosomes can be isolated from a variety of cells, and given the fact that these EVs participate in intercellular communication and in the maintenance of normal and pathological conditions, there are several studies regarding their use for diagnostic and therapeutic purposes. For example, exosomes were used to detect tumours in patients with ovarian, prostate and breast cancer [33–35]. Some of these applications and therapeutic effects are schematized in Figure 6. Regarding the use of exosomes in therapeutics, these vesicles can induce tissue regeneration with the delivery of lipids, proteins, growth factors and nucleic acids, for example [36].

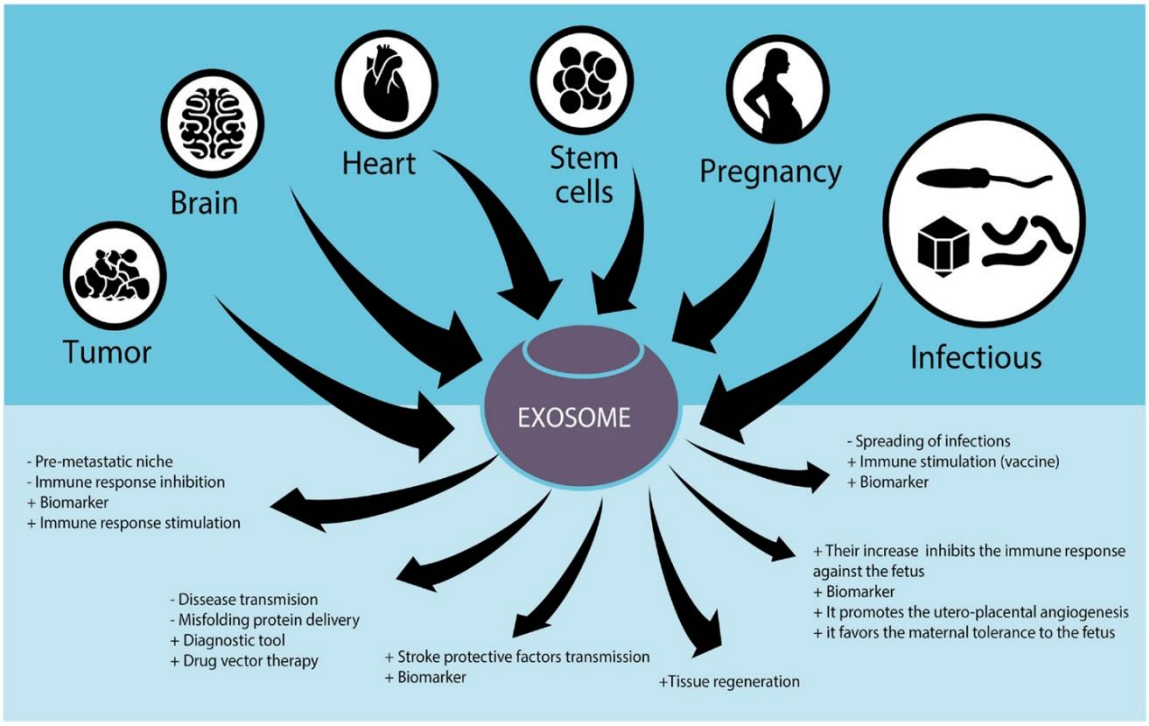

Figure 6 – The role of exosomes in different tissues and their possible therapeutic applications. Figure adapted from reference [29].

1.1.4. International Society for Extracellular Vesicles position in the definition of extracellular vesicles

The extracellular milieu, like serum and plasma, may be very complex and contain a diversity of non-vesicular materials such as extracellular RNA, protein complexes and lipoproteins. Separation of these non-vesicular materials from EVs is not fully achieved by common isolation protocols, like ultracentrifugation and commercial precipitation kits.

Consequently, there is a need to determine the distinct contributions of EVs in any experiment that describes the molecular content or the functional role of the isolated material. So, the ISEV (*International Society for Extracellular Vesicles*) has adopted a set of requirements that researchers can use to discriminate EV from non-EV components [37]. One of the first requirements to define EVs is that they should be isolated from extracellular fluids, like conditioned cell culture medium or body fluids. Here, an important aspect is that the collection of EV-containing fluid must be gentle, limiting cell disruption, which may contribute to the isolation of vesicles from the intracellular compartments. The second requirement regards to the characterization of these EVs is that a general overview of their protein composition must be provided, including description or quantification of necessarily expected proteins, like those shown in Table 1. ISEV suggested that investigators should report at least 3 or more proteins (and, at least, in a semi-quantitative manner) expected to be present in the EVs of interest, like transmembrane proteins and proteins from the cytosol that were linked to the membrane (Table 1, groups 1 and 2, respectively). The amount of proteins not expected to be present in EVs should also be determined, such those associated with cellular structures different from the cell or endosome membranes (Table 1, group 3). Furthermore, protein isolates should be compared with those described for other EVs, by searching within databases, like *EVpedia* and *Vesiclepedia*. The presence of extracellular proteins (Table 1, group 4) in EVs preparations should be regarded very carefully. For example, acetylcholinesterase (AChE) has been used as a EV marker but ISEV requires confirmation of the presence of this protein by other techniques such as Western blotting or by performing assays where inhibitors of AChE are used. The third and last requirement for the definition of EVs, is the characterization of single vesicles within a mixture to get information on the heterogeneity of the EV preparation. As a rule, at least 2 different technologies should be used to characterize individual EVs. When using electron microscopy (EM) or atomic force microscopy (AFM), images should show a wide field (so that several vesicles can be observed) and high-magnification images of individual vesicles. Size distribution measurement of EVs obtained, for example, by nanoparticle-tracking analysis, dynamic light scattering or resistive pulse sensing, may also provide valuable information, representative of the whole EV population. However, the results acquired using these techniques should be compared with data from transmission EM (TEM), AFM or other microscopy techniques, since they are not able to distinguish between vesicles and other particles of similar size [37].

Table 1 – Different proteins expected in EVs isolates, including some examples (non-exclusive). Adapted from reference [37].

1. Transmembrane or lipid-bound extracellular proteins	2. Cytosolic proteins	3. Intracellular proteins	4. Extracellular proteins
Argues presence of a membrane in the isolate	With membrane- or receptor-binding capacity	Associated with compartments other than plasma membrane or endosomes	Binding specifically or non-specifically to membranes, co-isolating with EVs
Present or enriched in EVs/exosomes	Present or enriched in EVs/exosomes	Absent or under-represented in EVs/exosomes, but present in other types of EVs	Variable association with EVs
Examples: Tetraspanins (*CD9*, *CD63*, *CD81*) Integrins (*ITG***) or cell adhesion molecules (*CAM**) Growth factor receptors Heterotrimeric G proteins (*GNA***) Phosphatidylserine-binding *MFGE8*/lactadherin	Examples: Endosome or membrane-binding proteins (*TSG101*, annexins = *ANXA**, Rabs = *RAB**) Signal transduction or scaffolding proteins (syntenin)	Examples: Endoplasmic reticulum (Grp94 = *HSP90B1*, calnexin = *CANX*) Golgi (*GM130*) Mitochondria (cytochrome C = *CYC1*) Nucleus (histones = *HIST*H**) Argonaute/RISC complex (*AGO**)	Examples: Acetylcholinesterase (*ACHE*) Serum albumin Extracellular matrix (fibronectin = *FN1*, collagen = *COL*A**) Soluble secreted proteins (cytokines, growth factors, matrix metalloproteinases = *MMP**)

At least one protein of each category 1, 2 and 3 should be quantified in the EV preparations. EV association of proteins of category 4 should be demonstrated by other means.
Italics: official gene names; *, ** denotes different possible family members.

1.2. Exosome isolation methods

The techniques used in the isolation of exosomes should have a high efficiency, independently of the sample source. After, the quality of the exosome suspensions should be analysed by several physical and chemical/biochemical techniques [38]. With the fast evolution of science and technology, different techniques have been developed for the isolation of exosomes that are able to provide a high quantity of these vesicles with a elevated degree of purity. Each technique has a set of unique advantages and disadvantages for exosome isolation, and these will be discussed in the next sections.

1.2.1. Ultracentrifugation-based isolation techniques

When a suspension is submitted to a centrifugal force, the particles in the suspension will sediment according to their physical properties, such as the size, density and shape. The sedimentation process will also depend on the applied centrifugal force, as well as on solvent density and viscosity. Normally, in ultracentrifugation processes, one can reach high centrifugal forces, up to 1 000 000 x g. The ultracentrifugation-based approaches are the gold standard for exosome isolation, accounting for 56 % of the exosome isolation reports [39]. Exosomes can be isolated by preparative

ultracentrifugation. There are two types of preparative ultracentrifugation, the differential ultracentrifugation and the density gradient ultracentrifugation.

The differential ultracentrifugation is based on the use of different centrifugation cycles at different centrifugal forces and periods of time to isolate exosomes from other components in a sample. Before exosome isolation, normally a clean-up step is carried out to remove large particles from plasma or serum [40]. Between the centrifugation cycles, and depending on the centrifugal force used, the pellet or the supernatant is resuspended in an isotonic solution, such as Phosphate buffered saline (PBS). This method normally is referred as the pelleting or the simple ultracentrifugation method [41].

In the density gradient ultracentrifugation, separation of exosomes is accomplished according to their mass, density and size in a density gradient medium pre-constructed in a centrifuge tube. The sample is layered in the top of the tube containing the gradient and then submitted to an extensive ultracentrifugation. After applying a specific centrifugal force, the solutes, including the exosomes, move to different zones, according to their specific sedimentation rate. Then, the exosomes can be recovered by a simple fraction collection [41].

1.2.2. Precipitation-based approaches

Water-excluding polymers, such as polyethylene glycol (PEG), can be used to alter the solubility or dispersability of exosomes, and consequently, the precipitation of these vesicles in biological fluids [42]. This water-excluding polymers act by tying up the water molecules and forcing less soluble components to precipitate [42,43]. Normally, the samples are incubated with PEG having a molecular weight of 8 kDa [44]. Then, after incubation at 4ºC overnight, the samples are centrifuged at low speeds and the exosomes pelleted [42]. The precipitation is easy and does not require the use of expensive and specialized equipment [45].

There are several exosome precipitation kits in the market for different biofluids, such plasma, serum, urine, ascites, cerebrospinal fluid and culture medium. However, before precipitation, the samples need to be pre-cleaned from different interferents, such whole cells and cellular debris. Also, one disadvantage of the polymer-based precipitation is the co-precipitation of other contaminants, such as proteins and polymeric materials [39]. The use of pre- and post-isolation steps can reduce these problems. The pre-isolation steps can be used to remove particles, such as lipoproteins, and the post-

isolation steps to remove polymeric materials with the use, for example, of a Sephadex G-25 column, for example.

1.2.3. Immunoaffinity capture-based techniques

Due to their natural and cellular biogenesis, exosomes have a highly diverse set of proteins and receptors both in the lumen and membrane. This offers the possibility for the development of high selective isolation techniques, based on the interaction between those proteins (antigens) and their antibodies. Normally, the exosome biomarkers used in immunoisolation are localized in the exosome membranes.

For example, a microplate-based enzyme-linked immunosorbent assay (ELISA) was developed for the capture and quantification of exosomes from urine, plasma and serum [39]. Other variants based on immunoaffinity capture were developed. For example, Zarovni *et al*. [39] used submicron-size magnetic particles coated with specific antibodies for the isolation of exosomes from cell culture. The CD63 membrane protein, that is highly expressed in most of human exosomes, was the first characterized member of the tetraspanin family [43,46]. Having this is mind, this surface protein became of high interest in the development of immunoisolation techniques for exosomes in complex sample matrices. Some investigations suggested that immunoaffinity-based isolation techniques have a higher efficiency in the isolation of exosomes from human colon cancer cell culture media compared to ultracentrifugation techniques [47]. In comparison to the microplate-based technique, the use of magnetic beads for the immunoisolation of exosomes is more efficient and sensitive due to the a larger surface area available for interaction and a more homogenous capture process. Also, the starting sample volume in magnetic-based isolation approaches does not represent an imposition, and this kind of approach can be applied to a diverse set of sample volumes.

1.2.4. Microfluidics-based isolation techniques

The advances in the microfabrication technologies led to the development of microfluidics-based devices for the efficient and quick isolation of exosomes. These devices mainly work based on the physical and biochemical properties of exosomes at the microscale, like their size, density and immunoaffinity. Other innovative mechanisms are also being proposed for microfluidics-based exosome isolation that involve

electrophoretic and electromagnetic manipulations [48], as well as acoustic processes [49].

To increase the specificity and the possibility of studying subpopulations of exosomes, Chen *et al.* [50] tried to integrate the use of immunoaffinity capture in a microfluidic chip for the isolation of exosomes. Like it was mentioned before, this immunocapture technique relies in the interaction between the exosome membrane proteins (antigens) and the antibodies immobilized on the chip. There are already some microchips commercialized for exosome capture, specifically the ExoChip. The ExoChip is a microfluidic device functionalized with tetraspanin CD63, a largely expressed protein in the human exosomes surface. Then, a fluorescent carbocyanine dye (DiO) stains the membrane of exosomes, and the quantification is performed with the use of a microplate reader. The experimental design of this chip is summarized in Figure 7.

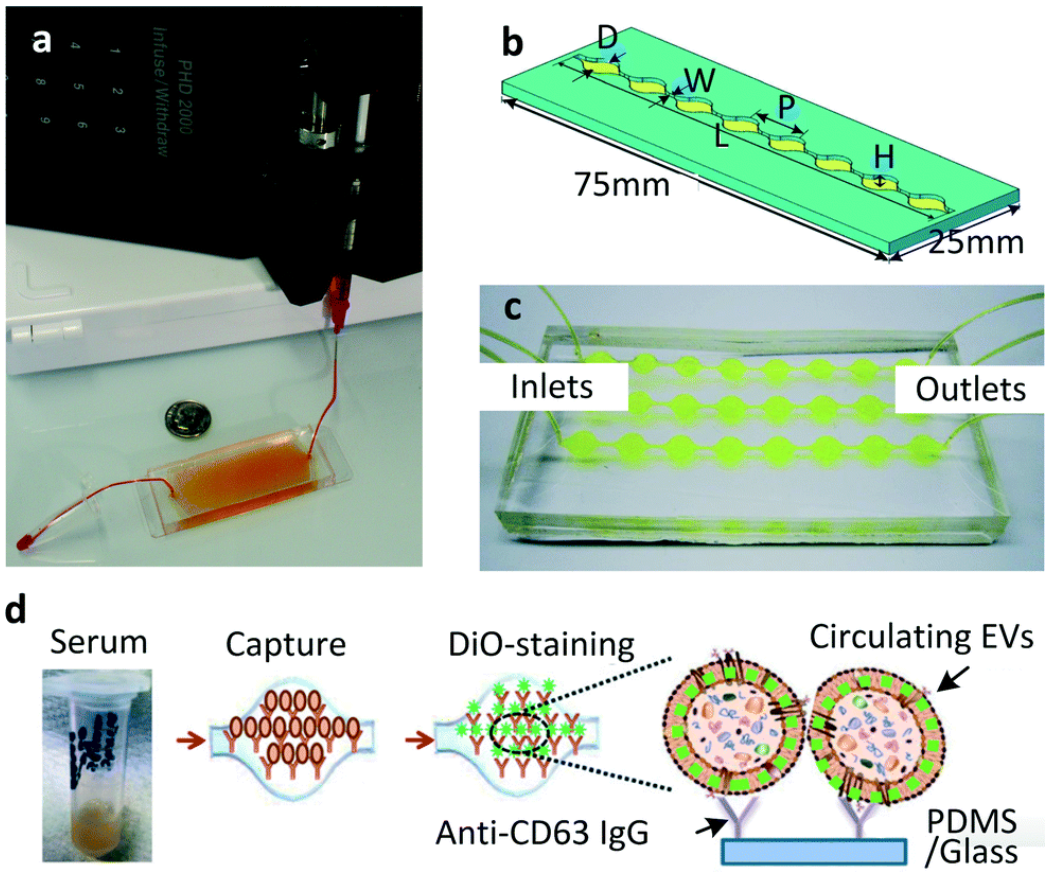

Figure 7 – Experimental design of the ExoChip. (a) The first chip designed for the isolation of exosomes. (b) A modified design of the same chip, the ExoChip with a single channel (W = 0.75 mm, L = 73 mm, P = 9 mm, H = 100 µm). (c) Experimental scheme of a 3 channel ExoChip. (d) Working scheme of the ExoChip, which involves three steps: (i) the capture of CD63-positive exosomes from a blood infusion. (ii) staining with the DiO fluorescent dye and (iii) Chip analysis with conventional methods. Figure adapted from reference [51].

1.3. Characterization of extracellular vesicles

Due to the complexity of EVs structure and composition, there is a need for the development of methods capable of a) characterizing their biochemical content and b) determining their physical properties. The biomolecular characterization of EVs involves the determination of their protein, nucleic acid and lipid content, while the physical characterization involves the determination of parameters such as morphology, size, charge, mechanical properties and density. Together, these characteristics can give us information about the biological function and origin of EVs.

1.3.1. Physical characterization of EVs

In the last decades, there was a great attention towards the physical characterization of small EVs, because there was an enormous development in techniques that can detect objects with a size below 200 nm. In this section, the physical techniques that are currently more often used in the physical characterization of EVs will be described.

1.3.1.1. Dynamic light scattering

Dynamic light scattering (DLS) technique is the most used optical technique for the determination of nanoparticles size in solution. This technique is based on the incidence of a laser beam in a colloidal solution, where there is dispersion of this light by nanoparticles in the solution, resulting in fluctuations of the scattered light intensity. These nanoparticles are under Brownian motion effect, which is related to their hydrodynamic size. So, it is possible to determine particle size distribution through a mathematical formula, known as the Stokes-Einstein equation. It is important to refer that this equation assumes that all the nanoparticles are spherical. This technique can detect particles and vesicles with nanoscale sizes, which makes this technique suitable for the characterization of EVs [52,53]. One of the limitations of DLS is that it does not work that well with polydisperse samples, because the larger objects can scatter more light and may hide the smaller particles [54]. For the characterization by DLS, EVs can be isolated from cell culture medium [54,55] or from plasma samples [56].

To overcome some of the limitations that were mentioned, the samples can be submitted to size exclusion chromatography, in order to remove the bigger particles or

aggregates, like proteins or larger vesicles, making the technique more suitable for the EV population under study [57].

1.3.1.2. Nanoparticle tracking analysis

The nanoparticle tracking analysis (NTA) has recently been used as an alternative technique to DLS for the determination of EVs size, especially for the smallest ones, like exosomes. The NTA technique is similar to DLS since it also detects the scattered light of particles with the use of a laser beam. However, the NTA technique uses a conventional microscope, allowing the direct visualization of the light scattering particles (Figure 8). The tracking of the Brownian motion allows the determination of the hydrodynamic size of single particles [58].

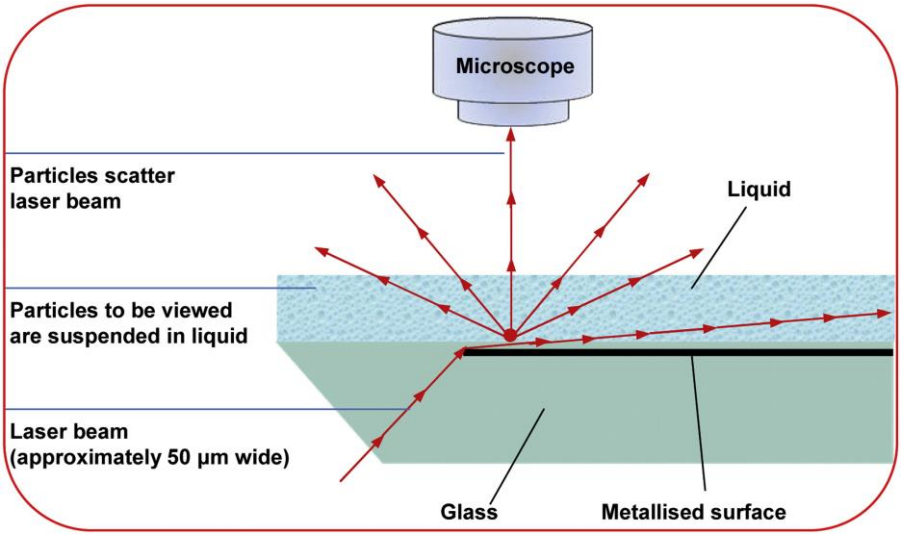

Figure 8 – Representation of the nanoparticle tracking analysis (NTA) technique. Figure adapted from reference [58].

One of the advantages of this technique in relation to DLS, is the fact that the concentration of particles can be measured. Also, NTA is more suitable for the analysis of polydisperse samples, because particles are analysed in an individual basis, instead of the ensemble-average signal used in DLS.

One of the limitations of NTA is the fact that small particles scatter few light, making this technique only suitable for particles with a size bigger than 50 nm [59,60]. Another limitation is the analysis of vesicles in complex biological samples, which cannot be

distinguished from other kind of particles, like protein aggregates [57,61]. Nevertheless, NTA remains a convenient and fast technique in the characterization of EVs [61,62].

This technique has been used in diverse studies, for example, in the determination of EVs sample stability and quality [63], and in the characterization of EVs found in blood samples of cancer [64] and Parkinson´s disease patients [65,66].

1.3.1.3. Tunable resistive pulse sensing

Electrical methods, based on the Coulter principle, have been proposed as an alternative to optical methods for the size determination of EVs. Normally, the setup of these electrical techniques is based in two chambers filled with an electrolyte solution that are separated by a pore. The passage of a nanoparticle through the pore results in the decrease of the ionic conductivity across the aperture, referred as blockade event (Figure 9). The amplitude of the blockade event is related to the particle volume.

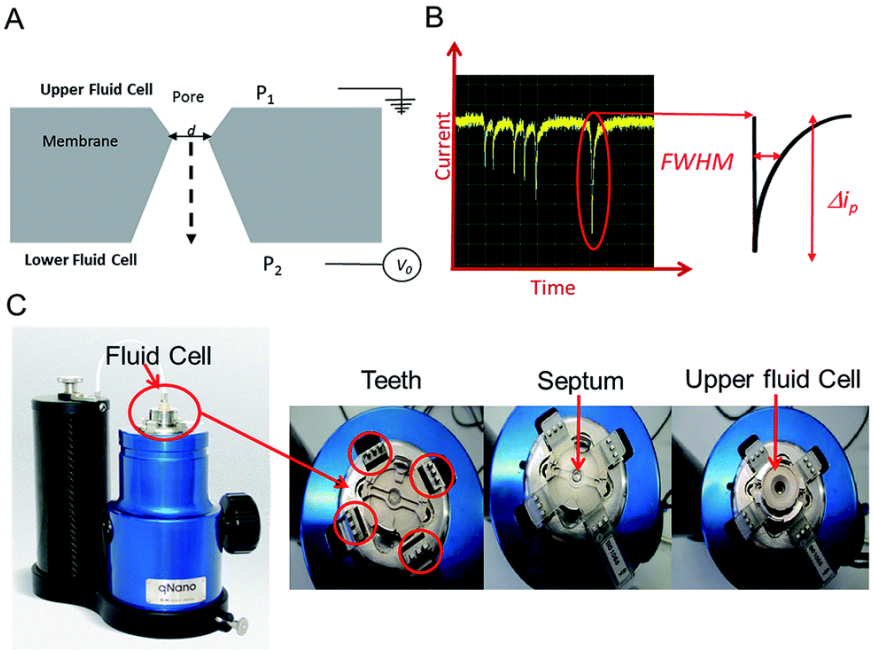

Figure 9 – Tunable resistive pulse sensing (A) Sectional scheme of a pore. The sample is normally placed in the upper fluid cell. (B) Example of a baseline and blockade event (current dips) that are caused by the passage of a particle through the pore. Each event is analysed for full width half maximum (FWHM) duration, related to the particle surface charge, and Δi_p, related to the particle volume. (C) The Izon qNano instrument, showing the fluid cell, teeth and the membrane with the aperture. Figure adapted from reference [67].

This technology, referred as tunable resistive pulse sensing (TRPS), can detect vesicles down to 50 nm, using, for example, the qNano device, commercialized by Izon [68–70]. One of the major advantages of this technique is the use of an elastic pore, which size can be tuned to increase the detection range for bigger particles, making this technique suitable for polydisperse samples. This technique has already been used in the characterization of EVs in many contexts. For example, Böing *et al*. [71] used TRPS to investigate the role of caspase-3 in the production of EVs from breast cancer cells.

1.3.1.4. Flow cytometry

Flow cytometry is a technique that detects both the fluorescence and scattering signal from individual particles through the incidence of a laser beam while these particles flow through a nozzle.

When the light's wavelength is smaller than the particles, the forward scattering light can be used to determine the size of cells. For smaller particles, such EVs, the signal can be deconvoluted through their side scattering, if the structure and refractive index value are known. However, like it was mentioned before, normally the suspensions of EVs are very heterogeneous in size, making this strategy uncertain. So, the calibration through the use of beads of known refractive index and size is being suggested for a more precise determination of liposome [72] and EV [73] size. As an alternative, the membrane of EVs can be labeled with fluorescent probes to determine their size, since homogenous membrane staining results in a fluorescence intensity that is proportional to the surface area [74].

However, the detection of vesicles with sizes of few manometers remains a hard task in conventional flow cytometry [75,76]. Some optimized systems and protocols can detect particles with sizes down to 100 nm [75]. These limitations are due to the fact that small EVs or particles have a low scattering signal, and can be affected by the Swarm effect, where multiple objects are detected just as a single event [77].

1.3.1.5. Atomic force microscopy

The atomic force microscopy (AFM) is a surface imaging technique, that can have a sub-nanometer resolution. One of the advantages of this technique is that the measurements can be directly done in aqueous environments, like most part of biological solutions. This technique is based on the use of a very sharp tip, mounted in the end of a cantilever. The interaction between the tip and the sample surface is monitored through the deflection of the cantilever. AFM can be used to study the sample topography, but also to study other sample characteristics, like its chemical and mechanical properties. The topographical images can be acquired by the contact (Figure 10-ii) and non-contact mode (Figure 10-iii) [78]. The tapping mode is normally used for the characterization of soft particles, such EVs, because the contact mode can result in vesicle deformation and rupture. However, when using AFM in the characterization of EVs, one should have attention on the sample preparation, specially sample immobilization in the surface [79]. Sharma *et al.* [80] used AFM tips coated with anti-CD63 to show that the increase in tip-vesicle binding force was related to the increase in the density of this receptor per vesicle in patient samples.

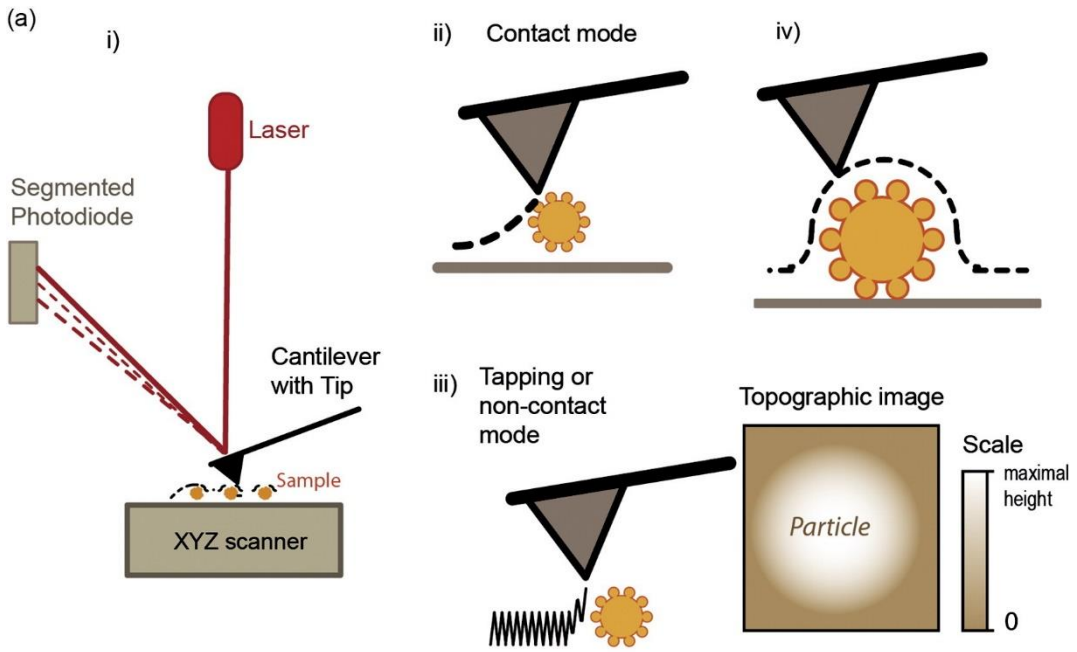

Figure 10 – Atomic force microscopy imaging of extracellular vesicles. I) working principle of AFM. The AFM can operate in ii) contact mode, iii) in tapping mode yielding a topographical image of the surface (iv). Figure from reference [81].

1.3.1.6. Electron microscopy

Due to their small size, EVs cannot be detected by standard optical microscopy. Instead, an electron microscopy (EM) can be used to visualize these vesicles. EM uses electrons instead of photons to create images with resolutions down to nanometers. Because of this capacity, EM has become the gold method for visualization of EVs, and to study their morphology and structure. There are two main EM techniques, the scanning electron microscopy (SEM) and the transmission electron microscopy (TEM). In the first one, the topographical image of the surface is acquired through the detection of secondary electrons originated from the incidence of an electron beam in the sample. However, one of the drawbacks of SEM, is that samples must have a conductive surface, being necessary, sometimes, to coat the surface with a thin layer of a conductive material, like gold. Despite the use of SEM and other variants, in the characterization of EVs [63,82], TEM is mostly used. In TEM the samples do not need to have a conductive surface, and therefore ultra-thin samples can be directly analysed in transmission mode. However, in standard TEM, samples need to be fixated and dehydrated due to the applied vacuum. Also, the samples are normally stained for a better contrast and visualization. One of the advantages of TEM is the possibility to do immuno-electron microscopy. This allows for the detection of specific biomolecules in the outer membrane of the EVs with the use of gold-conjugated antibodies. TEM in combination with immunostaining has been used to investigate diverse EVs populations [83].

1.3.2. Chemical/Biochemical characterization of EVs

One of the most commonly used methods for the identification of proteins in EVs is Western blotting. In this technique, a mixture of proteins is separated based on their molecular weight through a gel electrophoresis. Then, the proteins are transferred to a membrane of nitrocellulose, Polyvinylidene difluoride (PVDF) or nylon. Membrane sites with unbound protein are blocked with a blocking solution, such as Bovine serum albumin (BSA) or non-fat dry milk. Then the membrane is incubated with antibodies specific for the protein of interest. In this process, a primary antibody labelled with an enzyme can be used or, alternatively, a primary antibody will be used first followed by the addition of a secondary antibody labelled with an enzyme. The unbound antibody is washed, leaving only the antibody bound to the protein of interest. The bound antibody is then detected by exposure to a specific substrate, which gives a detectable signal [84]. For a more deeper analysis, proteomic approaches, like Sodium dodecyl sulphate-Polyacrylamide

gel electrophoresis (SDS-PAGE) or High-performance liquid chromatography (HPLC) followed by mass spectrometry can be used [85]. Conde-Vancells *et al*. [86] have done an extensive proteomic characterization of exosomes secreted by hepatocytes using both methods. The lipid content of exosomes can also be analysed by lipidomic approaches. Llorente *et al.* [87] did an extensive analysis of exosome lipid contents and of their cells of origin. There are diverse databases, such *Vesiclepedia*, in which the protein and lipid contents of EVs are described [88].

1.4. Mesenchymal stem cells (MSCs) as the source of exosomes

One important aspect when using exosomes for drug delivery applications is their origin, that is, the cell source used for obtaining them. For example, exosomes isolated from dendritic cells can be loaded with antigenic peptides for T cell proliferation, and thus be of great potential as a vaccine in cancer and infectious diseases [89]. However, exosomes derived from dendritic cells are immunogenic, which does not make them a suitable vehicle for drug delivery. Thus, the ideal cell source would be one capable of producing non-immunogenic exosomes in abundance. In fact, for drug delivery, it is described that the best option is to use mesenchymal stem cells derived exosomes [90].

1.4.1. Background of mesenchymal stem cells

MSCs are multipotent stem cells that can be found in diverse adult tissues, such as adipose tissue, periosteum, liver, lung, spleen, muscle connective tissue, amniotic fluid, placenta, umbilical cord blood, dental pulp and aborted foetal tissues [90]. According to the International Society for Cellular Society, MSCs must be plastic adherent when maintained in standard culture conditions; they must express CD105, CD73 and CD90, and lack expression of CD45, CD34, CD14 or CD11b, CD79α or CD19 and HLA-DR surface molecules. At last, they must be able to differentiate into osteoblasts, adipocytes and chondroblasts *in vitro* [91]. The differentiation potential of MSCs is shown in Figure 11. Although several research papers report the differentiation of MSCs towards cells of ectoderm and endoderm origin, this is still controversial.

1.4.2. Clinical and therapeutic applications of MSCs

Mesenchymal stem cells are the most studied stem cells, with more than 49000 publications cited in Web of Science since 1900. This could be attributed to their application in a wide range of diseases and injuries [92], to their easy availability from different tissues (such as bone marrow and fat tissue) and to their capacity for large *ex vivo* expansion [93]. Until 2015, the database of the US National Institutes of Health (NIH) registered about 493 MSC-based clinical trials [94]. MSCs have been explored in four main fields: local implantation of MSCs to treat local diseases; systemic transplantation of MSCs; use of stem cell therapy together with gene therapy; and use of MSCs in tissue engineering procedures [92]. Regarding the local implantation of MSCs, these cells were shown to be efficient in the treatment of bone diseases [95]. For example, some clinical reports demonstrated

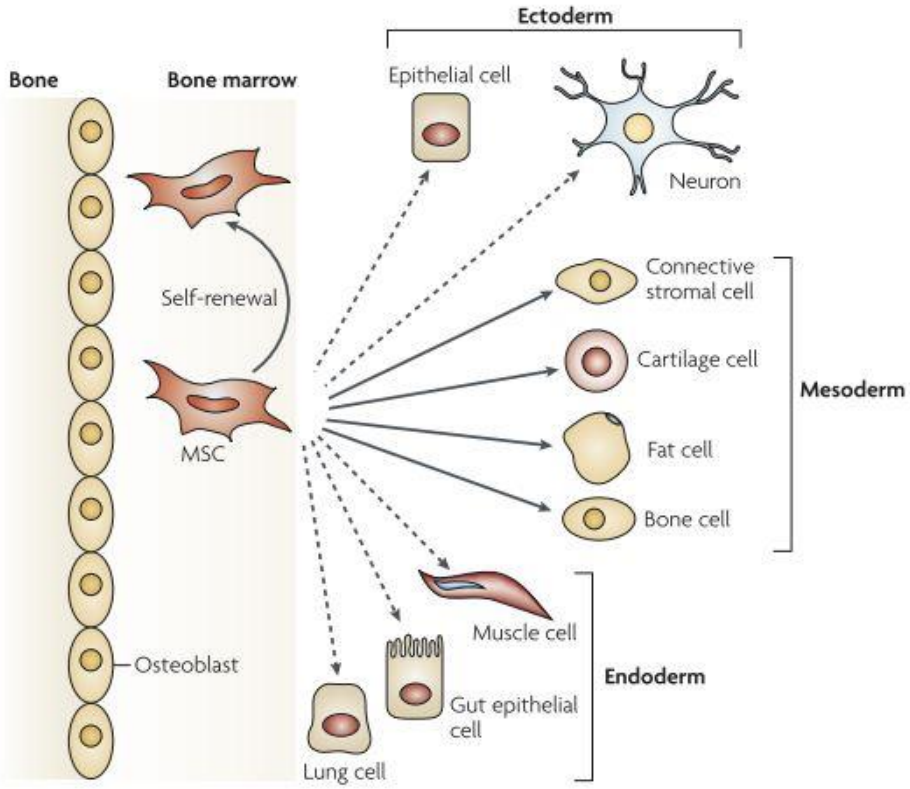

Figure 11- The differentiation capacity of MSCs. The figure shows the ability of MSCs to self-renew (curved arrow) and to differentiate into mesodermal lineage (solid arrows). The reported capacity to transdifferentiate in cells of other lineages (ectoderm and endoderm) is showed by dashed arrows (even though this is still controversial). Figure adapted from reference [96].

the capacity of autologous MSCs in the treatment of large bone defects, when injected *ex vivo* [97]. Also, some studies applied MSCs in the repair of cartilage tissue [98]. The MSCs can also be used for the treatment of vascular diseases, like vascular ischemia, peripheral arterial disease [99] and coronary artery disease [100]. These studies showed very good results, but more trials are needed in a bigger number of randomized patients.

Beyond the possibility of direct differentiation into different cell types, MSCs are able to secret several biochemical factors that have local paracrine and autocrine actions (throphic factors), as shown in Figure 12 [101]. For example, the secretion of trophic factors led to a reduction in the infarct incidence and improved the cardiac functions in a pig model of chronic ischemia [102]. Later, it was shown that these therapeutic factors were released inside membrane vesicle, more specifically in the exosomes [103].

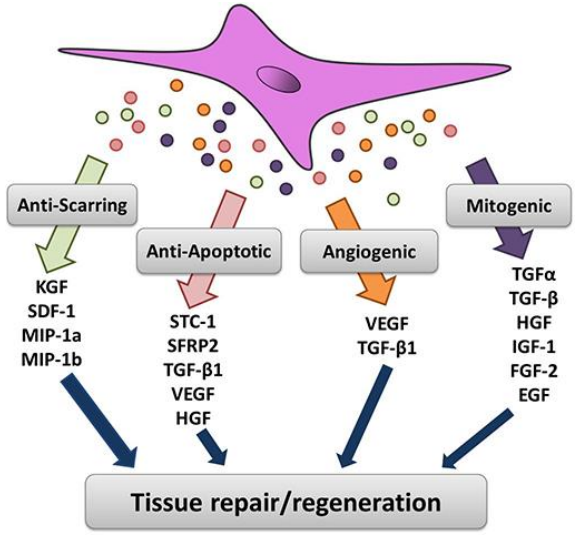

Figure 12 – Paracrine factors release by mesenchymal stem cells which may play an important role in mitogenesis, angiogenesis, apoptosis and scarring. Figure adapted from reference [104].

1.4.3. Advantages of using MSCs as exosome producers for drug delivery

Mesenchymal stem cells present many features that make them ideal candidates as producers of exosomes. For example, these cells present a large *ex vivo* expansion capacity, and since they can be isolated from human adult tissues, their use is ethically non-controversial. Also, as there are already several reports that describe the safe clinical transplantation of MSCs, one can conclude that the use of exosomes derived from these cells will not lead to adverse effects. The administration of human MSC-derived exosomes in an immunocompetent mouse model for acute myocardial ischemia was shown to have therapeutic effects, and without adverse effects [105,106].

One of the most important aspects in the clinical use of MSCs is their ability to make use of suppressive and regulatory effects over the innate immune cells and independently of their autologous or allogeneic origin [107]. This immunomodulatory ability can result in a longer exosome longevity and bioavailability of their therapeutic cargo. Another important aspect of the MSCs is their high *ex vivo* proliferative capacity. Although this expansion is finite, some studies were made regarding this question. For example, Chen *et al*. [108] created an immortalized MSC line with the myc oncogene. The immortalization compromised the differentiation capacity of these cells but did not affect the production and therapeutic effect of the exosomes. The immortalization of MSCs could reduce the need for constant new batches of these cells, also reducing the need for constant derivation, testing and validation and therefore making the production of MSC exosomes more commercially sustainable. One last topic that should be addressed related to the use of MSCs as candidates for the production of exosomes is that these cells are among the most prolific producers of exosomes [109]. All these properties are presented in Figure 13.

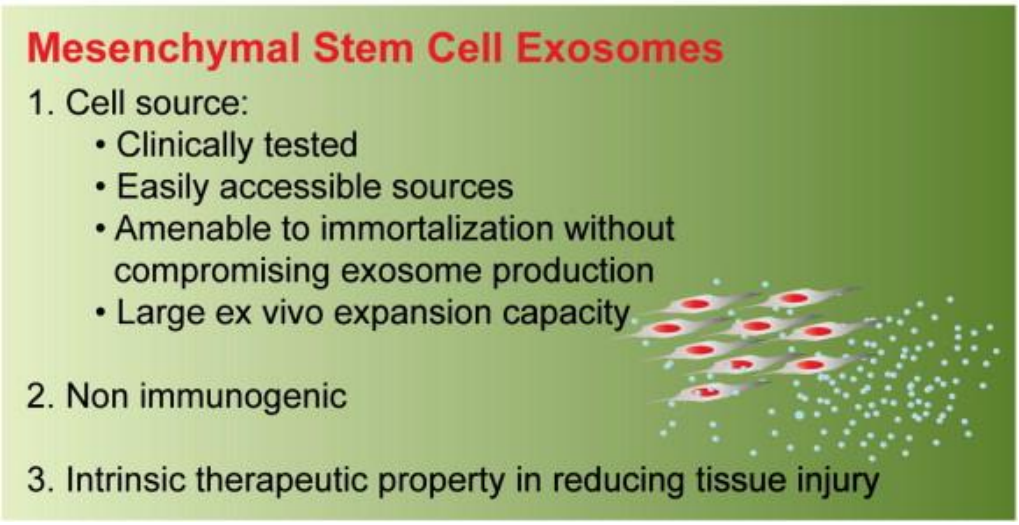

Figure 13 – Advantages of using mesenchymal stem cells as a source of exosomes. Figure adapted from reference [4].

1.5. Methods for the loading of therapeutic cargo into exosomes

Exosomes have a lipid bilayer membrane that serves like a natural barrier for the protection of their cargo in order for it to not be degraded in the bloodstream. However, the presence of this membrane makes exosome loading a challenging task. Indeed, the successful delivery of the therapeutic cargo transported by exosomes depends directly

on the efficiency of the selected loading method [110,111]. Exosome loading methods can be classified in two groups: (1) after EV isolation; and (2) before EV isolation (like schematized in Figure 14). A brief description of the most important methods used is presented in the following sections.

1.5.1. Exosome loading methods after EV isolation

1.5.1.1. Electroporation

When exosomes (or cells) are submitted to an electrical field, pores can be created in the membranes, facilitating the sorting of cargo into the lumen of EVs [112]. For example, Alvarez-Erviti *et al*. [113] loaded small interfering RNA (siRNA) in exosomes with the use of the electroporation technique. Other studies also used this method for the incorporation of therapeutic cargo, with voltages in the range of 150-700 V. Interestingly, the applied voltage for efficient exosome loading by electroporation may vary with the type of donor cell (immature dendritic cells, monocytes and HeLa cells, for example) [114,115].

Electroporation may be a good option for exosome loading since it is easy to control the experimental parameters. However, some authors believe that it may induce adverse effects in the loaded cargo or in exosome integrity.

For example, Kooijmanns *et al*. [111] showed that the process of electroporation can induce the formation of siRNA aggregates, and that only 0.05 % of the siRNA was successfully incorporated in exosomes using this method. Other work showed that electroporation can also induce the aggregation of exosomes themselves,; however, when the parameters are optimized, the aggregation can be significantly reduced, still allowing the incorporation of iron particles [110]. This method was also used for the incorporation of doxorubicin in targeted exosomes, showing that it can represent an efficient way to load chemotherapeutics in exosomes. Moreover, the drug was able to maintain its biological function [114].

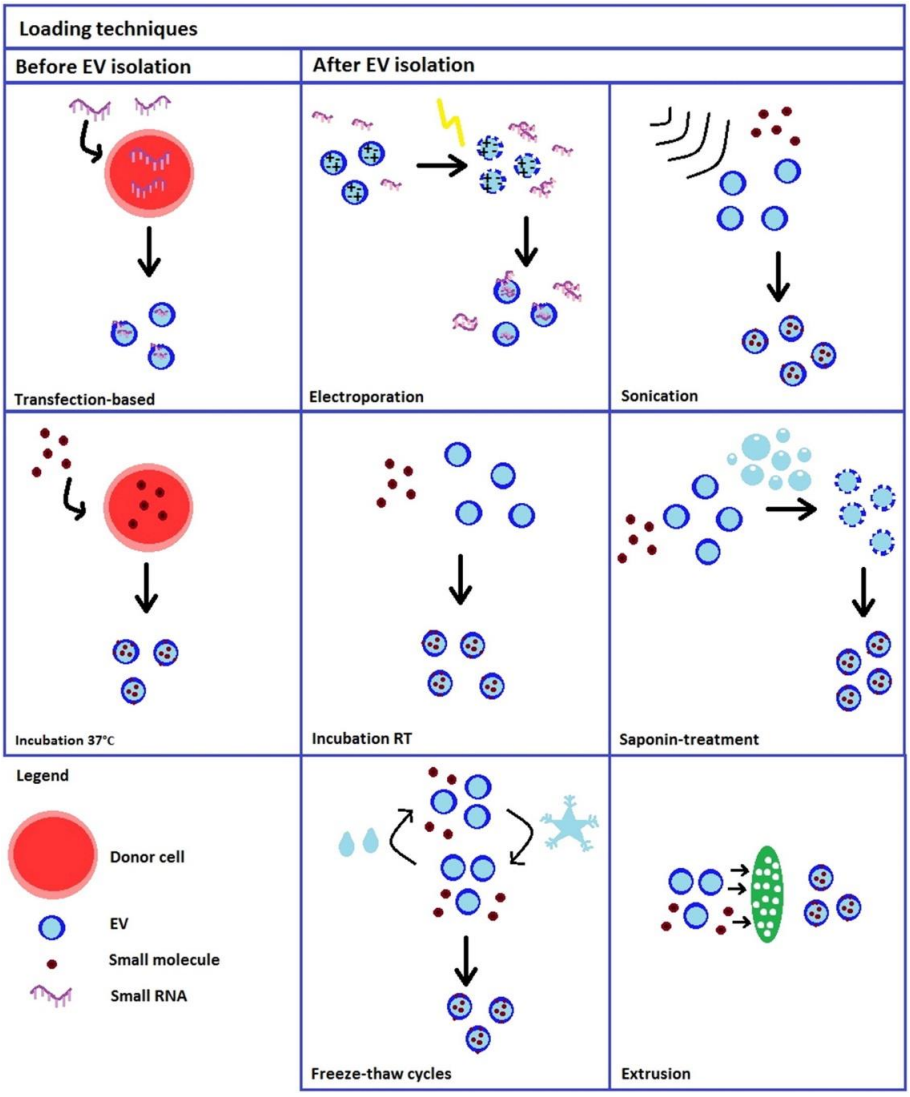

Figure 14 – Scheme with the different strategies for exosome loading. Left side: Incorporation of the therapeutic cargo before exosome isolation. Transfection of cells with a vector encoding a protein and by simple exposure to a therapeutic molecule. Right side: Incorporation of the therapeutic cargo after exosome isolation. Electroporation, simple incubation, application of ultrasonic frequencies, repeated freeze-thaw cycles, treatment with detergent-like molecules, such as saponin, and extrusion. Figure adapted from reference [116].

1.5.1.2. Simple incubation

Simple incubation of the therapeutic cargo with exosomes is a common method for exosome loading. Only 5 minutes of incubation was needed to efficiently incorporate curcumin in exosomes at 22 ºC, and result in a significant anti-inflammatory effect in different disease models [117,118]. Curcumin can induce lipid rearrangement and changes in the membrane fluidity, and for this reason the incorporation of this molecule

in the exosome lumen is an easy process [119,120]. Some other therapeutic cargo was loaded in exosomes through incubation at 37 ºC for 1h and 2h, such as miR-150 and doxorubicin [121,122]. The relative small size of these molecules may be the reason for their successful incorporation in exosomes.

1.5.1.3. Use of transfection agents

Commercial transfection agents can be used for the incorporation of a therapeutic cargo in exosomes. Normally, the cargo loaded in exosomes through this method is siRNA. There are at least two studies that used transfection reagents for the incorporation of siRNA in exosomes. They showed that the use of *HiPerFect transfection reagent* was less efficient than electroporation, and that the use of the very common *Lipofectamine 2000* reagent resulted in the incorporation of siRNA in exosomes, decreasing gene expression after being delivered inside cells [115,123]. However, the effect of the loaded exosomes alone was not confirmed, because of the presence of captured siRNA in leftover micelles. So, the chemical-based transfection method does not seem adequate for the loading of therapeutic cargo, such as siRNA, in exosomes.

1.5.1.4. Other methods

Besides the methods already described, some other methods have been also used for the incorporation of therapeutic cargo in exosomes. For example, Haney *et al.* [124] tried to load the enzyme catalase in exosomes through different methods, such as saponin permeabilization, sonication, freeze-thaw cycles and extrusion. The most efficient methods were the sonication, saponin treatment and extrusion. Also in this study, the effect of these treatments in the morphology and size of exosomes was observed. Extrusion and sonication resulted in an increase of the exosome size as analysed by DLS, NTA and AFM. A similar study was performed by Fuhrmann *et al.* [125]. They observed an eleven-fold increase in the incorporation of porphyrins in exosomes through saponin permeabilization in comparison to simple incubation and extrusion. These methods for the incorporation of therapeutic cargo in exosomes are represented in Figure 14.

1.5.2. Exosome loading methods before EV isolation

1.5.2.1. Cell exposure to the therapeutic cargo

A possible method to load exosomes is by simply exposure of cells in culture to the therapeutic cargo. Pascucci *et al.* [126] showed the incorporation of Paclitaxel in EVs of mesenchymal stromal cells. This was accomplished by the exposure of MSCs to high dosages of Paclitaxel. Consequently, the cells produced EVs loaded with Paclitaxel that were able to inhibit *in vitro* tumour growth.

1.5.2.2. Transfection of exosome producing cells

Transfection of cells is probably the most used method for the incorporation of therapeutic cargo in exosomes. This is accomplished by transfection of exosome producing cells with a gene of interest that, when overexpressed, will give rise to the production of the protein of interest (therapeutic protein or gene product) which will then be incorporated in the lumen or membrane of exosomes [127,128]. For example, MSCs were transfected with a miR-46b vector, leading to the production of miR-146b-expressing exosomes, which were then successful in the inhibition of tumour growth [128]. This study showed the capacity of using exosomes in cancer treatment. Also, another similar study demonstrated the production of exosomes with a targeting peptide that allowed their targeted delivery after intravenous injection [127]. In the literature, one can also find reports on the use of cell transfection for overexpression and incorporation of a specific protein in exosome membranes [129,130]. There are already commercial products for exosome engineering, like the incorporation of targeting peptides in the exosome membrane. The System Biosciences (SBI) company sells a product, called *XStamp*™, that makes use of a Lentivector for transfection and subsequent expression of a gene product incorporated in exosomes surface [131]. Figure 15 shows the vector used in this technology.

However, one must keep in mind that cell engineering for production and presence of targeting peptides in exosomes surface, and incorporation of large amounts of cargo in their lumen, can be a laborious procedure. This can represent a problem in clinical applications, where patient cells are used for the production of engineered exosomes. Therefore, production of non-autologous exosomes with non-immunogenic properties would be of very great interest.

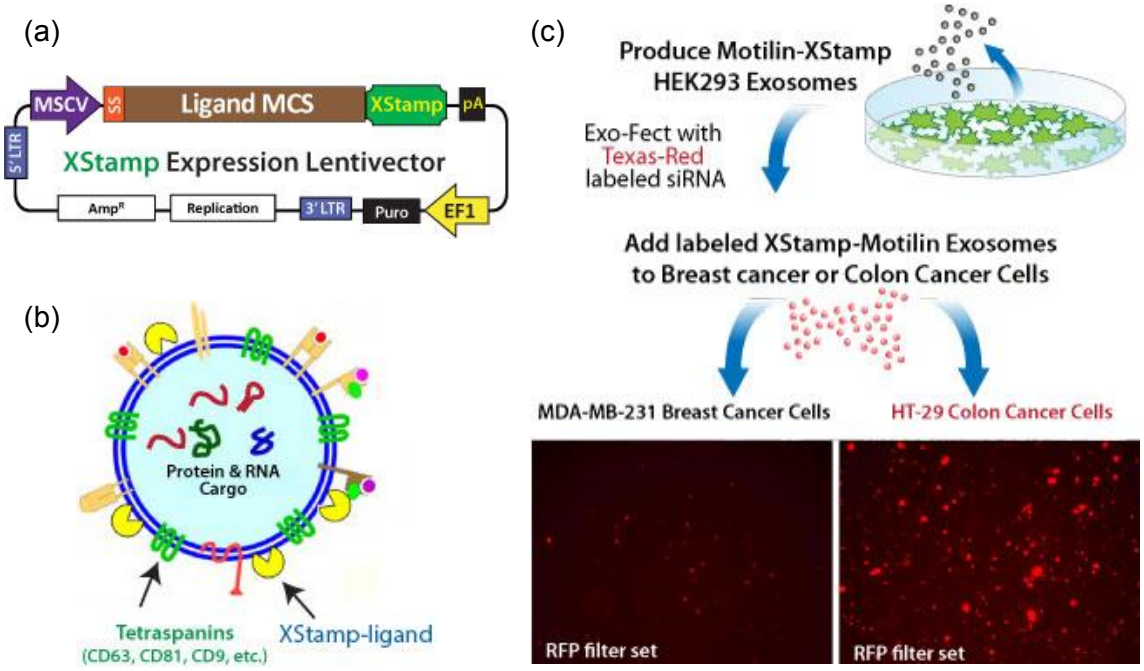

Figure 15 – *XStamp*™ technology commercialized by System Biosciences company: (a) Lentivector with a ligand MCS for insertion of the gene of interest. (b) Representation of an exosome with the localization of the XStamp-ligand. (c) Scheme to produce XStamp-Motilin exosomes. Motilin is a 22-amino acid sequence polypeptide hormone that binds specifically to motilin receptor in the intestine cells. After being produced, the exosomes were added to the MDA-MB-231 breast cell line (motilin receptor negative) and HT-29 colon cancer cell line (motilin receptor positive). After 24 h, the cells were visualized in a fluorescence microscope, and the HT-29 cells took up the exosomes at much higher rate than the MDA-MB-231 cells. Figure adapted from reference [131].

1.6. Dendrimers as nanocarriers for drug delivery

"Dendrimer" comes from the Greek word *dendron*, which means "tree" and the word *meros* which means "part". Dendrimer is a term internationally accepted, but other terms can be used, like "arborols" and "cascade molecules". The first dendrimers were synthesized in the research group of Fritz Vögtle in 1978 [132]. After that, many different families of dendrimers were synthesized, like the poly(amidoamine) (PAMAM) dendrimer family that appeared in 1983 by the hands of Donald Tomalia [133,134]. PAMAM dendrimers are commercially available and are, by far, the most studied dendrimer family.

1.6.1. Characteristics and molecular structure of PAMAM dendrimers

Dendrimers are large and complex polymer molecules with a well-defined chemical structure. They possess three different architectural components: (i) an initiator

core, consisting of a molecule with at least two identical chemical groups, (ii) interior layers (generations), composed of repeating units radially attached to the core, and (iii) many functional groups (multivalency), located in the surface of the dendrimers (Figure 16). These surface groups are responsible for the important properties of dendritic macromolecules such as charge and solubility. When compared to other carrier systems, like linear polymers, dendritic structures have a huge potential because of their unique shape, nanoscale size and monodispersity [135].

"Monodispersity" means that dendrimers possess a well-defined molecular structure. The monodispersity of dendrimers has been confirmed using techniques such as gel electrophoresis, mass spectrometry, size exclusion chromatography and transmission electron microscopy. Mass spectrometry analysis, for example, has shown, that PAMAM dendrimers (Figure 17) from generations 1 to 5, produced by the divergent method, are very monodisperse [136].

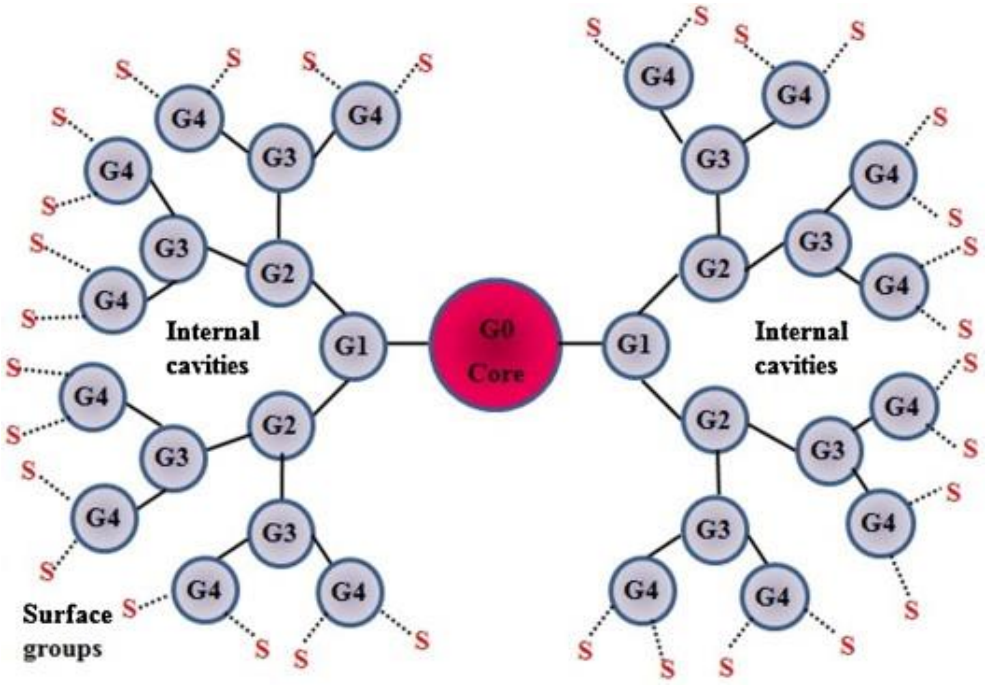

Figure 16 – Representation of the general structure of dendrimers. Figure adapted from reference [132].

The size of dendrimers increases with the number of generations, from several to tens of nanometers in diameter. Dendrimers can have sizes resembling some biological structures - for example, generation 5 PAMAM dendrimer has a size (5.5 nm) and a shape similar to those of hemoglobin (Hb). Dendrimer size is also relevant for its three-dimensional shape. Lower generation dendrimers tend to have an open and amorphous structure, whereas the higher generations can adopt more spherical

conformations, being capable of incorporating guest molecules (like therapeutic compounds) within their branches [137].

Like it was mentioned before, dendrimers are composed of three structural units: the core, the branching units and the terminal functional groups. These end groups may possess a negative, positive or neutral charge, which is fundamental in the exploration of these macromolecules as drug delivery carriers. This periphery charge can play an important role in dendrimer applications – for instance, cationic dendrimers such as PAMAM dendrimers with amino termini can be used for gene delivery purposes since they can form complexes with the anionic charged deoxyribonucleic acid (DNA) (Figure 18). Also, the positive charge of dendrimers can facilitate the interaction with cell membranes, which are slightly negative due to surface glycoproteins, making them a suitable candidate for intracellular drug delivery. However, one problem associated with these positively charged dendrimers is the fact that they can induce some cytotoxicity, hemolysis, among others. Fortunately, this aspect can be overcome with dendrimer surface modification using different molecules, such as PEG, carbohydrates and acetate [138].

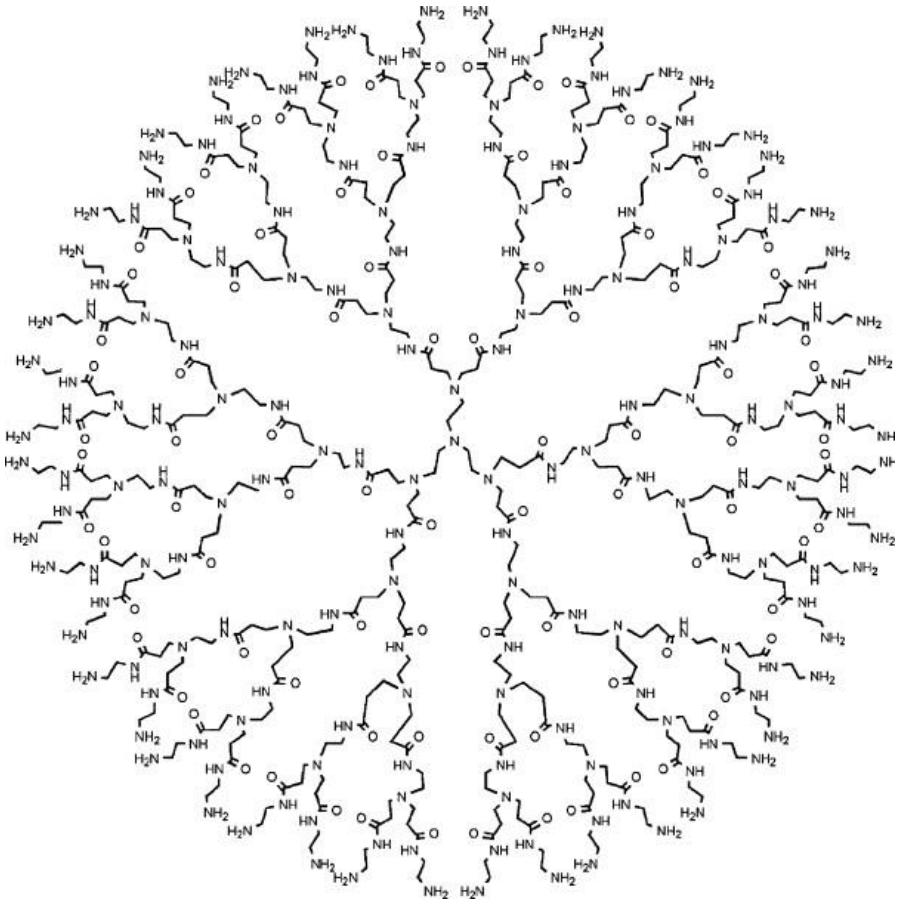

Figure 17 – Molecular structure of PAMAM dendrimers. Figure adapted from reference [138].

1.6.2. Biomedical applications of PAMAM dendrimers

The unique properties of dendrimers (nanometric size, tailor-made surface groups, extensive branching, excellent stability and monodispersity) have attracted the attention of researchers for their possible biomedical applications, such as nucleic acid delivery, controlled delivery of therapeutic compounds and use for imaging and diagnostic purposes.

An extensive literature is available concerning the application of dendrimers in nucleic acid delivery, especially related with the use of amino terminated PAMAM dendrimers. The existence of amino groups at the dendrimer surface enhances nucleic acid transfection efficiency. Normally, the complexes formed by dendrimers and nucleic acids are called “dendriplexes”. Dendrimers showed good transfection efficiencies in the delivery of a variety of genetic materials, such as aptamers, antisense oligonucleotides, siRNA and genes [139]. The mechanism of nucleic acid delivery is represented in Figure 18, specifically for the delivery of a gene. Briefly, the first step consists in the cellular uptake of the dendriplex by endocytosis, then followed by endosomal disruption and release of the complex into the cytosol. After, the DNA is disassembled from the dendrimer, it enters the nucleus and is replicated with the host DNA. After the transcription is accomplished, the product, mRNA, is released as a biosignal and translated into the protein of interest [140].

The intracellular delivery of a therapeutic cargo is one of the most promising applications of dendrimers. These macromolecules have been successfully used in different studies for intracellular delivery of diverse kinds of drugs which can be chemically conjugated to the dendrimers or just linked by physical means (like surface adsorption or encapsulation within dendrimer internal cavities) [138]. However, to achieve that purpose, it is necessary to prevent non-specific interactions between dendrimers and the systemic circulation, as well as a quick removal of the dendriplexes from the systemic compartment by renal clearance or phagocytosis by macrophages [138].

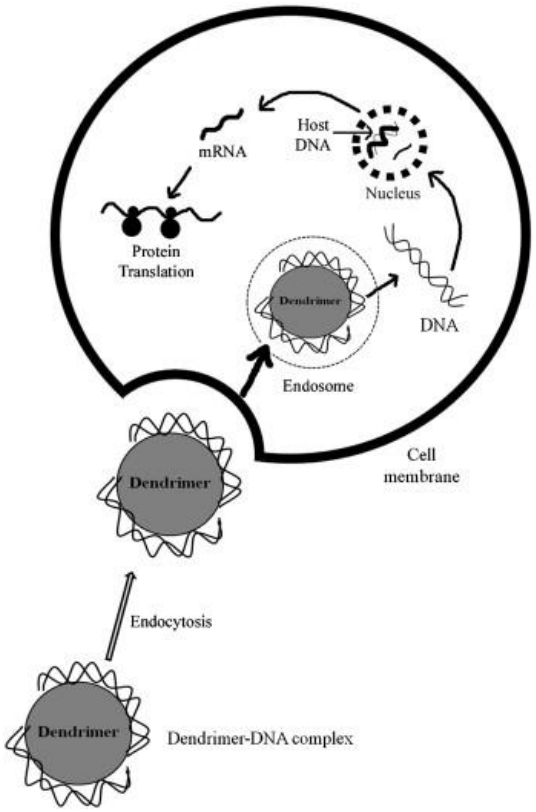

Figure 18 – Gene delivery mediated by dendrimers. Figure adapted from reference [132].

For example, conjugates of PAMAM dendrimers and methylprednisolone were rapidly internalized by human lung carcinoma epithelial cells [141]. The activity of the free drug was comparable to the one of the dendritic complex. Kolhe *et al*. demonstrated that ibuprofen covalently linked to PAMAM dendrimers was rapidly taken by A549 cells, and also that a sustained release of the drug was achieved. Indeed, dendrimers can be used for the successful intracellular delivery of therapeutic compounds and, also, as controlled drug delivery systems which will assure the release of the drug for a prolonged period [142].

One last and important application of the dendrimers in the biomedical field is their application as imaging agents [143]. Nanomaterials based on dendrimers have been efficiently used as imaging agents in a diverse group of imaging techniques, like magnetic resonance imaging (MRI), computed tomography (CT) imaging, fluorescence imaging and positron-emission tomography (PET). For example, MRI is a non-invasive diagnostic technique, based in the different relaxation times of protons in different tissues that often uses gadolinium complexes as contrast agents. However, the Gd(III) ions are highly toxic due to their high affinity for serum proteins and are also quickly cleared from the systemic circulation limiting the time for medical analysis. To overcome this problem,

Gd(III) have been complexed to high molecular weight compounds, such as dextran, albumin, polylysine and dendrimers [144] . Dendrimers combined with gold nanoparticles may also find applicability as contrast agents in CT imaging to substitute the iodine compounds traditionally used that also raise problems of toxicity [143]. In fact, dendrimers can even be used as scaffolds for the construction of theranostics nanomaterials that can be applied for therapy and, simultaneously, for imaging purposes [143].

1.7. Thesis objectives

The main objective of this Master thesis was to evaluate the possibility of using exosomes derived from human mesenchymal stem cells (hMSCs) as carriers of dendrimers, more precisely generation 4 (G4) poly(amidoamine) dendrimers with amino termini (PAMAM(NH_2)).

Assuming the hypothesis that exosomes could be loaded before their isolation from cells by cell exposure to a dendrimer-containing solution, it was designed a set of experiments, in particular:

a) The labelling of PAMAM dendrimers with rhodamine B isothiocyanate (RITC) and further characterization by Nuclear Magnetic Resonance (^{1}H NMR), Fourier Transformed Infrared Spectroscopy (FTIR), UV/Vis spectroscopy, and fluorescence spectroscopy;
b) the effect of the pH in the stability of the fluorescence emission of PAMAM(NH_2)-RITC conjugates;
c) the cytotoxicity of the PAMAM(NH_2)-RITC conjugates using cells in culture;
d) the kinetics of PAMAM(NH_2)-RITC conjugate cell uptake by fluorescence spectroscopy and fluorescence microscopy;
e) establishment of an exosome isolation protocol using a precipitation-based approach and the physical and biochemical characterization of the isolated exosomes, for example, by Dynamic Light Scattering (DLS), detection of acetylcholinesterase (AChE) activity and Transmission Electron Microscopy (TEM);
f) the exposure of hMSCs to PAMAM(NH_2)-RITC conjugates and stimulation of exosome release; isolation of the exosomes and the confirmation of the presence of dendrimers in the exosome fraction by fluorescence spectroscopy;

Part 2. Materials and methods

Contents

2. Materials and methods

2.1. Synthesis and characterization of PAMAM(NH_2)-RITC conjugates

2.1.1. Materials

Rhodamine B isothiocyanate (RITC, mixed isomers, BioReagent) was from Sigma-Aldrich. Generation 4 (G4) PAMAM dendrimers with ethylenediamine core, in methanol, with 100 % -NH_2 end groups, were from Dendritech® (Midland, MI, USA). Dimethyl sulfoxide (DMSO, analytical grade) was from Fisher Scientific. The dialysis membranes were from SpectrumLabs (Spectra/Por ® 7 Dialysis Membrane with molecular weight cut-off (MWCO) of 6000-8000 Da). The ultra-pure (UP) water used in all experiments was obtained through a Millipore Milli-Q purification system with a resistivity higher than 18.2 MΩ.cm (at 25°C).

2.1.2. Preparation and characterization of PAMAM(NH_2)-RITC conjugates

For the preparation of PAMAM(NH_2)-RITC conjugates, G4 PAMAM dendrimers with 100 % -NH_2 surface groups were used. The synthesis conditions to obtain a specific number of RITC molecules attached to each dendrimer molecule were previously optimized and determined in our lab. The conditions for the conjugation are presented in Figure 19. To attach one molecule of RITC to one G4 PAMAM dendrimer (in average), RITC was used in excess (1.5 mol of RITC to 1 mol of dendrimer). As such, 33.7 mg of lyophilized dendrimer was firstly dissolved in 4.5 ml of DMSO. Then, the conjugation was started with the addition of 1.9 mg of RITC dissolved in 0.5 ml of DMSO. The reaction was performed for 18 h under stirring, in a dark environment, and at room temperature. After that, the solution was extensively dialysed against distilled water for 3 days. Then, the obtained purple solution was lyophilized, leaving 31 mg of conjugate.

To assess the successful conjugation of RITC to the dendrimer, the conjugates and the non-conjugated PAMAM dendrimers and RITC molecules were characterized by different techniques, namely ^{1}H NMR, UV/Vis, FTIR, and fluorescence spectroscopy.

For the ^{1}H NMR characterization, a Bruker Avance II+ 400 MHz equipment at 25 ºC (probe temperature) was used. The chemical shifts (δ) are presented in ppm and calibrated based on the residual solvent peaks. All the compounds were dissolved in

deuterated water (D_2O). All NMR data was treated using the Mnova NMR ® software, v9.1.

The UV/Vis spectra were obtained using a Perkin-Elmer Lambda 25 spectrophotometer. All the measurements were done using a stopped quartz cell and for a scan interval between 190 and 900 nm. The conjugated and non-conjugated compounds were dissolved in UP water and analysed at the concentration of 1 µM.

The FTIR spectra were obtained through an ATR coupled Perkin Elmer Spectrum Two spectrometer. The IR spectra were collected by pressing small amounts of the sample on a Diamond/ZnSe crystal. All the spectra were acquired at the resolution of 4 cm^{-1}, with a minimum number of 20 scans and along the spectral range of 4000 to 400 cm^{-1}.

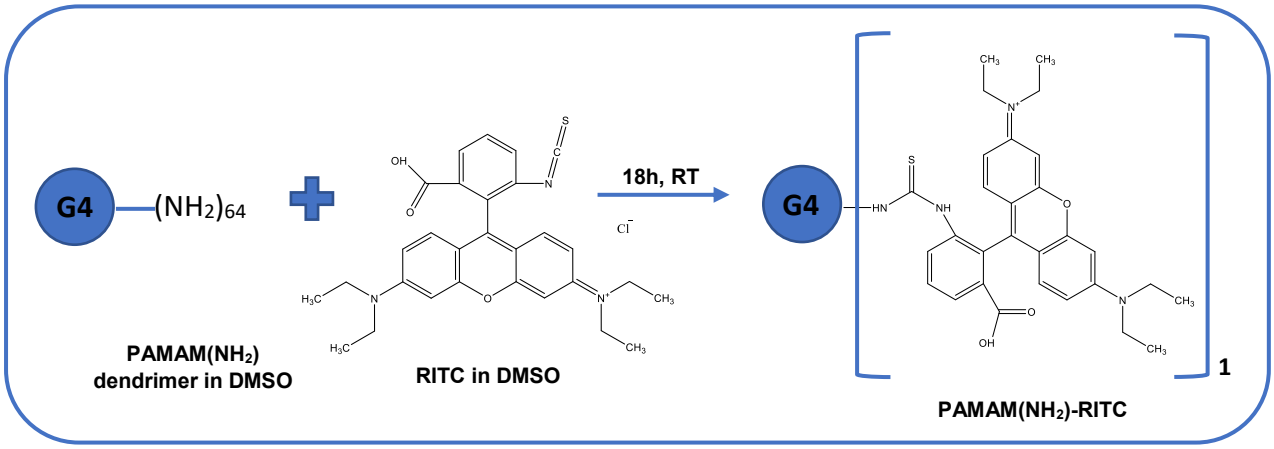

Figure 19 – Conjugation conditions for the preparation of G_4 PAMAM(NH_2)-RITC conjugates (1:1.5 PAMAM:RITC molar ratio).

2.1.3. Effect of the pH in the photostability of PAMAM(NH_2)-RITC conjugates

To evaluate the photostability of the conjugates during the events of uptake and endosomal maturation, the fluorescence intensity of PAMAM(NH_2)-RITC conjugates was measured at different pH values.

Briefly, 100 µL of a 10 µM solution of the conjugates was dispersed at different pH values (3-10) in 4,9 ml of a buffer containing 31 mM $C_6H_8O_7$ (citric acid), 29 mM KH_2PO_4 (monopotassium phosphate), 29 mM H_3BO_3 (boric acid) and 29 mM of $C_8H_{12}N_2O_3$ (diethylbarbituric acid). Then, 200 µL of each solution was transferred to an opaque 96 well plate, and the fluorescence intensity was measured with a microplate reader (Victor^3 1420, PerkinElmer) at λ_{ex} = 530 nm, λ_{em} = 590 nm.

2.2. Cytotoxicity studies of PAMAM(NH_2)-RITC conjugates

To determine the best concentration for the "*in vitro*" inclusion of the PAMAM(NH_2)-RITC conjugates into the exosomes, as well as the concentration that would be the most suitable for cell uptake and colocalization studies, cytotoxicity assays were done. All the conditions applied for these studies are described in the next sections.

2.2.1. Cell culture conditions for cytotoxicity analysis

All cytotoxicity assays were accomplished using human mesenchymal stem cells (hMSCs). The human mesenchymal stem cells were isolated from the bone marrow present in the trabecular bone of healthy adults which was obtained during surgical interventions after trauma. Only tissue that would have been discarded was used with the approval of the Ethical Local Committee (Hospital Dr. Nélio Mendonça, Funchal). First, primary hMSC cultures were established based on cells adherent to the plastic surface of the cell culture dish (VWR). Afterwards, cells were passaged using a standard protocol using trypsin (Gibco) and their number was expanded. Cells were always grown in 100 mm cell culture dishes using α-Minimum essential medium (α-MEM) (Gibco) supplemented with 1 % (v/v) of an antibiotic/antimycotic solution (AA, Gibco) and 10 % (v/v) of Fetal Bovine Serum (FBS, Gibco) - referred as "complete medium" from now on. The cells were cultured in an incubator (at 37ºC with 5 % CO_2 atmosphere) until the desired number of cells were achieved and before reaching confluence.

2.2.2. Effect on cell viability of PAMAM(NH_2)-RITC conjugates

Non-conjugated generation 4 PAMAM dendrimers and PAMAM(NH_2)-RITC conjugates were used in the cytotoxicity studies.

The cytotoxicity of these compounds was evaluated through the resazurin reduction assay. This assay relies on the assessment of metabolic active cells that can convert the non-fluorescent dye, resazurin, into a fluorescent product resorufin, which emits a fluorescence signal that can then be measured using a microplate reader. This assay assumes that there is a direct correlation between cell metabolic activity and the number of viable cells. As such, cell viability was determined as a percentage in relation to the non-exposed cells (control). For this purpose, the hMSCs were exposed to

different concentrations of compounds (1 – 0,1 μM). Cell viability was determined 24, 48 and 72h of cell culture.

Briefly, the hMSCs were seeded in 48-well plates (VWR) at the density of 1 x 10^5 cells per well with α-MEM complete medium, and left to incubate at 37 ºC in a 5 % CO_2 atmosphere. After 24 h, the medium was replaced with 450 μL of fresh one. Then, 50 μL of each dendrimer stock solution in UP water were added to each well to obtain the intended concentration.

After 24 h (exposure time), the cell culture medium was removed and complete, fresh, α-MEM medium containing 10 % (v/v) of a 0.1 mg/ml resazurin solution (Sigma-Aldrich) was added to each well. The cells were then left to incubate for 4 h at 37 ºC and 5 % CO_2. After this time, 100 μL of the medium, from each well, were transferred to a 96 opaque well-plate and fluorescence was measured using a microplate reader, at λ_{ex} = 530 nm, λ_{em} = 590 nm. Then, the wells were washed three times with PBS 1x (Sigma-Aldrich), and 500 μL of α-MEM complete medium were added to each well. The same procedure was repeated after 48 and 72 h of culture. All the samples were analysed based on six replicates.

2.3. Kinetics of cell uptake of PAMAM(NH_2)-RITC conjugates

Having in mind the idea of loading exosomes with PAMAM(NH_2)-RITC conjugates before their isolation from cells, the kinetics of cell uptake was studied. In these experiments, hMSCs were seeded at a density of 2x10^4 cells per well in a 24-well plate. Then, after 24 h, cells were exposed to 1 μM of conjugate (final concentration) in complete medium during different periods of time (6-30 h). Although this concentration resulted in some cellular toxicity, this value was selected in order to make the observable expected effects more evident. After that, medium was removed and the wells were washed 3 times with PBS 1x. Cells were then lysed with 100 μL of RIPA buffer (Amresco, VWR), supplemented with Protease inhibitor cocktail Set III, EDTA-free (Calbiochem, Merck Millipore) in the proportion of 1:200, and scrapped with a pipette tip. After this, 100 μL of cellular suspension was transferred to an opaque 96-well plate, and fluorescence intensity was read in a microplate reader (Victor3 1420, PerkinElmer) at λ_{ex} = 530 nm and λ_{em} = 590 nm. Cells under the same conditions were visualized in an inverted fluorescence microscope (Nikon Eclipse TE 2000-E).

2.4. Establishment of an exosome isolation protocol

2.4.1. Definition of the protocol

For the establishment of an exosome isolation protocol, NIH 3T3 cells were used due to their easy maintenance and fast proliferation in culture. NIH 3T3 cells were cultured in Dulbecco's modified eagle medium (DMEM) (Gibco), supplemented with 10 % (v/v) FBS and 1 % (v/v) AA. Exosome-depleted FBS (Gibco) was always used when the objective was to harvest cell supernatants for exosome isolation.

Isolation of exosomes from cell culture media was based on a precipitation-based approach using a commercial reagent, the *Total Exosome Isolation Reagent (from cell culture media)* from Invitrogen. This reagent makes less-soluble components, like exosomes, become insoluble, allowing their recovery by low-speed centrifugation. The guidelines recommended in the *Total Exosome Isolation Reagent* product sheet (see the annex) were generally followed, with adaptations. Briefly, when cells reached 70-80 % of confluence, cell culture medium was replaced with α-MEM supplemented with 10 % (v/v) of exosome-depleted FBS and 1 % (v/v) AA. Cells were incubated for 48 h, then the medium was harvested and submitted to differential centrifugation to remove cell debris and other types of extracellular vesicles. Cell culture medium was centrifuged at 300 x g for 10 min to remove cell debris and the obtained supernatant was further centrifuged at 2 000 x g for 20 min to remove apoptotic bodies; again, the supernatant was centrifuged at 10 000 x g for 30 min to remove microvesicles. The supernatant was then mixed with half of its volume of *Total Exosome Isolation Reagent* and was incubated overnight at 4ºC. The samples were then centrifuged at 10 000 x g for 1h at low temperature. The exosome-containing pellet was then resuspended in a phosphate buffered saline (PBS, Sigma) solution and, depending on the experiment, immediately analysed or stored at -80ºC.

As exosomes are described in the literature as having a size below 200 nm [25], the introduction of a filtration purification step before addition of the commercial reagent to the exosome-containing medium was evaluated. For this, NIH 3T3 cells were used as exosome producers and the exosome-containing medium was filtrated using a 0.22 µm polyethersulfone filter (VWR). Also, since a big volume of supernatant was always harvested with a large amount of *Total Exosome Isolation Reagent*, the possibility of concentrating cell supernatants by exploring an ultrafiltration process was evaluated in order to not spend large quantities of the isolation reagent. Thus, the use of Amicon 15-Ultra Centrifugal Filter Units 3 kDa MWCO (Millipore, Merck) was tested for supernatant

concentration after the mentioned filtration step. In these experiments, the presence of exosomes in the final solutions was assessed using the Dynamic Light Scattering (DLS) technique since it gives information regarding the hydrodynamic size of particles. A scheme of this study can be found in Figure 20. Samples were analysed immediately after exosome isolation. A control consisting of medium not exposed to cells was used. Overall, it was concluded that the filtration step did not have an impact on the quality of the DLS analysis whereas the concentration step improved it. Also, to diminish the expenditure with the *Total Exosome Isolation Reagent*, it was decided to keep the concentration step in the process of exosome isolation.

After these preliminary experiments, the final protocol for isolation of exosomes was established which included an extra concentration step performed using Amicon 15-Ultra Centrifugal Filter Units with 3 kDa MWCO (Millipore, Merck) in addition to the other procedures described in the second paragraph of this section,

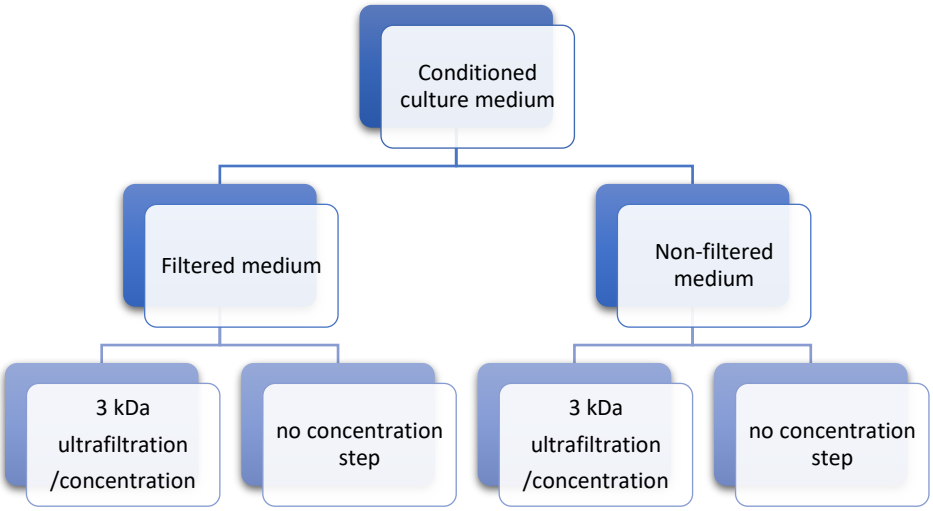

Figure 20 - Scheme for testing the influence of filtration and concentration steps in the isolation of exosomes.

2.4.2. Effect of storage temperature on the stability of exosome solutions

The influence of the storage temperature in the stability of exosome solutions was also studied. For this, hMSCs were used to produce exosome-containing solutions. hMSCs cells were cultured in α-MEM (Gibco) supplemented with 10 % (v/v) FBS (Gibco) and 1 % (v/v) AA (Gibco). Only cells from passages 3 to 7 were used to obtain exosomes. Exosomes were isolated following the established protocol. After getting the exosome solutions, they were stored at different temperatures, namely 25ºC (room temperature), 4ºC, -20ºC and -80ºC for one week. Then, the hydrodynamic size of the particles in

solution was evaluated using the DLS technique to assess the quality of the exosome solutions. As a control, exosomes analysed immediately after exosome isolation were used.

2.4.3. Exosome characterization

2.4.3.1. Dynamic Light Scattering (DLS)

The hydrodynamic size of the isolated exosomes was analysed by a Malvern Zetasizer Nano ZS (Malvern, UK). For this purpose, exosome solutions stored at -80 ºC were thawed, diluted in PBS 1x at different concentrations and then analysed at 25 ºC with a measurement angle of 173º. All the experimental conditions were maintained constant in all the measurements.

2.4.3.2. Transmission Electron Microscopy (TEM)

Exosomes were prepared and visualized in an analytical TEM Hitachi 8100, equipped with a ThermoNoran light elements EDS detector and digital image acquisition. Preparation of the samples was assessed as described previously by Lötvall *et al*. [145]. The exosome solutions were thawed from -80 ºC and drops were placed in *Parafilm* film. Then, with the help of a forceps, a formvar carbon coated nickel grid was placed on the top of each drop for 30-60 min. After this, each grid was washed thrice with 30 µL of PBS 1x. Samples were then fixed in a drop of 2 % paraformaldehyde (Sigma) for 10 min and washed thrice with 30 µL of PBS 1x. Samples were contrasted by adding a drop of 2 % uranyl acetate for 10 min. Excess liquid was removed by gently using absorbing paper, and the grids were air dried for 5 min before analysis.

2.4.3.3. Acetylcholinesterase (AChE) activity

To verify and validate the presence of exosomes in solution, the activity of acetylcholinesterase was measured. AChE is an enzyme that is specific to these vesicles [146]. The acetylcholinesterase activity was assessed as previously described by Savina *et al*. [147]. Briefly, 40 µL of exosome suspension was diluted in 110 µL of PBS 1x. Then, 37.5 µL of this diluted suspension was added to a transparent 96-well microplate. Then,

1.25 mM of acetylthiocholine iodide (Sigma Aldrich, Merck) and 0.1 mM of 5,5'-dithiobis(2-nitrobenzoic acid) (Sigma Aldrich, Merck) were added to each well to a final volume of 300 µL, and incubated at 37 ºC. The change in absorbance at 412 nm was read each 5 min for 30 min. The control contained complete medium supplemented with 10 % (v/v) exosome-depleted FBS and 1 % (v/v) AA. All the measurements were done in triplicate.

2.5. Exosome loading with PAMAM(NH_2)-RITC conjugates

In this thesis, it was hypothesized that exosomes could be loaded with PAMAM(NH_2)-RITC conjugates before their isolation from cells, a technique described in the literature as being successful for other cargo [26]. Briefly, the hMSCs were seeded in 100 mm *Petri* dishes. After attaining 70-80 % of cell confluency, the medium was replaced by fresh medium with 1 µM of conjugates (final concentration) and exposed for 24h (exposition time to conjugates). Then, cells were washed with PBS and cultured during two more days. After this period, the medium was collected and exosomes were isolated according to the protocol previously established.

Since there is also the possibility that the conjugates are integrated into microvesicles, a parallel study was performed where microvesicle release was stimulated by culturing cells in FBS-free medium for 2 days after 24h exposition time to conjugates (this will be referred as the "activation step"). It is reported that a serum-depleted medium induces cell stress, which can increase the release of microvesicles [140]. In this case, the microvesicle fraction was collected by differential centrifugation and analysed.

Both microvesicles and exosome pellets were resuspended in PBS. After, 100 µL of each suspension were transferred to an opaque 96-well plate, and fluorescence intensity was measured in a microplate reader. Also, an aliquot of the microvesicles suspension was placed on microscope slides and observed under an inverted fluorescence microscope; the same was not done for exosomes since the optical microscope does not have enough resolution for their observation. In these studies, control experiments were done with PAMAM(NH_2)-RITC non-exposed cells.

2.6. Intracellular distribution of PAMAM(NH_2)-RITC conjugates

Since the presence of PAMAM(NH_2)-RITC conjugates was not detected in microvesicles and exosomes, the fate of the conjugates inside cells was investigated using fluorescence microscopy. In these experiments, besides hMSCs, MCF-7 cells were also used due to their easy maintenance and fast proliferation in culture. hMSCs cells were cultured as mentioned before and MCF-7 cells were cultured in RPMI (Gibco), supplemented with 10 % (v/v) FBS (Gibco), 1 % (v/v) NEAA (non-essential amino acids, Gibco), 1mM of pyruvic acid (Sigma-Aldrich), 10 µg/ml of human insulin (Sigma-Aldrich) and 1 % (v/v) AA (Gibco).

First, hMSCs and MCF-7 cells were seeded at a density of $2x10^4$ cells per well in a 24-well plate. Then, cells were exposed to 1 µM of conjugates for 24 h in complete medium. After incubation with the conjugates, cells were labelled with specific cell organelle fluorescent probes (Invitrogen, ThermoFisher). To label the endoplasmic reticulum, cells were washed three times with PBS 1x and then incubated with 2 µL of CellLightTM ER-GFP, BacMam 2.0 (green fluorescence colour) in complete medium, overnight, at 37ºC. To label the Golgi complex, cells were washed three times with PBS 1x, fixed with 4 % of paraformaldehyde and permeabilized with 0.2 % of Triton X-100. Then, cells were incubated with 50 µg/ml of Lectin HPA (green fluorescence colour) in complete medium for 45 min. To label actin (microtubules), the same procedure as the Golgi complex staining was followed, but in the end, Alexa Fluor 488™ Phalloidin stain was added and left to incubate for 30 min. All the cells were counterstained with the nuclear stain DAPI (blue fluorescence colour) (Sigma-Aldrich, Merck). Briefly, a 1:2500 solution of DAPI in PBS 1x was prepared from an existent stock solution (5 mg/ml in PBS 1x). Then, a volume of diluted DAPI solution sufficient to cover the cells was added to the wells and left for 15 min at room temperature. After this, cells were washed three times with PBS 1x and visualized under an inverted fluorescence microscope (Nikon Eclipse TE 2000-E).

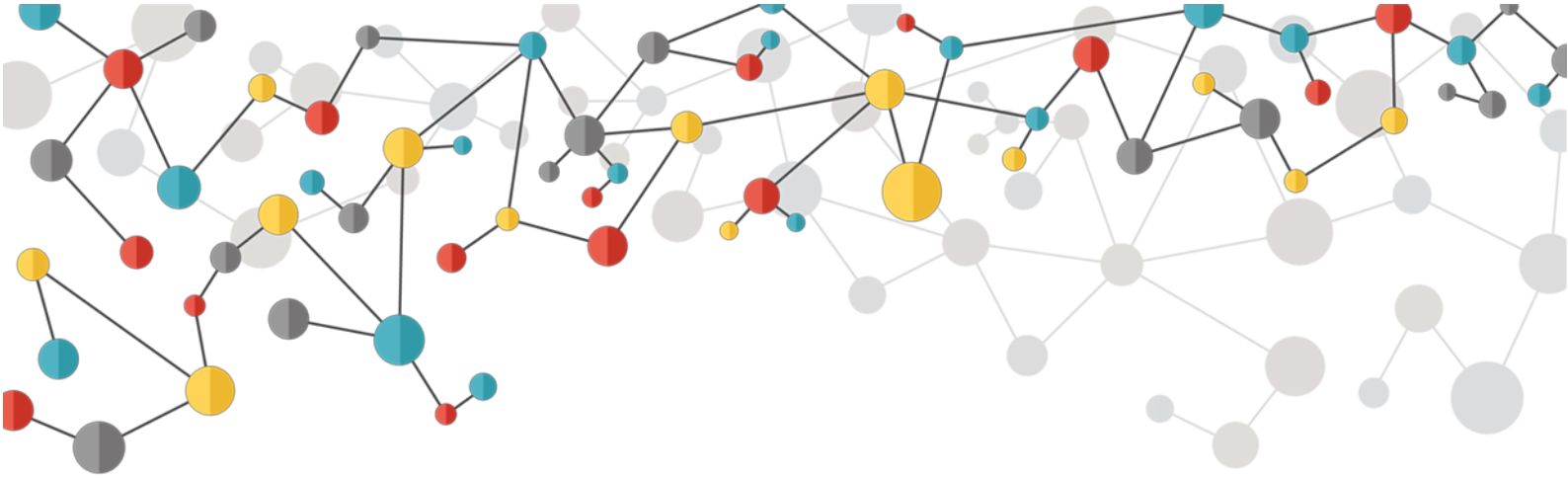

Part 3. Results and Discussion

Contents

3. Results and discussion

3.1. Synthesis and characterization of PAMAM(NH_2)-RITC conjugates

Since the main objective of this Master thesis was to evaluate the possibility of using exosomes derived from human mesenchymal stem cells (hMSCs) as carriers for dendrimers, the first experimental step was to label them with a fluorescence probe. As such, generation 4 (G4) poly(amidoamine) dendrimers with amino termini (PAMAM(NH_2)) were reacted with rhodamine B isothiocyanate (RITC) to get PAMAM(NH_2)-RITC conjugates. The reaction is between the isothiocyanate group in RITC and a primary amine (acting as a nucleophile) at the surface of a PAMAM dendrimer, resulting in a thiourea bond. There are many reports in the literature regarding this type of reaction between primary amines and isothiocyanate groups. In fact, a lot of dyes have been attached to proteins through this kind of reaction, because these dyes are rich in primary amines [148]. Moreover, several works mention the functionalization of PAMAM dendrimers with the fluorescein isothiocyanate (FITC) dye that also has an isothiocyanate group which can directly form a thiourea bond with the primary amines of the dendrimer [149–151]. One should keep in mind that, normally, this kind of reaction is highly selective for primary amines [152].

As show in Figure 21, this reaction begins with a nucleophilic attack of the amine to the electrophilic carbon of the RITC isothiocyanate group. This reaction leads to an electron shift that results in the formation of a thiourea bond between the RITC and the PAMAM dendrimer. It has been reported that the conjugation between primary amines and isocyanate groups takes about 18 h [153].

Thiourea bonds have a limited stability due to hydrolytic events that may occur, specially at room temperature [154]. So, these conjugates were maintained at a low temperature (4ºC) to reduce hydrolytic events and consequently increase the lifespan of the conjugates.

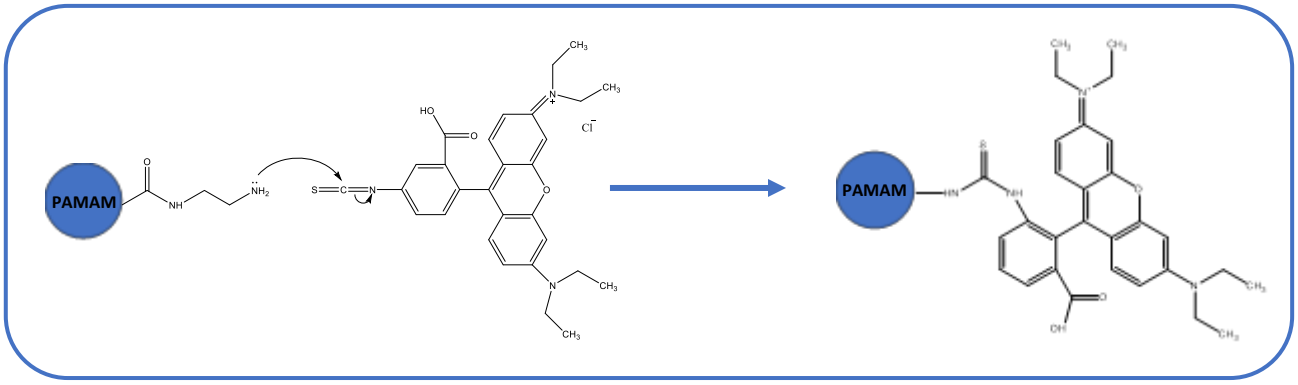

Figure 21 – Representation of the reaction between the primary amines in the PAMAM dendrimer and the electrophilic carbon of the RITC isothiocyanate group.

It is important to keep in mind that one should functionalize the surface of dendrimers with the minimum number of fluorescent molecules for diverse reasons. One of the most important reasons is that an extensive functionalization of the nanomaterial would result in a different dendrimer surface, consequently leading to a different biological response. Other important aspect, is that the higher degree of functionalization could result in self-quenching effects due to spatial proximity between fluorescent molecules [155]. So, in this work, the reaction was done to obtain only one molecule of RITC per dendrimer (in average). Previous work done in our group showed that to obtain this result the reaction should be done at a PAMAM dendrimer:RITC molar ratio of 1:1.5.

The success of labeling of the PAMAM(NH_2) G_4 dendrimer with RITC was assessed through different techniques, such as Nuclear Magnetic Resonance (^{1}H NMR), Fourier Transformed Infrared Spectroscopy (FTIR), UV/Vis spectroscopy, and fluorescence spectroscopy. The ^{1}H NMR spectrum of the PAMAM(NH_2)-RITC conjugates is shown in Figure 22. There, one can see the characteristic peaks of PAMAM(NH_2) G_4 around δ=3.5 - 2 ppm, identified with the letter a. Also, one can confirm the successful conjugation of the RITC molecule to the dendrimer by the appearance of a new peak around δ=6.96 ppm. Like it was demonstrated in previous studies [156], this peak is characteristic of the formed thiourea bond, and is identified in Figure 22 with the letter b. It should be referred that the visualization of the peaks characteristic of the RITC is very difficult, due to the large difference in the number of protons between the dendrimer and the RITC molecule. For comparative effects, the ^{1}H NMR of both the non-conjugated dendrimer and RITC molecule are presented in the Annexes Section A. The conjugation of 1 molecule of PAMAM dendrimer to 1 molecule of RITC was confirmed by calculating the ratio between signal integrals.

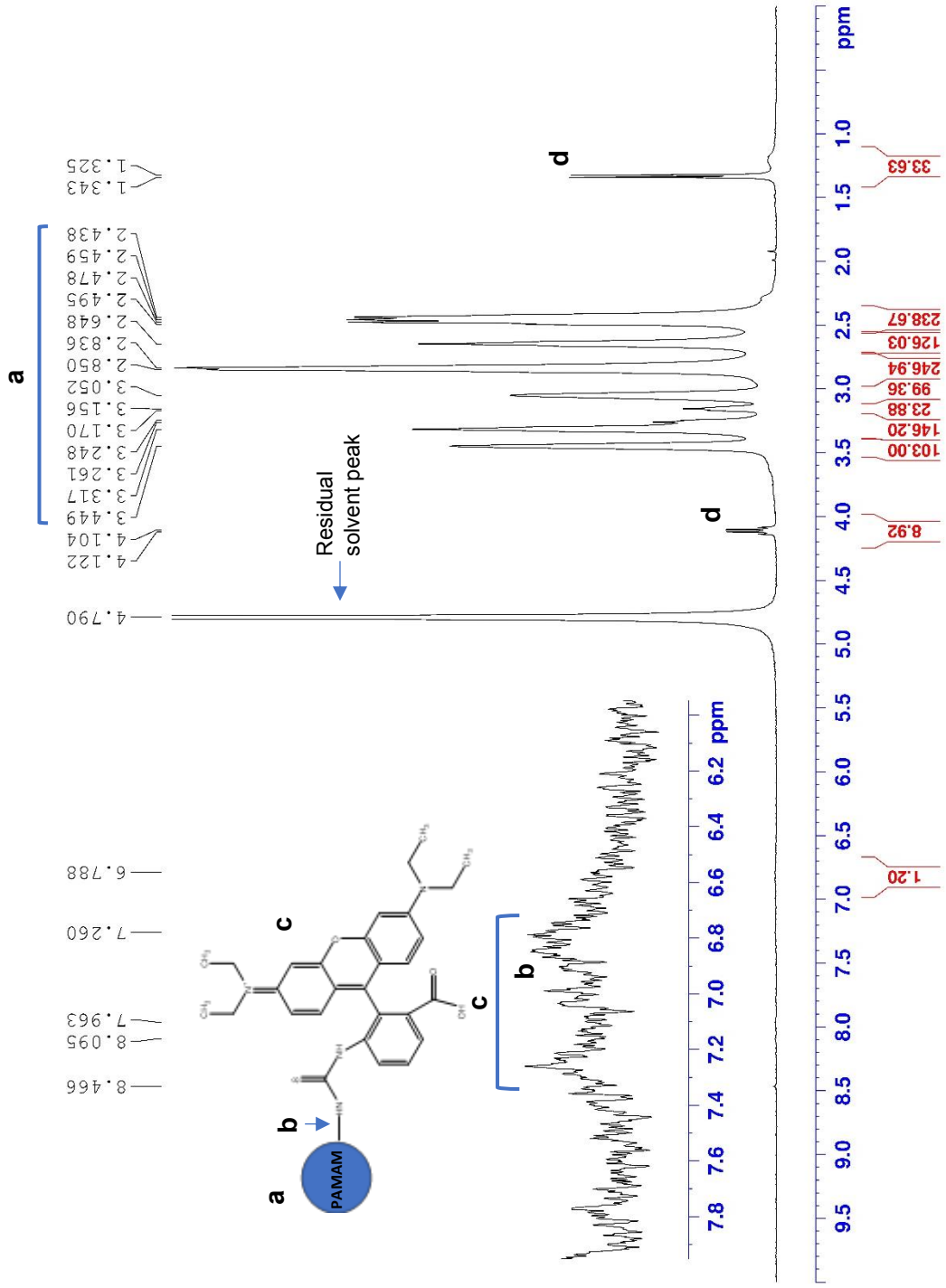

Figure 22 – The ^{1}H NMR spectrum of the PAMAM(NH_2)-RITC conjugate in D_2O (400 MHz). a: PAMAM(NH_2) G_4 dendrimer; b: thiourea; c: RITC; d: urea.

To confirm the success of conjugation, the compounds were analysed with other spectroscopic techniques. In Figure 23, the FTIR-ATR spectrum for the PAMAM(NH_2)-RITC conjugate is shown. The appearance of bands around 1100-1300 cm^{-1} are probably associated with the stretching of the formed thiourea bond [157].

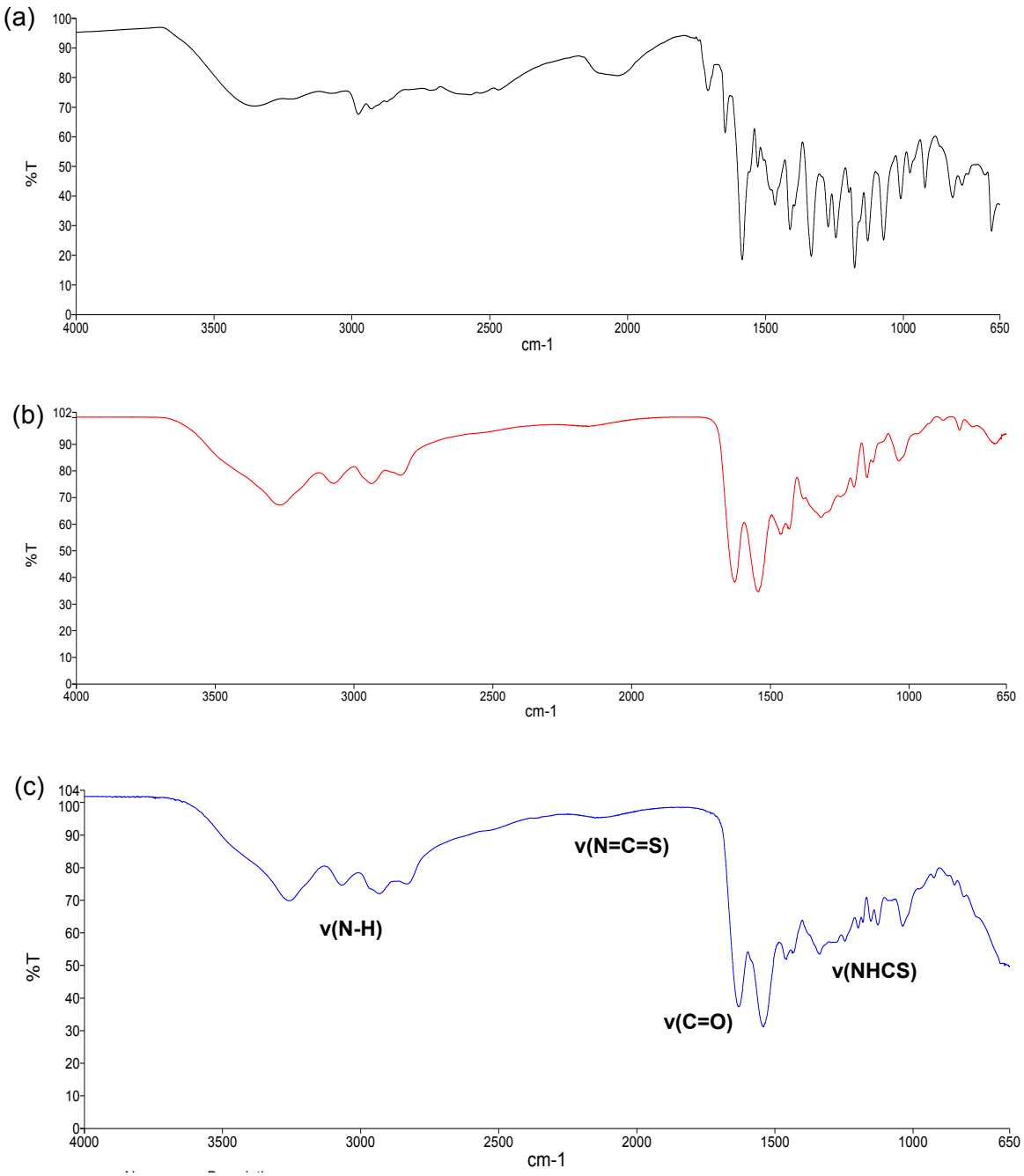

Figure 23 – FTIR-ATR spectra of (a) RITC molecule, (b) PAMAM(NH_2) G4 dendrimer and (c) PAMAM(NH_2)-RITC conjugate.

However, the existence of a weak broad peak around 2100 cm^{-1}, characteristic of the stretching of the isothiocyanate group, points out that some non-conjugated RITC molecules can be associated with the dendrimers by physical interactions and not by chemical means.

Figures 24 and 25 show the UV/Vis (absorption) and fluorescence emission spectra of the prepared PAMAM(NH_2)-RITC conjugate, respectively. The analysis of the UV/Vis (absorption) spectrum of the conjugate shows a band of absorption with a maximum at 560 nm that can only be attributed to the presence of the rhodamine label. A slight bathochromic shift (red shift) in the wavelength of maximum absorption could be observed for the conjugate (560 nm) in relation to free RITC (558 nm). This behaviour is also described in the literature for other kinds of materials labelled with RITC, like microspheres [97,158]. As expected and in agreement with previous data, the emission spectrum of the PAMAM(NH_2)-RITC conjugate shows two bands of emission at wavelengths close to those shown by free RITC. Also, there is a slight red shift in the wavelength of maximum emission when RITC is conjugated to the dendrimer.

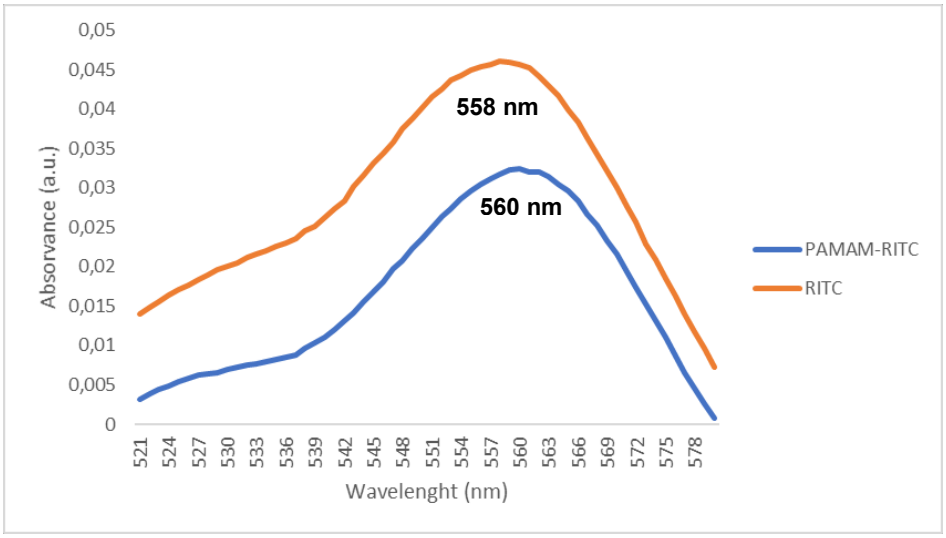

Figure 24 - UV/Vis spectra for the PAMAM(NH_2)-RITC conjugate and the free RITC. Both compounds were analysed at a concentration of 1 µM.

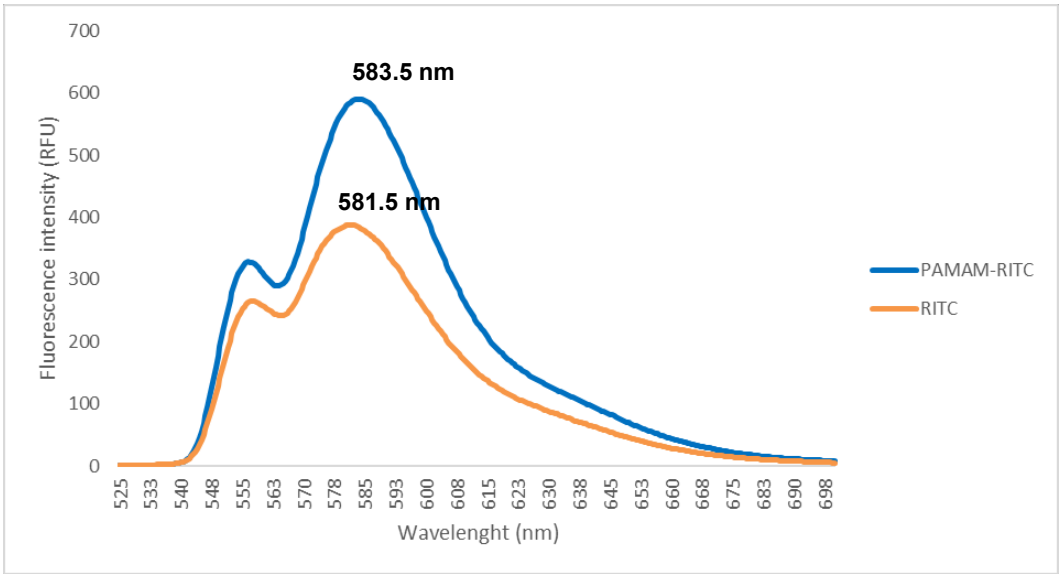

Figure 25 – Emission spectra for the PAMAM(NH_2)-RITC conjugate and the free RITC. Both compounds were analysed at a concentration of 1 μM.

3.2. Effect of the pH in the fluorescence intensity of PAMAM(NH_2)-RITC conjugates

The labelling of nanomaterials with different fluorescent probes is a widely employed method to study the efficiency of their cellular internalization and the localization of these nanomaterials once inside cells. According to literature, nanomaterials can follow different endocytic routes during cell uptake involving a set of vesicle maturation and acidification events (Figure 26). The pH inside these vesicles can go from 6.2 - 6.5 in early endosomes to 4.5 - 6 in late endosomes and lysosomes [159]. Since the present work also involves the tracking of PAMAM(NH_2)-RITC conjugates inside cells, it was decided to evaluate the effect of pH on their fluorescence intensity.

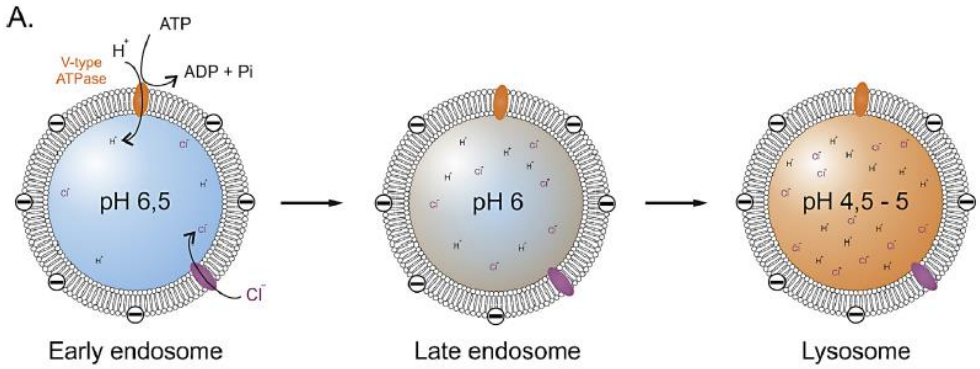

Figure 26 – Normal acidification of endosomes during their maturation to late endosomes and lysosomes. This occurs via transport of H^+ ions across the endosomal membrane by V-type ATPases, which produces an electrical gradient that is balanced by the influx of counter-ions, like Cl^- ions. Figure adapted from reference [160].

Rhodamine dyes are fluorophores from the xanthene's family, along with fluorescein and eosin. In acidic conditions, the rhodamine dyes are found in their cationic form due to the protonation of the carboxylic groups. At neutral pH, the carboxylic groups are deprotonated, and because of the positively charged nitrogen in the alkyl arms, these dyes are found in the zwitterionic form, as shown in Figure 27. Under alkaline conditions, the zwitterionic form undergoes a reversible conformation to a lactone, which results in the interruption of the π-conjugation of the fluorophore [161]. Consequently, absorption of this lactones occur in the UV, and the quantum yield and lifetime are very low [162,163].

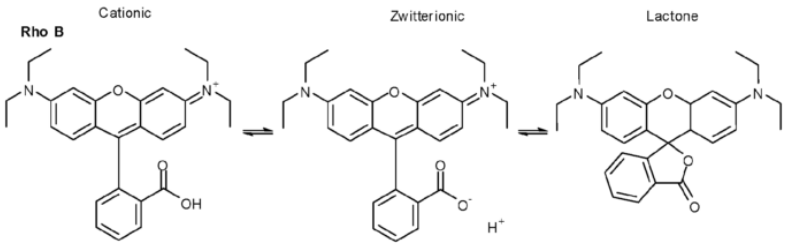

Figure 27 – Molecular structures of the three Rhodamine B forms. Image adapted from reference [161].

Figure 28 shows the impact of a range of pH values (3 – 10) on the fluorescence intensity of the conjugates. Through the analysis of this graphic, one can see that the fluorescence intensity is relatively stable in the pH range 3 – 7 and only starts to decrease at higher pHs (8 – 10). Considering what was mentioned before, this was the expected behaviour since rhodamine dyes have a higher fluorescence signal when they are in their cationic and zwitterionic forms present at acidic and neutral pH, respectively. Lee *et al.* [164] reported that RITC-incorporated silica oxide nanoparticles also showed a very stable fluorescence intensity behaviour under acidic conditions, without dissociation of RITC from the nanoparticles, and without any relevant changes in their size and surface charge. So, the present results reveal that the option to use RITC as a label for dendrimers was adequate, being a good fluorophore to track the conjugates upon their internalization in cells.

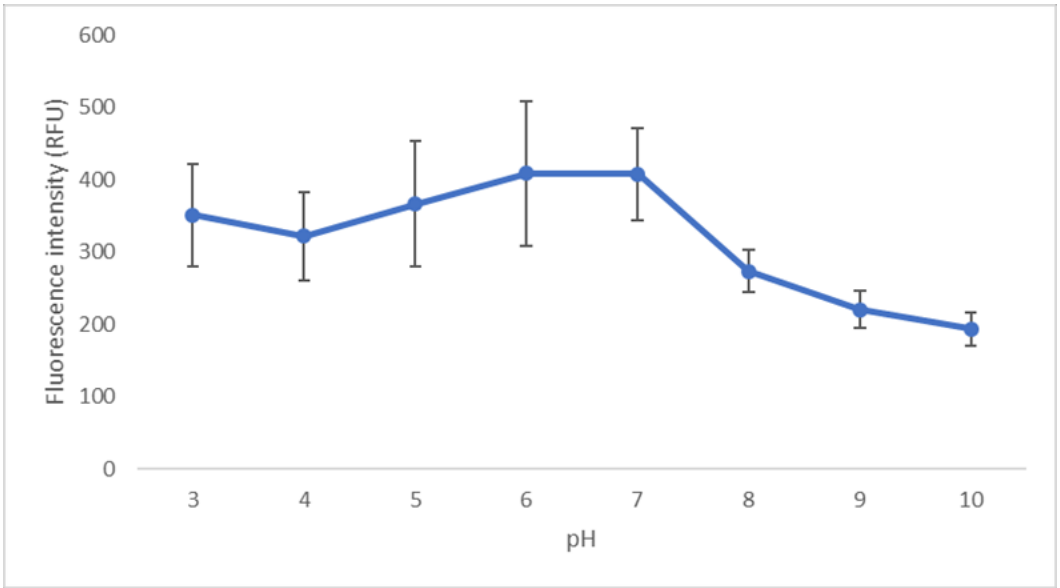

Figure 28 – Effect of pH change on the fluorescence intensity of the prepared PAMAM(NH_2)-RITC conjugates. The fluorescence intensity is presented as relative fluorescence units (RFU).

3.3. Cytotoxicity studies of PAMAM(NH_2)-RITC conjugates

Figures 29 and 30 show the cytotoxicity over hMSCs of non-conjugated and conjugated PAMAM dendrimers, respectively, as a function of concentration and time after an initial exposure period of 24 h. Results are presented as a percentage of cell viability in relation to the control (cells not exposed to the free dendrimers or conjugates). Cell viability was correlated with the metabolic activity of cells since the resazurin reduction assay was used. This method assumes that healthy metabolic active cells can convert the non-fluorescent resazurin molecule in a fluorescent product, resorufin, whereas non-viable cells cannot. Because both dyes are membrane-permeable, the resazurin can enter the cells and be reduced, while the product of this reduction, resorufin, can leave the cell through the plasma membrane and accumulate in the cell medium. So, after exposing the cells to free dendrimers or conjugates, the resazurin reagent was added to the cells, and left to incubate for a certain time. After, the fluorescence signal coming from the medium was measured using a microplate reader [165,166].

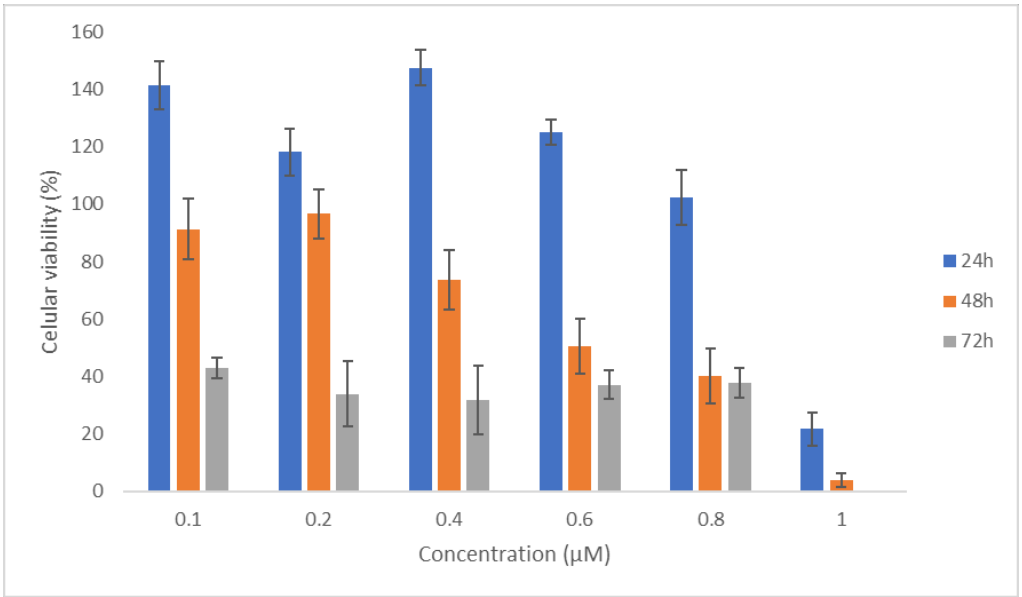

Figure 29– Cytotoxic behaviour of generation 4 PAMAM(NH_2) dendrimers over hMSCs. Each data set was plotted based on the mean and the corresponding relative standard deviation (RSD) of a single independent study with six replicates for each concentration.

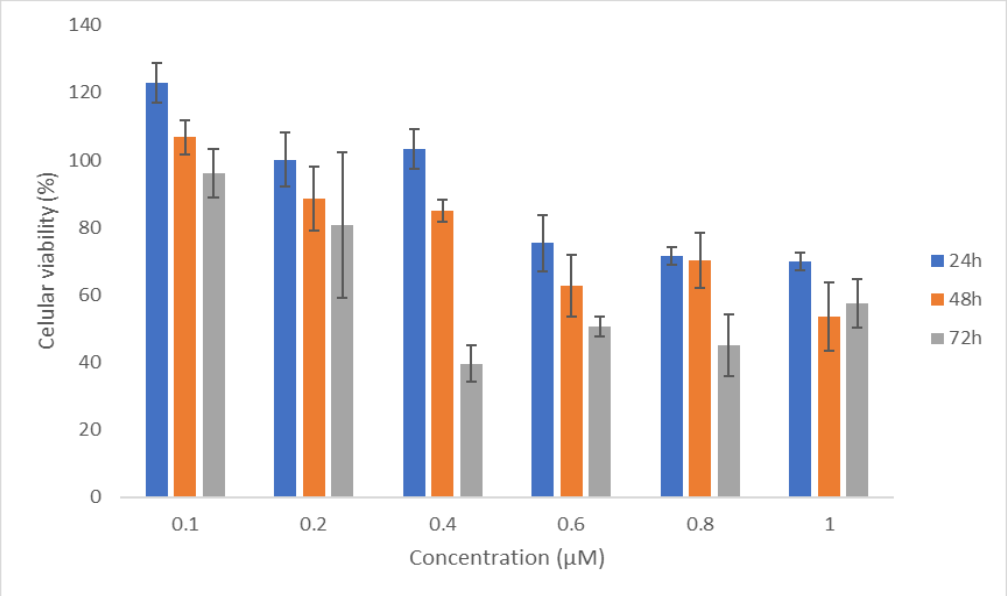

Figure 30 – Cytotoxic behaviour of PAMAM(NH_2)-RITC conjugates over hMSCs. Each data set was plotted based on the mean and the corresponding RSD of a single independent study with six replicates for each concentration.

Analysing figures 29 and 30, one can see that cytotoxicity increased with concentration and time after an initial exposure period of 24 h. Interestingly, there was a difference between the cytotoxic behaviour of the non-conjugated and conjugated PAMAM dendrimers. For all the concentrations tested, the non-conjugated dendrimer showed a much higher degree of cytotoxicity when compared to the dendrimer

conjugates. This may be due to dendrimer's amine termini that are protonated at physiological pH, leading to a strong positive charge in the molecule. The cells have negatively charged membranes, and when they are exposed to strongly positive molecules, such as cationic dendrimers, the difference in charge contributes for membrane destabilization, and consequently, to a higher cytotoxicity [167,168]. There are many reports in the literature highlighting the cytotoxicity behaviour of cationic PAMAM dendrimers and, also, referring different methodologies for decreasing their cytotoxicity. One possibility is to functionalize the dendrimer's surface and mask the positive charges [138]. For example, it has been reported that dendrimer's surface modification with polyethylenoglycol (PEG) chains results in a dramatic decrease of cytotoxicity [169]. Therefore, one can postulate that the presence of rhodamine at the dendrimer's surface acts in a similar way, reducing the dendrimer charge.

Based on these results, a concentration of 1 μM of conjugated dendrimer was used in the following studies, namely for the experiments related with the kinetics of cellular uptake, exosome loading and localization of conjugates inside cells. Indeed, this concentration was enough to give high fluorescence signals after the internalization of conjugates by cells without significantly affecting cell viability (higher than 60 % after 24h).

3.4. Kinetics of cell uptake of PAMAM(NH_2)-RITC conjugates

The intracellular components are protected from the external environment by the cytoplasmic membrane. The cell membrane is responsible for diverse important functions, such as cell homeostasis, ion concentration gradients, structural support, cell communication with the environment and entry/exit of nutrients and small molecules [170,171]. In nanomedicine, most of the nanomaterials must exert their therapeutic effect inside cells. However, the entry of nanoparticles in the cells remains a major challenge. Also, a more comprehensive understanding of nanoparticles uptake mechanisms is necessary for a better modulation of their physicochemical properties in order to achieve a higher efficiency and safety [172].

Before nanomaterials reach the cell membrane, they must first interact with the extracellular environment, like fibrosis, pH, extracellular matrix, and so on. This environment can induce some changes in the properties of nanomaterials. For instance, this interaction normally leads to the absorption of proteins in the surface of nanoparticles (the protein corona) affecting their interaction with the cytoplasmic membrane and

subsequently their intracellular distribution [173]. The capacity of nanoparticles to adhere and cross cell membranes is related to their physicochemical properties, such as size, charge and surface composition. Small and positive charged molecules, such as dendrimers with amine termini, are capable of crossing the cell membrane, where sometimes they can lead to membrane disruption and induce some cytotoxic effects [174].

As the main hypothesis of this thesis was to load exosomes with PAMAM(NH_2)-RITC conjugates before their isolation from cells, the kinetics of their cell uptake was studied. Cells were exposed to the conjugates at different times (6, 16, 24 and 30 h) and then lysed in a buffer to release their content. The fluorescence intensity due to conjugate internalization in cells was then measured using a microplate reader. The results are shown in Figure 31. In order to elucidate how dendrimers can increase the uptake of drugs, Goldberg *et al* [175] showed that PAMAM $G_{3.5}$-SN38 conjugates can enter Caco-2 cells more easily than free SN38, which showed only 5 % of the conjugates uptake. Therefore, one can see that with an increase of the exposure time, there is also an increase in the fluorescence signal, reaching a maximum at 24h. So, 24h of cell exposure to the PAMAM(NH_2)-RITC conjugates should be sufficient to apply in the exosome loading process.

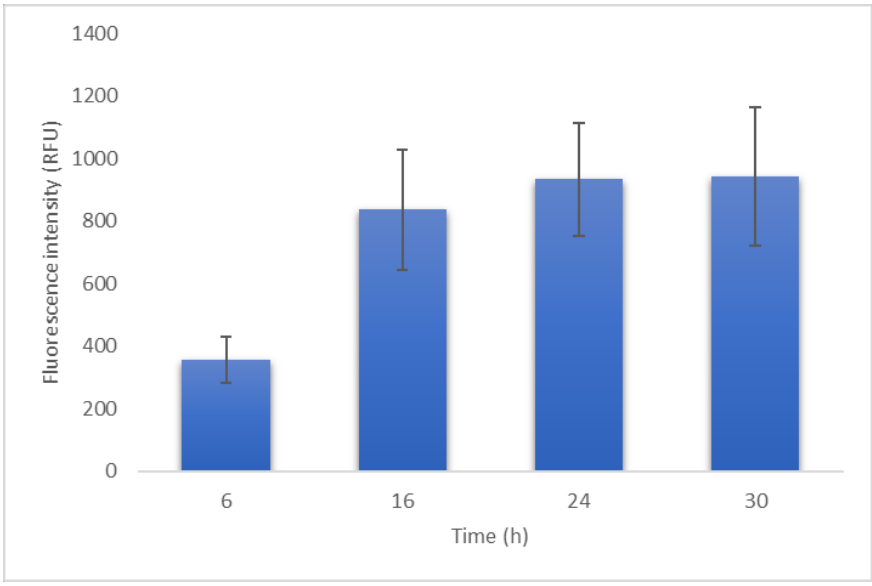

Figure 31 – Kinetics of cell uptake of PAMAM(NH_2)-RITC. hMSCs were exposed to conjugates during different times (6, 16, 24 and 30h). The fluorescence intensity is presented as relative fluorescence units (RFU).

Fluorescence microscopy was also used to follow the kinetics of conjugate cell uptake (Figure 32). First, using the bright field mode in the microscope, one could observe that cells had a healthy aspect, even after 72h of exposure to conjugates, which confirms that the conjugate concentration used was tolerable by cells. When using the fluorescence mode in the microscope, and in agreement with the quantitative results, one could see an increase with time of the red fluorescence signal coming from the internalized conjugates. Again, fluorescence intensity tended to stabilize after 24h of cell exposure to PAMAM(NH_2)-RITC conjugates. Curiously, as time passed, one noticed that the fluorescence signals seemed to be more concentrated in the cell perinuclear zone.

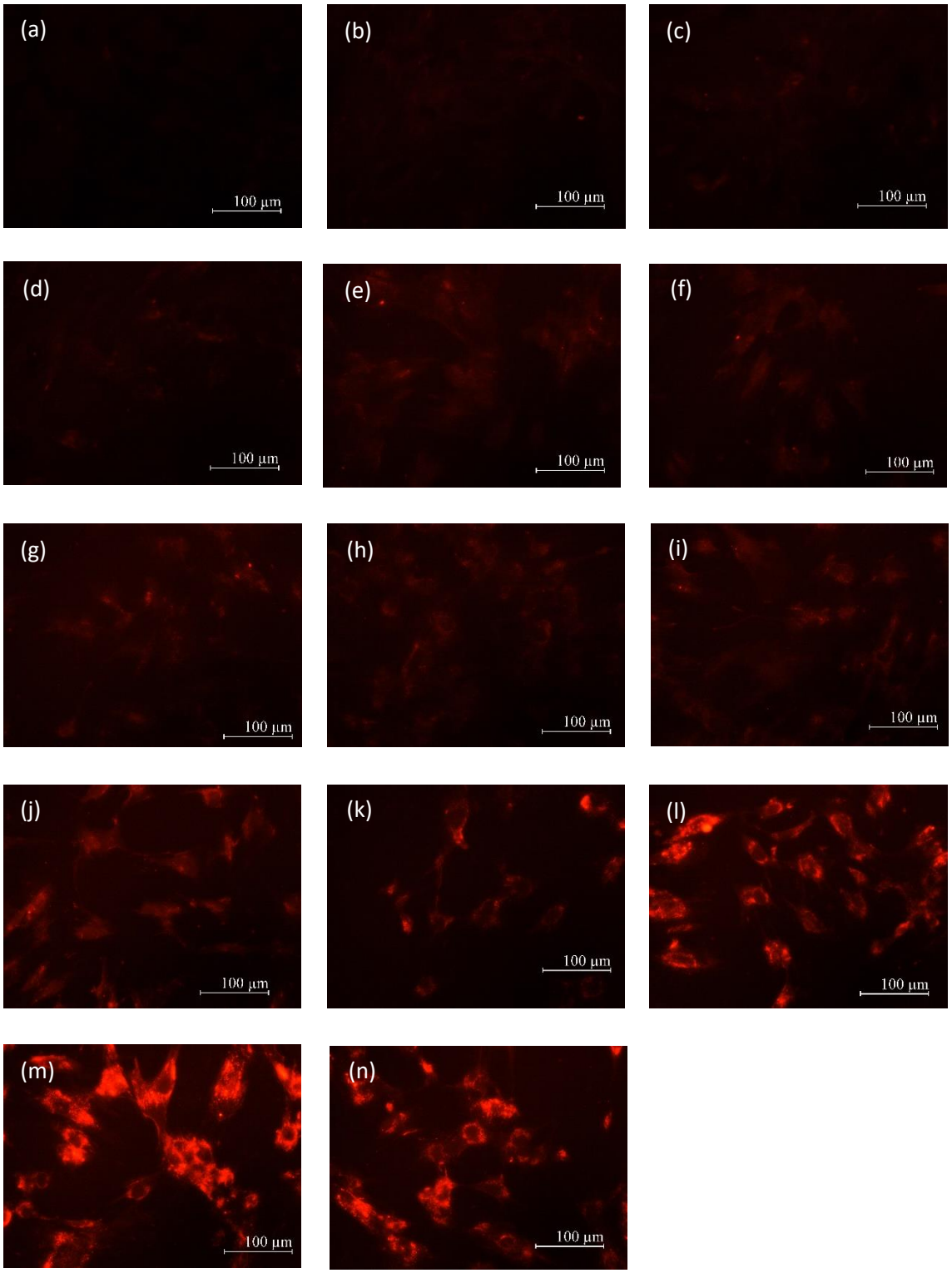

Figure 32 – Fluorescence microscopy images of hMSCs exposed to PAMAM(NH_2)-RITC conjugates during different times: a-30 min; b-1h; c-1h:30min; d-2h; e-3h; f-4h; g-5h; h-6h; i-7h; j-8h; k-12h; l-24h; m-48h; n-72h. All the images were taken with a magnification of 200 x.

3.5. Establishment of an exosome isolation protocol and exosome characterization

The advances in the understanding of the biological functions of exosomes have been unveiling the contribution of these vesicles for the physiological maintenance of the human body [176]. Consequently, the isolation of exosomes became a major area of interest, both in the field of research and clinical applications. Exosomes must be isolated in a reliably manner from diverse kinds of biofluids, like blood, urine and cerebrospinal fluid. As described in the introduction of this thesis in more detail, there are different techniques used for the isolation of exosomes, like ultracentrifugation, precipitation, immunoaffinity, microfluidics, among others. This thesis assumed as an initial hypothesis that exosomes could be loaded with the PAMAM(NH_2)-RITC conjugates before their isolation from cells by cell exposure to a solution containing these compounds. The cells would then excrete the exosomes into the cell culture medium. As such, a protocol to isolate exosomes from the cell culture medium had to be developed before further studies.

In this work and due to limitations of available equipment, a precipitation approach with a commercial reagent (*Total Exosome Isolation Reagent, from cell culture media*) was used for the isolation of exosomes. Typically, these commercial reagents contain a polymer that interferes with the solvent molecules (water in this case), thus forcing the less soluble components, like exosomes, to precipitate. The advantage of this method is that there is no need to use an ultracentrifuge to obtain the exosomes.

The guidelines for using the *Total Exosome Isolation Reagent* (see annex D), only include one centrifugation step before the use of the *Total Exosome Isolation Reagent* to obtain a pellet rich in exosomes: cell media is centrifuged at 2000 × g for 30 minutes to remove cells and debris. So, using this methodology, further purification steps (for example by affinity methods) would be required to get relatively pure exosomes. Having this is mind, it was decided to previously submit the cell culture media containing exosomes to a differential centrifugation process. That is, cell culture media was subjected to a series of centrifugation steps with increasing *g* forces and increasing centrifugation times: 300 x g for 10 min to remove cell debris; 2000 x g for 20 min to remove apoptotic bodies; and 10000 x g for 30 min to remove microvesicles. During these centrifugation steps, exosomes were always present in the supernatants. At the end, the last supernatant collected (already rich in exosomes) had to be mixed with half of its volume of *Total Exosome Isolation Reagent*.

In order to improve the exosome isolation protocol, the introduction of two other steps before addition of the commercial reagent to the exosome-containing medium was tested: (a) an early purification step (a filtration process using a 0.22 μm filter since exosomes have a size below 200 nm); (b) a concentration step (an ultrafiltration process using Centrifugal Filter Units with MWCO of 3 kDa in order to avoid the use of a large volume of *Total Exosome Isolation Reagent*,). In these experiments, NIH 3T3 cells were used for practical reasons related with their easy maintenance and fast proliferation in culture. The presence of exosomes in the final solutions was assessed using the Dynamic Light Scattering (DLS) technique since it gives information regarding the hydrodynamic size of particles. Results of these experiments are summarized in Figure 33 where the graphics show the hydrodynamic size distribution by intensity. The four plots in this figure always reveal the presence in the final solution of two families of particles having two distinct hydrodynamic diameters, represented by two peaks always clearly seen in the plots). Peak 1 can be attributed to the presence of the polymer in the *Total Exosome Isolation Reagent* together with other macromolecules from FBS (probably aggregates) or even small cell debris. Only the presence of the polymer cannot explain peak 1 since the analysis by DLS of the *Total Exosome Isolation Reagent* alone gives a peak around 3 nm (data in annex C). Peak 2 values are compatible with the characteristic size of exosomes. It is important to remember that, normally, exosome suspensions are very heterogenous in size, ranging from 50 to 150 nm [116]. Nevertheless, there are some studies, where the obtained exosome suspensions presented z-average values of 170 nm [55].

According to Figure 33, samples processed without the initial filtration and concentration steps presented the higher hydrodynamic diameter values and, also, the higher polydispersion index (PdI= 0.427). The introduction of a concentration step had an impact on the PdI value (PdI= 0.281) and resulted in smaller hydrodynamic diameter values. In case of samples processed with an initial filtration step, the concentration step also resulted in a diminishment of the polydispersion index (from PdI= 0.316 to PdI=0.214) and the measured hydrodynamic diameters. It seems, therefore, that DLS measurements in the more concentrated samples are more precise. For this reason, it was considered that a filtration step was not essential for the overall process of exosome isolation, whereas a concentration step would provide DLS measurements with higher quality. In addition, the concentration step has advantages as it is not necessary to use a larger volume of *Total Exosome Isolation Reagent*.

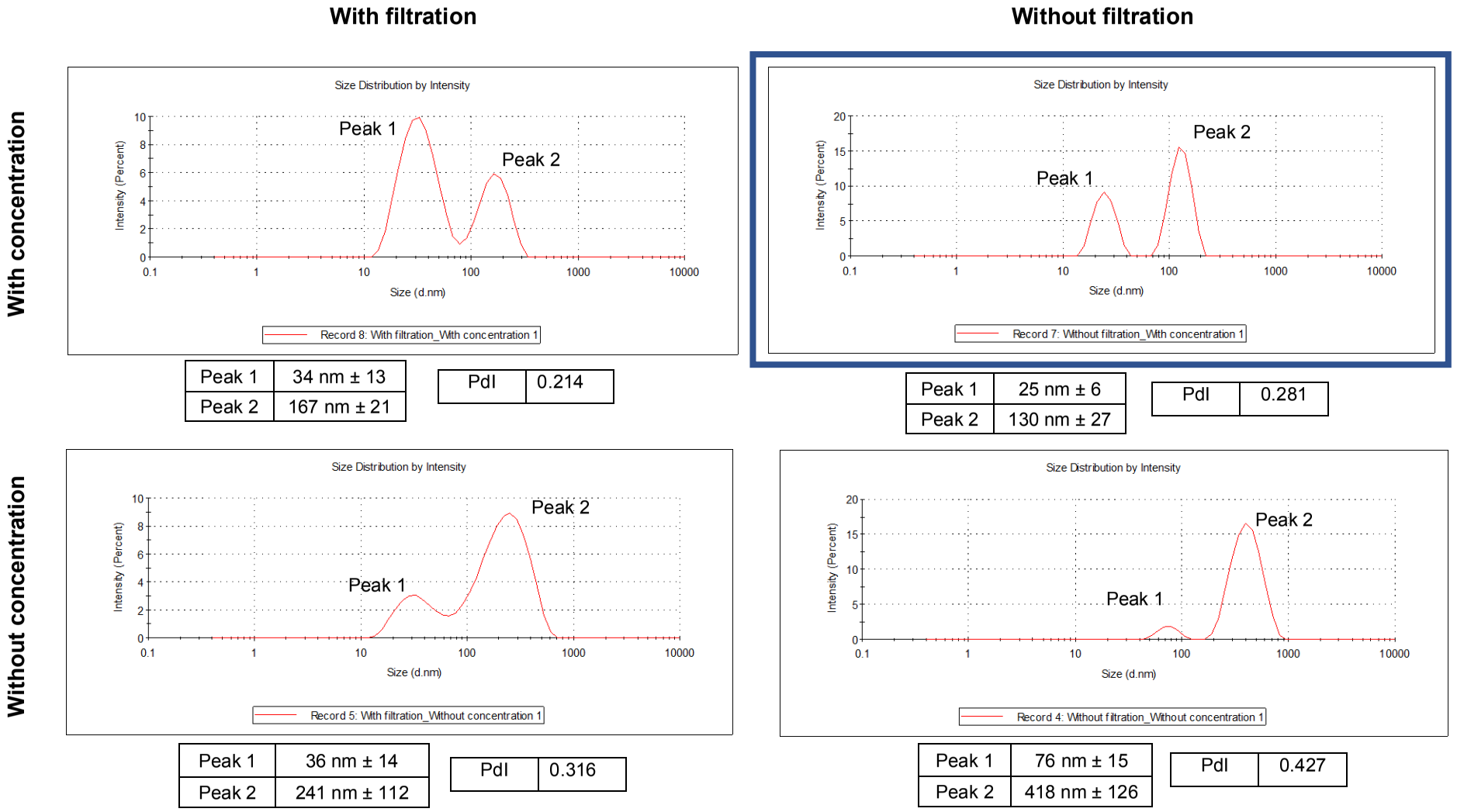

Peak 1	34 nm ± 13
Peak 2	167 nm ± 21

PdI	0.214

Peak 1	25 nm ± 6
Peak 2	130 nm ± 27

PdI	0.281

Peak 1	36 nm ± 14
Peak 2	241 nm ± 112

PdI	0.316

Peak 1	76 nm ± 15
Peak 2	418 nm ± 126

PdI	0.427

Figure 33 - Effect of the introduction of filtration and concentration steps in the protocol for exosome isolation from NIH 3T3 cells. The graphics obtained using the DLS technique show the hydrodynamic size distribution by intensity. The polydispersion (PdI) index is indicated.

A protocol to isolate exosomes from cell culture medium was then established that included a concentration step, which is schematized in Figure 34.

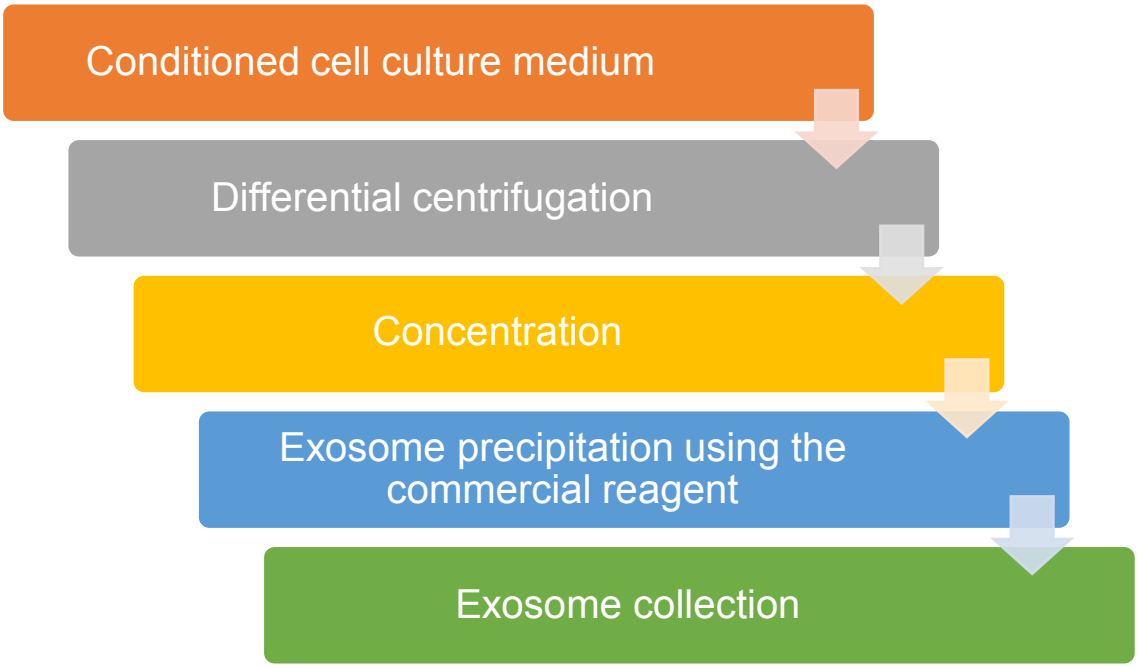

Figure 34 – Schematized protocol of the established exosome isolation protocol.

The influence of the storage temperature in the stability of exosome solutions was also evaluated. For this, hMSCs were used to produce exosome-containing solutions and exosomes were isolated following the previously established protocol. After obtainment of the exosome solutions, they were stored at different temperatures, namely 25ºC (room temperature), 4ºC, -20ºC and -80ºC for one week. Then, the hydrodynamic size of the particles in solution was once again evaluated using the DLS technique to assess the quality of the exosome solutions (Figure 35). As a control, exosomes analysed immediately after their isolation were used. Overall, the results demonstrated that exosomes can be stored for one week without relative changes in size even at room temperature. However, for longer periods of storage, it is obvious that they should be kept at -20/-80 ºC to prevent protein denaturation and microbial development.

Human mesenchymal stem cells present a high proliferative and immunosuppressive capacity, which makes them the ideal candidates for mass production of exosomes [90]. Since the aim of this thesis was to try to use exosomes from hMSCs as carriers for dendrimers, after establishing a protocol for exosome isolation, exosomes from hMSCs were isolated and characterized by DLS, TEM and detection of a biochemical marker, namely the acetylcholinesterase (AChE) enzyme.

Characterization of exosomes is important to confirm their presence at the end of the isolation process.

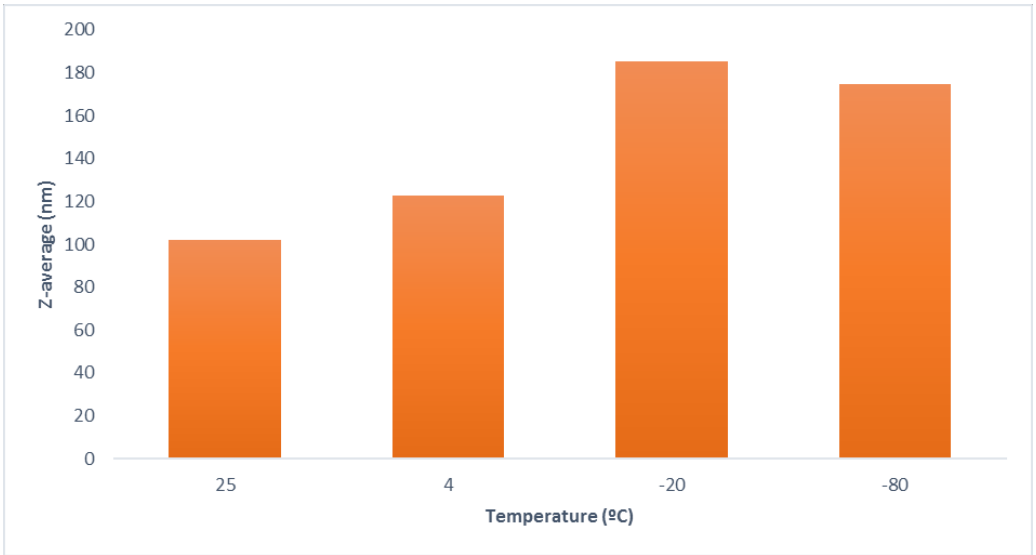

Figure 35 – Effect of storage temperature in the hydrodynamic size (Z-average) of the exosome solutions. Samples were analysed after being stored for 1 week.

Figure 36 represents the DLS analysis showing the hydrodynamic size distribution (by intensity) of the exosome solution isolated from hMSCs culture medium. Like it was seen for exosomes derived from NIH 3T3 cells, two populations of particles are evident in the plot: one with a peak around 25 nm (again this can be attributed to the presence of the reagent polymer together with other macromolecules from FBS or even small cell debris); and another one with a peak around 200 nm that should correspond to exosomes. It must be noticed that a relatively high PdI (0.563) was associated with this analysis, possibly revealing a higher heterogeneity nature of hMSCs exosomes when compared with NIH 3T3 exosomes.

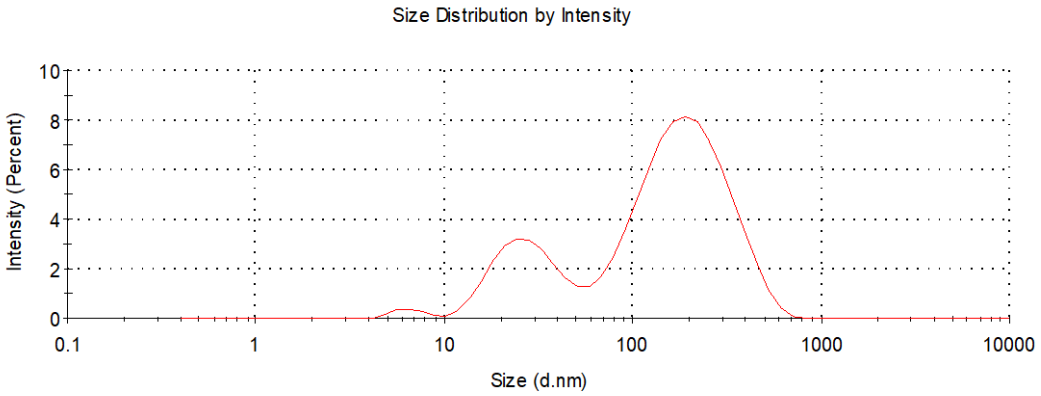

Figure 36 – Characterization of exosomes derived from hMSCs by DLS. The graphic shows the hydrodynamic size distribution by intensity.

Figure 37 is a micrograph from the exosome solution obtained by TEM analysis. The sample was stained with uranyl acetate that corresponds to the darker areas in the image. White circular spots, with and average diameter of 30-50 nm, can be seen and possibly correspond to exosomes due to their spherical morphology and size. They present a small size in comparison to the values determined by DLS since here they are in a dry state, whereas the size in DLS refers to their hydrodynamic diameter. Also, and like it was mentioned before, exosome suspensions are very heterogenous, and the image only represents a small observation field of the grid. Probably, if the grid was intensely analysed, other exosomes with different sizes would be found. Several reports in the literature show exosome images obtained using TEM where the size of these structures is around 50 nm or even less as exosomes tend to collapse upon drying [177]. The small white points in the image should correspond to the reagent polymer together with other macromolecules from FBS or small cell debris.

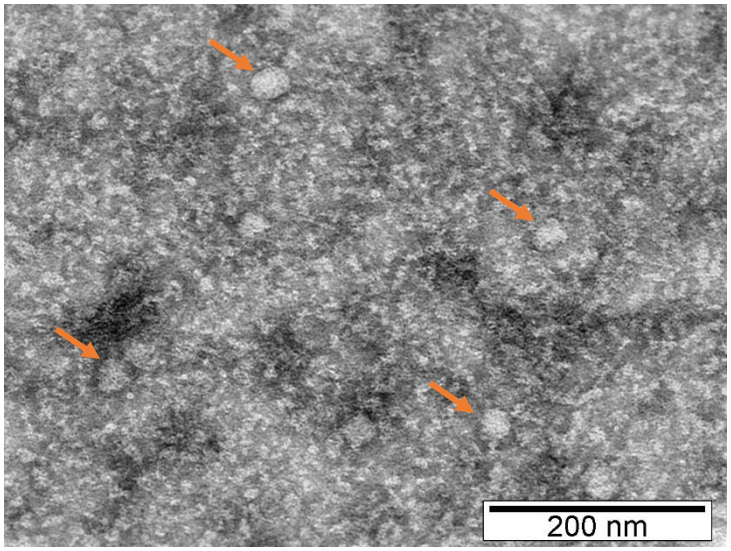

Figure 37 – Transmission electron microscopy image of a negative stained hMSCs exosome solution. The arrows point to white circular cup-shaped vesicles, exosomes.

Exosome presence was also validated by measuring the activity of acetylcholinesterase, according to the method of Savina *et al* [146]. AChE is an enzyme specific to exosomes [178] and, by analysis of Figure 38, one can see that AChE activity was much higher when analysing the exosome solution than in the control solution.

In conclusion, taken together, the exosome characterization results point out that the protocol established for exosome isolation was successful, independently of the cell source used.

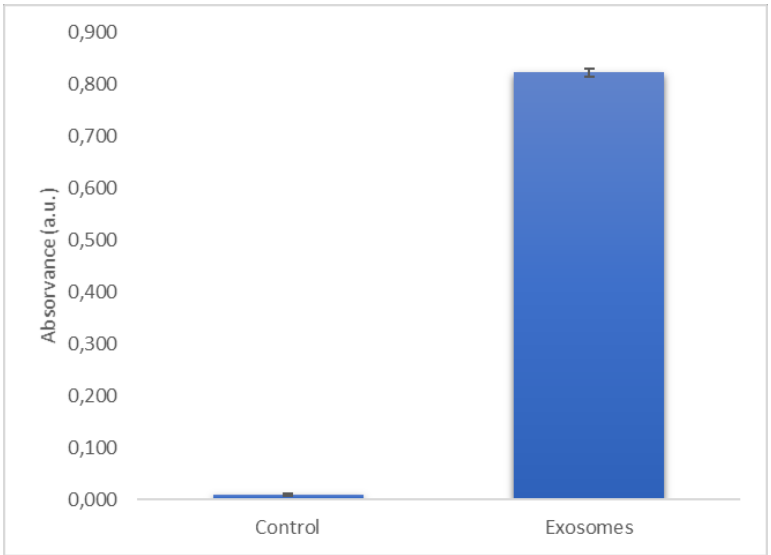

Figure 38 – Acetylcholinesterase assay of the exosome suspension obtained from hMSCs cells cell culture medium. Control used was based in the isolation from cell culture medium with no cells.

3.6. Exosome loading with PAMAM(NH_2)-RITC conjugates

After confirming that the PAMAM(NH_2)-RITC conjugates could be internalized by cells and after designing a successful protocol for recovering exosomes from cell culture medium, the following step was to try to obtain exosomes loaded with the conjugates only by subjecting hMSCs to their presence – that is, to load exosomes before their isolation from cells. As such, cells were exposed to PAMAM(NH_2)-RITC conjugates for 24h, washed with PBS and then cultured for more 48h. Next, the exosomes were isolated, lysed and fluorescence intensity was measured to check the presence of the conjugates. Simultaneously, as the conjugates could also be released inside microvesicles, an additional study was performed where cells passed through a process of activation to increase the production of microvesicles. For this, the microvesicle fraction was collected by differential centrifugation and analysed following the same methodology used for exosomes. In opposition to what was expected, the fluorescence intensity in all measured samples was close to zero, meaning that the conjugates were not present inside exosomes or microvesicles. Observation of microvesicles by fluorescence microscopy confirmed this finding (Figure 39).

Bright Field Red Filter Merged

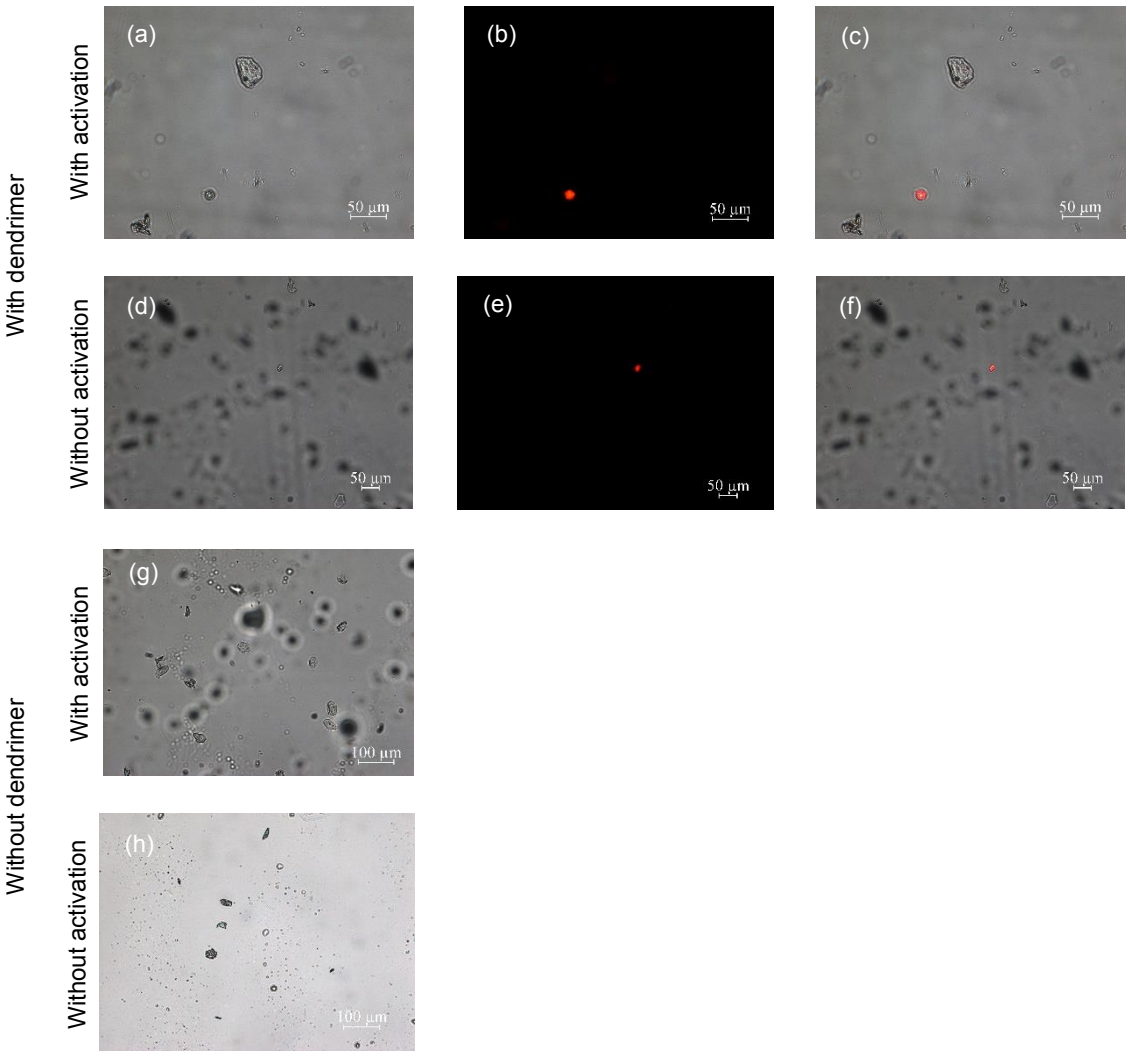

Figure 39 – Fluorescence microscopy images of the PAMAM(NH_2)-RITC conjugates inside microvesicles. These images are only of the microvesicles, because exosomes are not detectable with this kind of microscopy.

To elucidate the reason why the conjugates were retained inside the cell, it is crucial to understand some aspects regarding the intracellular trafficking of nanomaterials, and how they can affect their excretion by cells. According to Panyam *et al*. [179], there are two possible recycling processes for nanomaterials, one by the endosomes and other by the lysosomes/cytoplasm. So, after endocytosis, one part of the nanoparticles is delivered to the lysosomes or translocated from the endosomes to the cytoplasm, whereas the other part remains inside the endosomes or is recycled back to the cell surface (see Figure 40). As for the exocytosis of nanoparticles, it seems that at least two intracellular compartments are involved, one with a fast turnover and another one with a slow turnover. The velocity of this turnover appears to be related to some physical properties of the nanoparticles, such as the size [180,181]. For example, Cartiera *et al.* [182] showed that PLGA nanoparticles appear to be localized in early

endosomes, Golgi apparatus and Endoplasmic reticulum, which are slow recycling compartments.

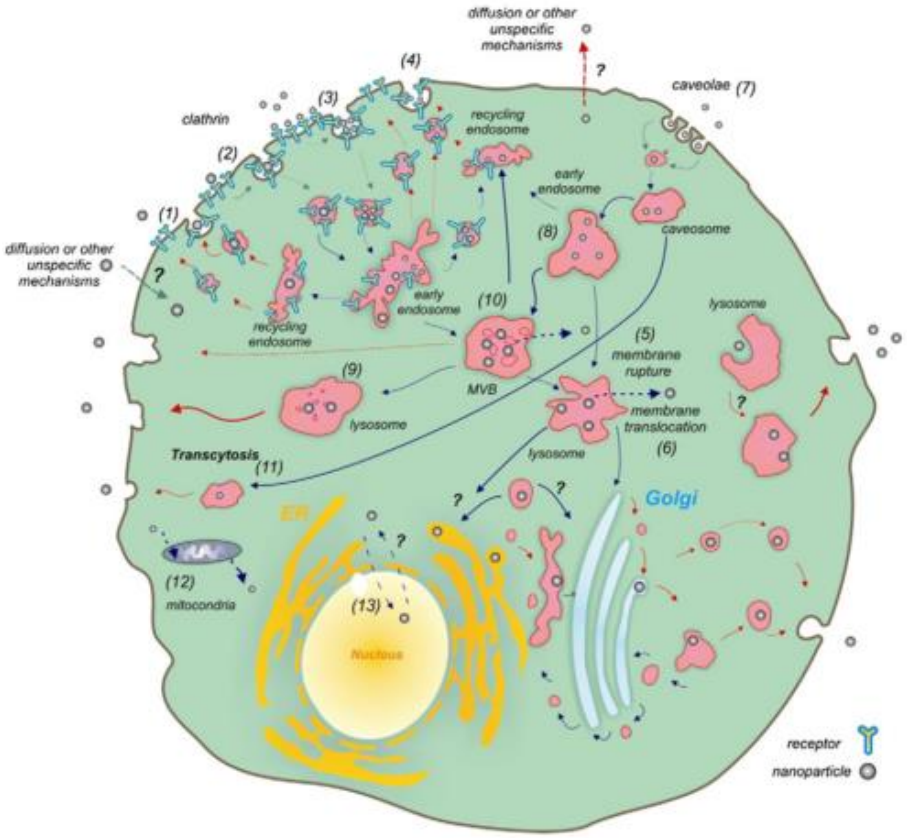

Figure 40 – Scheme showing the cellular excretion processes of nanoparticles (red arrows) along with their intracellular trafficking (blue arrows) and endocytosis mechanisms (green arrows). Figure adapted from reference [183].

3.7. Intracellular distribution of PAMAM(NH2)-RITC conjugates

Endocytosis is responsible for the transport of nanoparticles inside the cell through vesicles. Depending on their internalization route, nanomaterials can either be recycled and secreted from the cell through exocytosis, or trafficked to organelles, like lysosomes, Golgi complex and mitochondria (Figure 41).

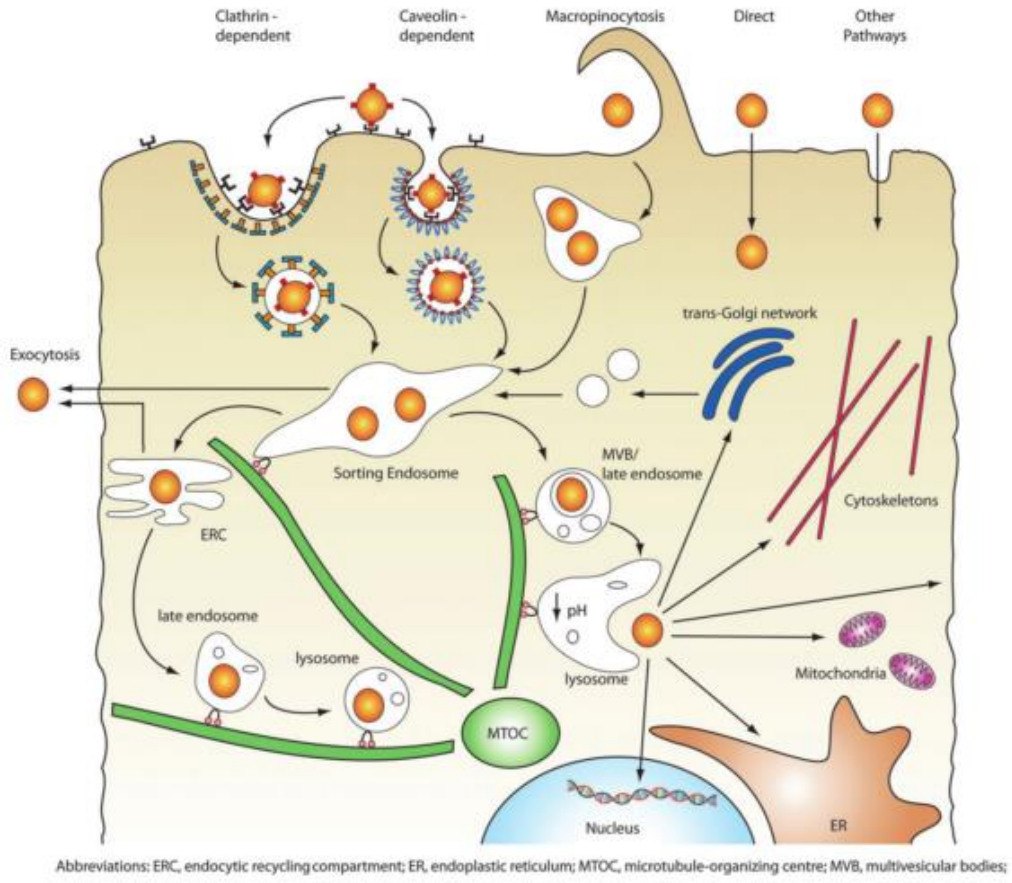

Figure 41 – Intracellular transport of nanoparticles. Figure adapted from reference [184].

The retention of nanomaterials inside vesicles is undesirable, because the maturation of vesicles into late endosomes and lysosomes is accomplished with a rapid acidification, with a pH decreasing from 6 to 4, and the recruitment of enzymes responsible for the degradation of the vesicular content. Polymers with amino groups, like PAMAM dendrimers, are known to escape from endosomes and lysosomes through the “proton-sponge effect” (Figure 42). In this effect, the polymer absorbs protons, inducing osmotic swelling of the endosome and, subsequently, its rupture [185,186].

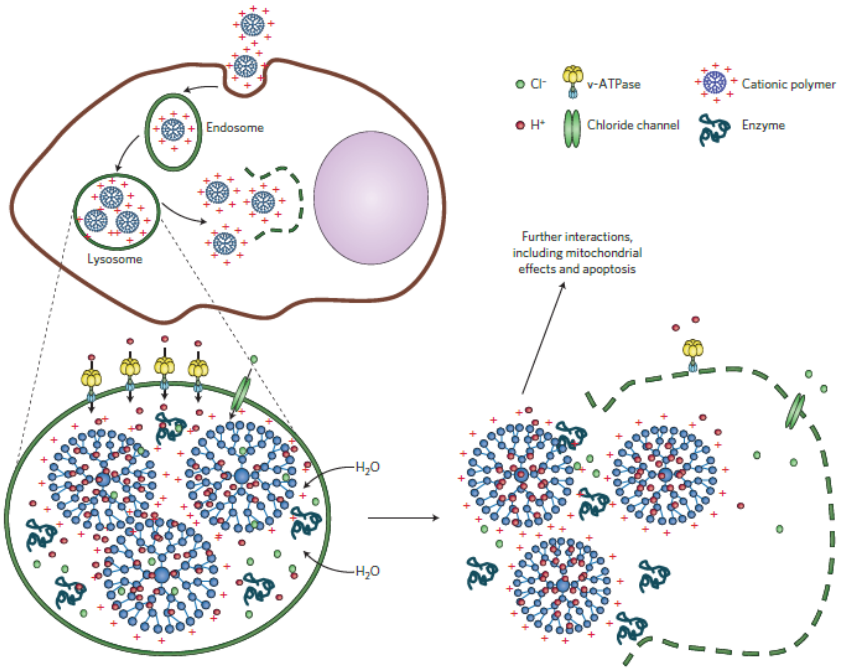

Figure 42 – Illustration of the proton sponge effect, leading to endosome and lysosome escape. Cationic polymers, like PAMAM(NH_2) dendrimers, are capable of sequestering protons by their amino groups. This process keeps the v-ATPase (proton pump) working, which leads to the retention of one Cl^- ion and one water molecule per proton. Subsequently, this results in the rupture of the endosome or lysosome, and in the spillage and deposition of the particles in the cytoplasm. Figure adapted from reference [187].

Once released from the endolysosomal compartments, nanoparticles must travel through the cytoplasm, to reach the target, and have the desired biological response. However, little is known about the intracellular transport of nanoparticles. Researchers are trying to answer this question using different fluorescent probes and proteins, to study the intracellular transport of nanoparticles using multicolour fluorescence imaging [188]. So, in this study, since no PAMAM(NH_2)-RITC conjugates were detected in the exosomes released by cells exposed to their presence, we were interested in knowing the localization/accumulation of the conjugates inside cells. To achieve this purpose, cells were exposed to the conjugates and were analysed using fluorescence microscopy and different fluorescent probes. MCF-7 cells were used in these studies for practical reasons.

Previously, during the conjugate uptake studies, accumulation of conjugates in the cell perinuclear region was already observed. As such, fluorescent probes for the endoplasmic reticulum and Golgi complex were used to see if there was co-localization of conjugates with these cellular structures since these are the organelles localized in that region of the cell. The results are exposed in Figure 43 and are coherent to the hypothesis that the PAMAM(NH_2)-RITC conjugates accumulate in these cellular

structures. One can find some studies in the literature regarding the localization of nanoparticles inside cells. For example, Oddone *et al*. [149] showed that PAMAM-FITC conjugates demonstrated a similar perinuclear distribution in 4T1 breast tumour cells. Greulich *et al*. [186] demonstrated that silver nanoparticles presented also a perinuclear distribution in hMSCs but they were co-localized with the endo-lysosomal compartments and not with Golgi apparatus or endoplasmic reticulum. This shows that the intracellular distribution of nanoparticles is a very complex topic, depending on diverse factors, such as the properties of the nanomaterial.

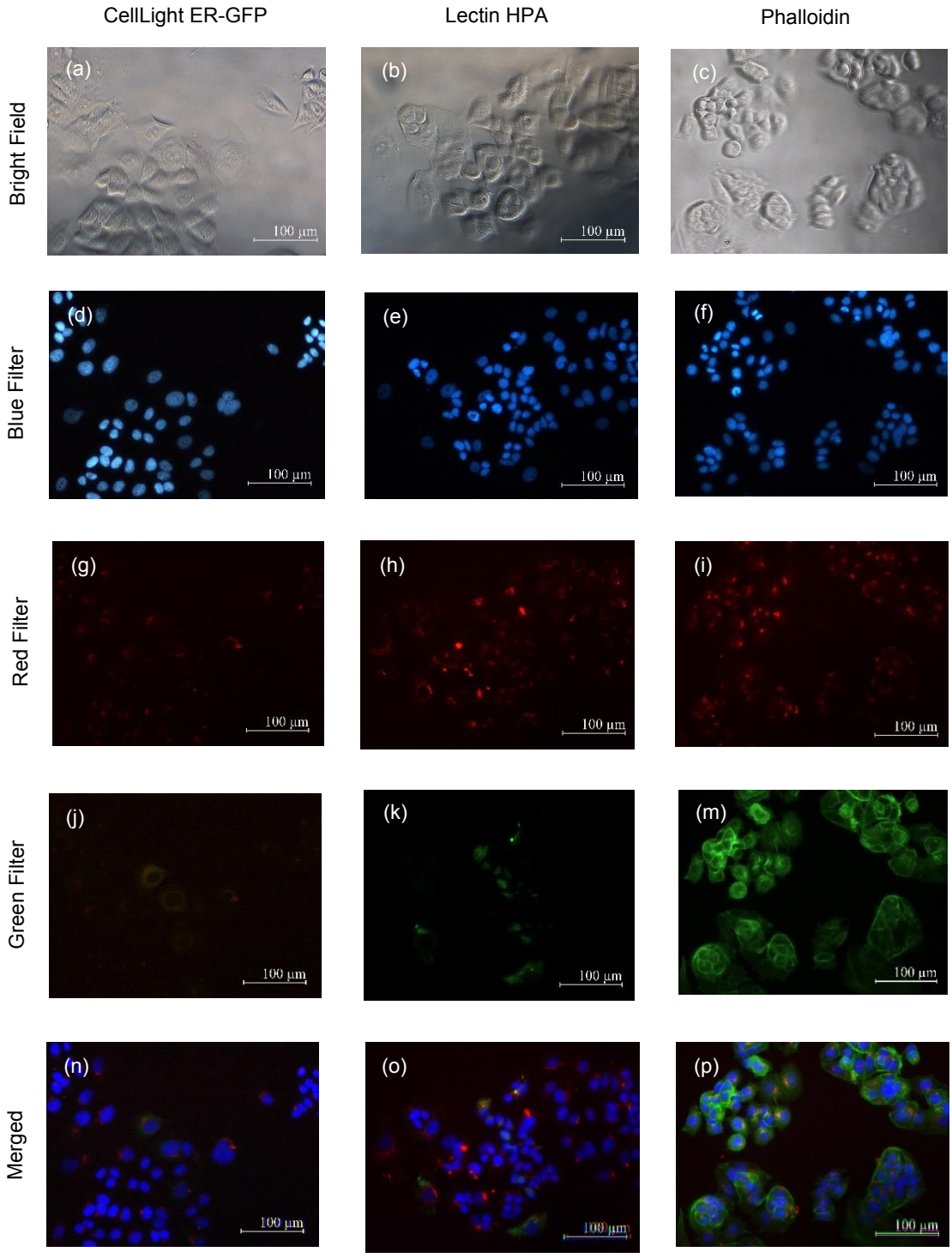

Figure 43 – Co-localization and intracellular distribution of the PAMAM(NH_2)-RITC conjugates in a MCF-7 cell line. CellLightER-GFP is responsible for staining of endoplasmic reticulum (green fluorescent colour), Lectin HPA for staining of Golgi apparatus (green fluorescent colour) and Phalloidin for Actin (microtubules) (green fluorescent colour) staining. The red fluorescence emission comes from the RITC and the blue colour from DAPI staining.

Part 4. Conclusions and Future Work

Conclusions and Future Work

Exosomes are considered a powerful tool in the bio- and nanomedicine fields. They can be used as biomarkers for several diseases, as well as for the inclusion of therapeutic cargo for treatment of several pathologies. However, they are still not very well understood and research about their biogenesis, properties and applications is greatly justified.

In this thesis, the possibility of using exosomes derived from hMSCs as vehicles for dendrimers, namely of generation 4 (G4) poly(amidoamine) dendrimers with amino termini (PAMAM(NH2)), was explored. In particular, the hypothesis that exosomes could be loaded before their isolation from cells by simple cell exposure to a dendrimer-containing solution was evaluated. Although, at the end, it was concluded that dendrimers accumulated in the cell perinuclear zone and were not excreted inside exosomes as expected, the following achievements were fulfilled:

a) PAMAM(NH_2)-RITC conjugates were successfully prepared and characterized, being possible to determine accurately the number of fluorochromes linked to the dendrimer;
b) the effect of pH in the stability of fluorescence emission of the PAMAM(NH_2)-RITC conjugates was studied showing that one can use RITC as a fluorochrome to track nanomaterials inside cells as its fluorescence intensity resists to acidic environments; the conjugation with the dendrimer did not affect the RITC fluorescence behaviour;
c) the cytotoxicity of the PAMAM(NH_2)-RITC conjugates was evaluated using hMSCs in culture; interestingly, the conjugation with RITC decreased the cytotoxicity of the dendrimer;
d) the kinetics of PAMAM(NH_2)-RITC conjugate cell uptake was studied revealing that a maximum in its cellular content was reached after 24h of culture;
e) an exosome isolation protocol was established using a precipitation-based approach and the isolated exosomes were successfully characterized by DLS, TEM and acetylcholinesterase (AChE) activity;
f) the localization/accumulation of the PAMAM(NH_2)-RITC conjugates inside cells was analyzed revealing a co-localization with the Golgi complex and the endoplasmic reticulum.

In the future, it will be necessary to make a deeper characterization of the isolated exosomes with the use of other techniques, such as Tunable Resistive Pulse Sensing (TRPS), flow cytometry, Western-Blotting, Atomic Force Microscopy (AFM), etc., and fully accomplish the requirements imposed by ISEV for the characterization of these vesicles. Also, it would be very interesting to explore the use of other nanomaterials for incorporation in different sets of EVs, such as exosomes and microvesicles.

References

References

1. Vader P, Breakefield XO, Wood MJA. Extracellular vesicles: Emerging targets for cancer therapy. Trends Mol Med 2014;20:385–393.

2. Raposo G, Stoorvogel W. Extracellular vesicles: Exosomes, microvesicles, and friends. J Cell Biol 2013;200:373–383.

3. Kalra H, Drummen G, Mathivanan S. Focus on Extracellular Vesicles: Introducing the Next Small Big Thing. Int J Mol Sci 2016;17:170.

4. Lai RC, Yeo RWY, Tan KH, Lim SK. Exosomes for drug delivery - A novel application for the mesenchymal stem cell. Biotechnol Adv 2013;31:543–551.

5. Jang SC, Kim SR, Yoon YJ, Park KS, Kim JH, Lee J, et al. In vivo kinetic biodistribution of nano-sized outer membrane vesicles derived from bacteria. Small 2015;11:456–461.

6. Ha D, Yang N, Nadithe V. Exosomes as therapeutic drug carriers and delivery vehicles across biological membranes: current perspectives and future challenges. Acta Pharm Sin B 2016;6:287–296.

7. Turturici G, Tinnirello R, Sconzo G, Geraci F. Extracellular membrane vesicles as a mechanism of cell-to-cell communication: advantages and disadvantages. Am Physiological Soc 2014;306:621-633.

8. Elmore S. Apoptosis: A Review of Programmed Cell Death. Toxicol pathol 2007;35:495-516.

9. Taylor, Rebecca C, Sean P, Martin, Seamus J. Apoptosis is a mode of cell death that is used by multi- cellular organisms to dispose of unwanted cells in a diversity of settings. Nat Rev Mol Cell Bio 2008;9:231-241.

10. Martínez MC, Freyssinet JM. Deciphering the plasma membrane hallmarks of apoptotic cells: Phosphatidylserine transverse redistribution and calcium entry. BMC Cell Biol 2001;2:20.

11. Erwig LP, Henson PM. Clearance of apoptotic cells by phagocytes. Cell Death Differ 2008;15:243–250.

12. Akers JC, Gonda D, Kim R, Carter BS, Chen CC. Biogenesis of extracellular vesicles (EV): exosomes, microvesicles, retrovirus-like vesicles, and apoptotic bodies. J Neuro-Oncol 2013;113:1-11.

13. Cocucci E, Racchetti G, Meldolesi J. Shedding microvesicles: artefacts no more. Trends Cell Biol 2009;19:43-51.

14. Leventis PA, Grinstein S. The Distribution and Function of Phosphatidylserine in Cellular Membranes. Annu Rev Biophys 2010;39:407–427.

15. Muralidharan-Chari V, Clancy J, Plou C, Romao M, Chavrier P, Raposo G. Article ARF6-Regulated Shedding of Tumor Cell-Derived Plasma Membrane Microvesicles. Curr Biol 2009;19:1875–1885.

16. Muralidharan-Chari V, Clancy JW, Sedgwick A, D'Souza-Schorey C. Microvesicles: mediators of extracellular communication during cancer progression. J Cell Sci 2010;123:1603–1611.

17. Harding C, Heuser J, Stahl P. Receptor-mediated Endocytosis of Transferrin and of the Transferrin Receptor in Rat Reticulocytes Recycling. J Cell Biol 1983;97:329–339.

18. Johnstone RM, Adam M, Hammond JR, Orr L, Turbide C. Vesicle formation during reticulocyte maturation. Association of plasma membrane activities with released vesicles (exosomes). J Biol Chem 1987 262:9412–9420.

19. Ludwig A-K, Giebel B. Exosomes: Small vesicles participating in intercellular communication. Int J Biochem Cell Biol 2012 44:11–15.

20. Marcus ME, Leonard JN. FedExosomes: Engineering therapeutic biological nanoparticles that truly deliver. Pharmaceuticals 2013;6:659–680.

21. Qin J, Xu Q. Functions and application of exosomes. Acta Pol Pharm 2014; 71:537-543.

22. Urbanelli L, Magini A, Buratta S, Brozzi A, Sagini K, Polchi A. Signaling Pathways in Exosomes Biogenesis, Secretion and Fate. Genes 2013;4:152–170.

23. Katzmann DJ, Odorizzi G, Emr SD. Receptor Downregulation and Multivesicular-Body Sorting. Nat Rev Mol Cell Biol 2002;3:893.

24. Raiborg C, Rusten E, Stenmark H. Protein sorting into multivesicular endosomes. Curr Opin Cell Biol 2003;15:446–455.

25. Vlassov A V., Magdaleno S, Setterquist R, Conrad R. Exosomes: Current knowledge of their composition, biological functions, and diagnostic and therapeutic potentials. Biochim Biophys Acta - Gen Subj 2012;1820:940–948.

26. Johnsen KB, Gudbergsson JM, Skov MN, Pilgaard L, Moos T, Duroux M. A comprehensive overview of exosomes as drug delivery vehicles - Endogenous nanocarriers for targeted cancer therapy. Biochimica et Biophysica Acta - Reviews on Cancer 2014;1846:75-87.

27. Andaloussi S, Lakhal S, Mäger I, Wood MJA. Exosomes for targeted siRNA delivery across biological barriers. Adv Drug Deliver Rev 2013;65: 391-397.

28. Colombo M, Raposo G, Théry C. Biogenesis, Secretion, and Intercellular Interactions of Exosomes and Other Extracellular Vesicles. Annu Rev Cell Dev Biol 2014;30:255–289.

29. Otaegui D, Krämer-Albers EM, Mongini C, Toro DJ, Toro J, Herschlik L. Emerging roles of exosomes in normal and pathological conditions: new insights for diagnosis and therapeutic applications. Front immunol 2015;6:203-215;

30. Ekström K, Valadi H, Ekström K, Bossios A, Sjöstrand M, Lee JJ. Exosome-mediated transfer of mRNAs and microRNAs is a novel mechanism of genetic exchange between cells. Nat Cell Biol 2007;9:654-659.

31. Kucharzewska P, Christianson HC, Welch JE, Svensson KJ, Fredlund E, Ringnér M, et al. Exosomes reflect the hypoxic status of glioma cells and mediate hypoxia-dependent activation of vascular cells during tumor development. Proceedings of the National Academy of Sciences 2013,110: 7312-7317.

32. Rosenberg DW, Yang S, Pleau DC, Greenspan EJ, Stevens RG, Rajan T V. Mutations in BRAF and KRAS Differentially Distinguish Serrated versus Non-Serrated Hyperplastic Aberrant Crypt Foci in Humans. Cancer research 2007;8:3551–3555.

33. Corcoran C, Friel AM, Duffy MJ, Crown J, O'Driscoll L. Intracellular and extracellular microRNAs in breast cancer. Clin Chem 2011;57:18–32.

34. Nilsson J, Skog J, Nordstrand A, Baranov V, Mincheva-Nilsson L, Breakefield X. Prostate cancer-derived urine exosomes: a novel approach to biomarkers for prostate cancer. Br J Cancer 2009;100:1603–1617.

35. Li J, Sherman-Baust CA, Tsai-Turton M, Bristow RE, Roden RB, Morin PJ. Claudin-containing exosomes in the peripheral circulation of women with ovarian cancer. BMC cancer 2009;9:244-255.

36. Iraci N, Leonardi T, Gessler F, Vega B. Focus on Extracellular Vesicles : Physiological Role and Signalling Properties of Extracellular Membrane Vesicles.

Int J Mol Sci 2016;17:171.

37. Lötvall J, Hill AF, Hochberg F, Buzás EI, Di Vizio D, Gardiner C. Minimal experimental requirements for definition of extracellular vesicles and their functions: a position statement from the International Society for Extracellular Vesicles. J Extracell vesicles 2014;3:26913.

38. Khatun Z, Bhat A, Sharma S, Sharma A. Elucidating diversity of exosomes: biophysical and molecular characterization methods. Nanomedicine 2016;11:2359–2377.

39. Zarovni N, Corrado A, Guazzi P, Zocco D, Lari E, Radano G. Integrated isolation and quantitative analysis of exosome shuttled proteins and nucleic acids using immunocapture approaches. Methods 2015;87:46-58.

40. Rechavi O, Erlich Y, Amram H, Flomenblit L, Karginov F V, Goldstein I. Cell contact-dependent acquisition of cellular and viral nonautonomously encoded small RNAs. Gene Dev 2009;23:1971-1979.

41. Yamashita T, Takahashi Y, Nishikawa M, Takakura Y. Effect of exosome isolation methods on physicochemical properties of exosomes and clearance of exosomes from the blood circulation. Eur J Pharm Biopharm 2016;98:1-8.

42. Zeringer E, Barta T, Li M, Vlassov A V. Strategies for Isolation of Exosomes. Cold Spring Harb Protoc 2015;4:319-323.

43. Kim DK, Nishida H, An SY, Shetty AK, Bartosh TJ, Prockop DJ. Chromatographically isolated CD63 extracellular vesicles from mesenchymal stromal cells rescue cognitive impairments after TBI. PNAS 2015;113:170-175.

44. Batrakova E V., Kim MS. Using exosomes, naturally-equipped nanocarriers, for drug delivery. J Control Release 2015;219:396–405.

45. Valadi H, Ekström K, Bossios A, Sjöstrand M, Lee JJ, Lötvall JO. Exosome - mediated transfer of mRNAs and microRNAs is a novel mechanism of genetic exchange between cells. Nat Cell Biol 2007;9:654-659.

46. Yáñez-Mó M, Barreiro O, Gordon-Alonso M, Sala-Valdés M, Sánchez-Madrid F. Tetraspanin-enriched microdomains: a functional unit in cell plasma membranes. Trends Cell Biol 2009;19:434–446.

47. Tauro BJ, Greening DW, Mathias RA, Ji H, Mathivanan S, Scott AM. Comparison of ultracentrifugation, density gradient separation, and immunoaffinity capture

methods for isolating human colon cancer cell line LIM1863-derived exosomes. Methods 2012;56:293–304.

48. Davies RT, Kim J, Jang SC, Choi E-J, Gho YS, Park J. Microfluidic filtration system to isolate extracellular vesicles from blood. Lab Chip 2012;12:5202.

49. Lee K, Shao H, Weissleder R, Lee H. Acoustic Purification of Extracellular Microvesicles. ACS nano, 2015;9:2321-2327.

50. Chen C, Skog J, Hsu C-H, Lessard RT, Balaj L, Wurdinger T. Microfluidic isolation and transcriptome analysis of serum microvesicles. Lab Chip 2010;10:505-511.

51. Liga A, Vliegenthart ADB, Oosthuyzen W, Dear JW, Kersaudy-Kerhoas M. Exosome isolation: a microfluidic road-map. Lab Chip 2015;15:2388–2394.

52. Parasassi T, De Spirito M, Mei G, Brunelli R, Greco G, Lenzi L. Low density lipoprotein misfolding and amyloidogenesis. The FASEB Journal 2008;22:2350-2356.

53. Maulucci G, De Spirito M, Arcovito G, Boffi F, Castellano AC, Briganti G. Particle Size Distribution in DMPC Vesicles Solutions Undergoing Different Sonication Times. Biophys J 2005;88:3545–3550.

54. Palmieri V, Lucchetti D, Gatto I, Maiorana A, Margherita, Marcantoni M, Maulucci G, Papi M, Pola R, Spirito M, Sgambato A. Dynamic light scattering for the characterization and counting of extracellular vesicles: a powerful noninvasive tool. J Nanopart Res 2014;16:2583.

55. Atay S, Gercel-Taylor C, Kesimer M, Taylor DD. Morphologic and proteomic characterization of exosomes released by cultured extravillous trophoblast cells. Exp Cell Res 2011;317:1192–1202.

56. Lawrie AS, Albanyan A, Cardigan RA, Mackie IJ, Harrison P. Microparticle sizing by dynamic light scattering in fresh-frozen plasma. Vox Sang 2009;96:206–212.

57. Varga Z, Yuana Y, Grootemaat AE, van der Pol E, Gollwitzer C, Krumrey M. Towards traceable size determination of extracellular vesicles. J Extracell Vesicles 2014;3:23298.

58. NOMES DOS AUTORES! Sizing and phenotyping of cellular vesicles using Nanoparticle Tracking Analysis. Nanomedicine Nanotechnology, Biol Med 2011;7:780–788.

59. Shang J, Gao X. Nanoparticle counting: towards accurate determination of the

molar concentration. Chem Soc Rev 2014;43:7267-7278.

60. Van der Pol E, Coumans FAW, Grootemaat AE, Gardiner C, Sargent IL, Harrison P. Particle size distribution of exosomes and microvesicles determined by transmission electron microscopy, flow cytometry, nanoparticle tracking analysis, and resistive pulse sensing. J Thromb Haemost 2014;12:1182–1192.

61. Van Der Pol E, Hoekstra AG, Sturk A, Otto C, Van Leeuwen TG, Nieuwland R. Optical and non-optical methods for detection and characterization of microparticles and exosomes. J Thromb Haemost. 2010;8(12):2596–607.

62. Gardiner C, Ferreira YJ, Dragovic RA, Redman CWG, Sargent IL. Extracellular vesicle sizing and enumeration by nanoparticle tracking analysis. J Extracell Vesicles 2013;2:19671.

63. Sokolova V, Ludwig A-K, Hornung S, Rotan O, Horn PA, Epple M. Characterisation of exosomes derived from human cells by nanoparticle tracking analysis and scanning electron microscopy. Colloids Surfaces B Biointerfaces 2011;87:146–150.

64. Gercel-Taylor C, Atay S, Tullis RH, Kesimer M, Taylor DD. Nanoparticle analysis of circulating cell-derived vesicles in ovarian cancer patients. Anal Biochem 2012;428:44–53.

65. Tomlinson PR, Zheng Y, Fischer R, Heidasch R, Gardiner C, Evetts S. Identification of distinct circulating exosomes in Parkinson's disease. Ann Clin Transl Neurol 2015;2:353–361.

66. Alvarez-Erviti L, Seow Y, Schapira AH, Gardiner C, Sargent IL, Wood MJA. Lysosomal dysfunction increases exosome-mediated alpha-synuclein release and transmission. Neurobiol Dis 2011;42:360–367.

67. Blundell ELCJ, Mayne LJ, Billinge ER, Platt M. Emergence of tunable resistive pulse sensing as a biosensor. Anal Methods 2015;0:1–12.

68. Anderson W, Lane R, Korbie D, Trau M. Observations of Tunable Resistive Pulse Sensing for Exosome Analysis: Improving System Sensitivity and Stability. Langmuir 2015;31:6577–6587.

69. Maas SLN, De Vrij J, Broekman MLD. Quantification and Size-profiling of Extracellular Vesicles Using Tunable Resistive Pulse Sensing. J Vis Exp 2014;92:1-7.

70. Weatherall E, Willmott GR. Applications of tunable resistive pulse sensing. Analyst 2015;140:3318-3334.

71. Böing AN, Stap J, Hau CM, Afink GB, Ris-Stalpers C, Reits EA. Active caspase-3 is removed from cells by release of caspase-3-enriched vesicles. BBA - Mol Cell Res 2013;1833:1844–1852.

72. Vorauer-Uhl K, Wagner A, Borth N, Katinger H. Determination of liposome size distribution by flow cytometry. Cytometry 2000;39:166–171.

73. Van Der Pol E, Van Gemert MJC, Sturk A, Nieuwland R, Van Leeuwen TG. Single vs. swarm detection of microparticles and exosomes by flow cytometry. J Thromb Haemost 2012;10:919–930.

74. Stoner SA, Duggan E, Condello D, Guerrero A, Turk JR, Narayanan PK. High sensitivity flow cytometry of membrane vesicles. Cytom Part A 2016;89:196–206.

75. Nolte- EN, van der Vlist EJ, Aalberts M, Mertens HC, Jan Bosch B, Bartelink W. Quantitative and qualitative flow cytometric analysis of nanosized cell-derived membrane vesicles. Nanomedicine Nanotechnology, Biol Med 2012;8:712–720.

76. Konokhova AI, Yurkin MA, Moskalensky AE, Chernyshev A V., Tsvetovskaya GA, Chikova ED. Light-scattering flow cytometry for identification and characterization of blood microparticles. J Biomed Opt 2012;17:57006.

77. Local T, Committee O, Witwer KW, Sahoo S, Gardiner C, Tahara H. The Fifth International Meeting of ISEV, ISEV2016, Rotterdam, The Netherlands, 4 – 7 May, 2016. J Extracell Vesicles 2016;5:31552.

78. Haugstad G. Atomic Force Microscopy: Understanding Basic Modes and Advanced Applications, First Edition. John Wiley & Sons, Inc. 2012. p.1-30.

79. Pignataro B, Steinem C, Galla HJ, Fuchs H, Janshoff A. Specific Adhesion of Vesicles Monitored by Scanning Force Microscopy and Quartz Crystal Microbalance. Biophys J 2000;78:487–98.

80. Sharma S, Gillespie BM, Palanisamy V, Gimzewski JK. Quantitative Nano-structural and Single Molecule Force Spectroscopy bio-molecular analysis of human saliva derived exosomes. Langmuir 2011;27:14394-14400.

81. Rupert DLM, Claudio V, Lässer C, Bally M. Methods for the physical characterization and quantification of extracellular vesicles in biological samples. Biochim Biophys Acta - Gen Subj 2017;1861:3164–3179.

82. Sharma S, Rasool HI, Palanisamy V, Mathisen C, Schmidt M, Wong DT. Structural-mechanical characterization of nanoparticle exosomes in human saliva, using correlative AFM, FESEM, and force spectroscopy. ACS Nano 2010;4:1921-1926.

83. Klang V, Valenta C, Matsko NB. Electron microscopy of pharmaceutical systems. Micron 2013;44:45–74.

84. Mahmood T, Yang P-C. Western blot: technique, theory, and trouble shooting. N Am J Med Sci 2012;4:429–434.

85. Turiák L, Misják P, Szabó TG, Aradi B, Pálóczi K, Ozohanics O. Proteomic characterization of thymocyte-derived microvesicles and apoptotic bodies in BALB/c mice. J Proteomics 2011;74:2025–2033.

86. Conde-Vancells J, Rodriguez-Suarez E, Embade N, Gil D, Matthiesen R, Valle M, Elortza F, Lu SC, Mato JM, Falcon-Perez JM. Characterization and Comprehensive Proteome Profiling of Exosomes Secreted by Hepatocytes Synopsis. J Proteome Res 2008;7:5157–5166.

87. Llorente A, Skotland T, Sylvänne T, Kauhanen D, Róg T, Orłowski A. Molecular lipidomics of exosomes released by PC-3 prostate cancer cells. Biochim Biophys Acta - Mol Cell Biol Lipids 2013;1831:1302–1309.

88. Abels ER, Breakefield XO. Introduction to Extracellular Vesicles: Biogenesis, RNA Cargo Selection, Content, Release, and Uptake. Cell Mol Neurobiol 2016;36:301-312.

89. Qazi KR, Gehrmann U, Domange Jordö E, Karlsson MCI, Gabrielsson S. Antigen-loaded exosomes alone induce Th1-type memory through a B-cell-dependent mechanism. Blood 2009;113:2673–2683.

90. Yeo RWY, Lai RC, Zhang B, Tan SS, Yin Y, Teh BJ. Mesenchymal stem cell: An efficient mass producer of exosomes for drug delivery. Adv Drug Deliv Rev 2013;65:336–341.

91. Dominici M, Le Blanc K, Mueller I, Slaper-Cortenbach I, Marini F, Krause D. Minimal criteria for defining multipotent mesenchymal stromal cells. The International Society for Cellular Therapy position statement. Cytotherapy 2006;8:315–7.

92. Abdallah B, Kassem M. Human mesenchymal stem cells: from basic biology to clinical applications. Gene Ther 2008;15:109–116.

93. Giordano A, Galderisi U, Marino IR. From the Laboratory Bench to the Patient's Bedside: An Update on Clinical Trials With Mesenchymal Stem Cells. J Cell Physiol 2007;211:27–35.

94. Squillaro T, Peluso G, Galderisi U. Clinical Trials with Mesenchymal Stem Cells: An Update. Cell Transplant 2015;25:1–53.

95. Bruder SP, Kurth AA, Shea M, Hayes WC, Jaiswal N, Kadiyala S. Bone Regeneration by Implantation of Purified, Culture-Expanded Human Mesenchymal Stem Cells. J Bone Joint Surg 1998;16:155–162.

96. Uccelli A, Moretta L, Pistoia V. Mesenchymal stem cells in health and disease. Nat Rev Immunol 2008;8:726–736.

97. Quarto R, Mastrogiacomo M, Cancedda R, Kutepov SM, Mukhachev V, Lavroukov A, Marcacci M. Repair of large bone defects with the use of autologous bone marrow stromal cells. N Engl J Med 2001;344:385-386.

98. Shiraishi K, Kamei N, Takeuchi S, Yanada S, Mera H, Wakitani S. Quality Evaluation of Human Bone Marrow Mesenchymal Stem Cells for Cartilage Repair. Stem Cells Int 2017;2017:1-9.

99. Tateishi-Yuyama E, Matsubara H, Murohara T, Ikeda U, Shintani S, Masaki H. Therapeutic angiogenesis for patients with limb ischaemia by autologous transplantation of bone-marrow cells: a pilot study and a randomised controlled trial. Lancet 2002;360:427–435.

100. Assmus B, Schächinger V, Teupe C, Britten M, Lehmann R, Döbert N. Transplantation of Progenitor Cells and Regeneration Enhancement in Acute Myocardial Infarction (TOPCARE-AMI). Circulation 2002;106:3009-3017.

101. Caplan AI, Dennis JE. Mesenchymal Stem Cells as Trophic Mediators. J Cell Biochem J Cell Biochem 2006;98:1076–1084.

102. Timmers L, Lim SK, Hoefer IE, Arslan F, Lai RC, van Oorschot AAM. Human mesenchymal stem cell-conditioned medium improves cardiac function following myocardial infarction. Stem Cell Res 2011;6:206–214.

103. Vrijsen KR, Sluijter JPG, Schuchardt MWL, van Balkom BWM, Noort WA, Chamuleau SAJ. Cardiomyocyte progenitor cell-derived exosomes stimulate migration of endothelial cells. J Cell Mol Med 2010;14:1064–1070.

104. Ramaswamy Y, Lim KS, Zreiqat H, Lu Z. Stem Cells for Bone Regeneration: Role

of Trophic Factors. Advanced Techniques in Bone Regeneration. InTech, 2016;56:604–609.

105. Lai RC, Arslan F, Tan S, Tan B, Choo A, Lee MM. Derivation and characterization of human fetal MSCs: An alternative cell source for large-scale production of cardioprotective microparticles. J Mol Cell Cardiol 2010;48:1215–1224.

106. Lai RC, Arslan F, Lee MM, Siu N, Sze K, Choo A. Exosome secreted by MSC reduces myocardial ischemia/reperfusion injury. Stem Cell Res 2010;4:214–222.

107. Marigo I, Dazzi F. The immunomodulatory properties of mesenchymal stem cells. Semin Immunopathol 2011;33:593–602.

108. Chen TS, Arslan F, Yin Y, Tan SS, Lai RC, Boon A. Enabling a robust scalable manufacturing process for therapeutic exosomes through oncogenic immortalization of human ESC-derived MSCs. J Transl Med 2011;9:47-57.

109. Ruenn Chai L, Tian Sheng C, Sai Kiang L. Mesenchymal stem cell exosome: a novel stem cell-based therapy for cardiovascular disease. Regen Med 2011;6:481-492.

110. Hood JL, Scott MJ, Wickline SA. Maximizing exosome colloidal stability following electroporation. Anal Biochem 2014;448:41–49.

111. Kooijmans SAA, Stremersch S, Braeckmans K, De Smedt SC, Hendrix A, Wood MJA. Electroporation-induced siRNA precipitation obscures the efficiency of siRNA loading into extracellular vesicles. J Control Release 2013;172:229–238.

112. Neumann E, Schaefer-Ridder M, Wang Y, Hofschneider PH. Gene transfer into mouse lyoma cells by electroporation in high electric fields. EMBO Joumal 1982;1:841–845.

113. Alvarez-Erviti L, Seow Y, Yin H, Betts C, Lakhal S, Wood MJA. Delivery of siRNA to the mouse brain by systemic injection of targeted exosomes. Nat Biotechnol 2011;29:341–345.

114. Tian Y, Li S, Song J, Ji T, Zhu M, Anderson GJ. A doxorubicin delivery platform using engineered natural membrane vesicle exosomes for targeted tumor therapy. Biomaterials 2014;35:2383-2390.

115. Shtam TA, Kovalev RA, Yu Varfolomeeva E, Makarov EM, Kil Y V, Filatov M V. Exosomes are natural carriers of exogenous siRNA to human cells in vitro. Cell Commun Signal 2013;11:88-98.

116. Vader P, Mol EA, Pasterkamp G, Schiffelers RM. Extracellular vesicles for drug delivery. Adv Drug Deliv Rev 2016;106:148-156.

117. Sun D, Zhuang X, Xiang X, Liu Y, Zhang S, Liu C, Barnes S, Grizzle W, Miller D, Zhang HG. A Novel Nanoparticle Drug Delivery System: The Anti-inflammatory Activity of Curcumin Is Enhanced When Encapsulated in Exosomes. Mol Ther 2010;18:1606–1614.

118. Zhuang X, Xiang X, Grizzle W, Sun D, Zhang S, Axtell RC. Treatment of Brain Inflammatory Diseases by Delivering Exosome Encapsulated Anti-inflammatory Drugs From the Nasal Region to the Brain. Mol Ther 2011;19:1769–1779.

119. Barry J, Fritz M, Brender JR, Smith PES, Lee DK, Ramamoorthy A. Determining the Effects of Lipophilic Drugs on Membrane Structure by Solid-State NMR Spectroscopy: The Case of the Antioxidant Curcumin. J Am Chem Soc 2009;131:4490-4498.

120. Jaruga E, Sokal A, Chrul S, Bartosz G. Apoptosis-Independent Alterations in Membrane Dynamics Induced by Curcumin. Exp Cell Res 1998;245: 303-312.

121. Jang SC, Kim OY, Yoon CM, Choi DS, Roh TY, Park J. Bioinspired exosome-mimetic nanovesicles for targeted delivery of chemotherapeutics to malignant tumors. ACS Nano 2013;7:7698–7710.

122. Bryniarski K, Ptak W, Jayakumar A, Püllmann K, Caplan MJ, Chairoungdua A. Antigen Specific Antibody Coated Exosome-Like Nanovesicles Deliver Suppressor T Cell miRNA-150 To Effector T Cells In Contact Sensitivity. J Allergy Clin Immunol 2013;132:170–181.

123. Wahlgren J, De T, Karlson L, Brisslert M, Sani FV, Rn Telemo E. Plasma exosomes can deliver exogenous short interfering RNA to monocytes and lymphocytes. Nucleic Acids Res 2012;40:130-142.

124. Haney MJ, Klyachko NL, Zhao Y, Gupta R, Plotnikova EG, He Z. Exosomes as Drug Delivery Vehicles for Parkinson's Disease Therapy. J Control Release 2015;207:18–30.

125. Fuhrmann G, Serio A, Mazo M, Nair R, Stevens MM. Active loading into extracellular vesicles significantly improves the cellular uptake and photodynamic effect of porphyrins. J Control Release 2015;205:35–44.

126. Pascucci L, Coccè V, Bonomi A, Ami D, Ceccarelli P, Ciusani E. Paclitaxel is incorporated by mesenchymal stromal cells and released in exosomes that inhibit in vitro tumor growth: A new approach for drug delivery. J Control Release 2014;192:262–270.

127. Ohno S, Takanashi M, Sudo K, Ueda S, Ishikawa A, Matsuyama . Systemically Injected Exosomes Targeted to EGFR Deliver Antitumor MicroRNA to Breast Cancer Cells. Mol Ther 2013;21:185–191.

128. Katakowski M, Buller B, Zheng X, Lu Y, Rogers T, Osobamiro O. Exosomes from marrow stromal cells expressing miR-146b inhibit glioma growth. Cancer Lett 2013;335:201–204.

129. Watson DC, Bayik D, Srivatsan A, Bergamaschi C, Valentin A, Niu G. Efficient production and enhanced tumor delivery of engineered extracellular vesicles. Biomaterials 2016;105:195–205.

130. Lee YS, Kim SH, Cho JA, Kim CW. Introduction of the CIITA gene into tumor cells produces exosomes with enhanced anti-tumor effects. Exp Mol Med 2011;43:281–290.

131. XStamp Cloning and Expression Lentivector - System Biosciences [Internet]. [cited 2017 Sep 25].

132. Kesharwani P, Jain K, Jain NK. Dendrimer as nanocarrier for drug delivery. Prog Polym Sci 2014;39:268–307.

133. Tomalia DA, Dewald JR. Dense star polymers having core, core branches, terminal groups. US Patent No. 4507466,1985.

134. Tomalia DA, Baker H, Dewald J, Hall M, Kallos G, Martin S, et al. A New Class of Polymers: Starburst-Dendritic Macromolecules. Polym J 1985;17:117-132;

135. Nanjwade BK, Bechra HM, Derkar GK, Manvi F V., Nanjwade VK. Dendrimers: Emerging polymers for drug-delivery systems. Eur J Pharm Sci 2009;38:185–196.

136. Journal P, Andrew D, Nanosynthons T, Tomalia DA. A New Class of Polymers : Starburst- Dendritic Macromolecules. 2016;(January 1985).

137. Esfand R, Tomalia DA. Poly(amidoamine) (PAMAM) dendrimers: from biomimicry to drug delivery and biomedical applications. Drug Discov Today 2001;6:427–436.

138. Jain K, Kesharwani P, Gupta U, Jain NK. Dendrimer toxicity: Let's meet the challenge. Int J Pharm 2010;394:122–42.

139. Gérard HC, Mishra MK, Mao G, Wang S, Hali M, Whittum-Hudson JA. Dendrimer-enabled DNA delivery and transformation of Chlamydia pneumoniae. Nanomedicine Nanotechnology, Biol Med 2013;9:996–1008.

140. Tekade RK, Kumar PV, Jain NK. Dendrimers in Oncology: An Expanding Horizon. Chemical reviews 2008;109:49-87.

141. Khandare J, Kolhe P, Pillai O, Kannan S, Lieh-Lai M, Kannan RM. Synthesis, Cellular Transport, and Activity of Polyamidoamine Dendrimer-Methylprednisolone Conjugates. Bioconjugate chem 2005;16:330-337.

142. Kolhe P, Misra E, Kannan RM, Kannan S, Lieh-Lai M. Drug complexation, in vitro release and cellular entry of dendrimers and hyperbranched polymers. Int J Pharm 2003;259:143–160.

143. Qiao Z, Shi X. Dendrimer-based molecular imaging contrast agents. Prog Polym Sci 2015;44:1–27.

144. Kobayashi H, Kawamoto S, Star RA, Waldmann TA, Tagaya Y, Brechbiel MW. Micro-magnetic Resonance Lymphangiography in Mice Using a Novel Dendrimer-based Magnetic Resonance Imaging Contrast Agent. Cance Res 2003;63:271–276.

145. Lässer C, Eldh M, Lötvall J. Isolation and Characterization of RNA-Containing Exosomes. J Vis Exp 2012;59:1-12.

146. Savina A, Vidal M, Colombo MI. The exosome pathway in K562 cells is regulated by Rab11. J Cell Sci 2002;115:2505-2515.

147. Savina A, Furlá M, Vidal M, Colombo MI. Exosome Release Is Regulated by a Calcium-dependent Mechanism in K562 Cells. J Biol Chem 2003;278:20083-20090.

148. Brinkley M. A brief survey of methods for preparing protein conjugates with dyes, haptens and crosslinking reagents. Bioconjug Chem 1992;3:2–13.

149. Oddone N, Lecot N, Fernández M, Rodriguez-Haralambides A, Cabral P, Cerecetto H. In vitro and in vivo uptake studies of PAMAM G4.5 dendrimers in breast cancer. J Nanobiotechnology 2016;14:45-57.

150. Oddone N, Zambrana AI, Tassano M, Porcal W, Cabral P, Benech JC. Cell uptake mechanisms of PAMAM G4-FITC dendrimer in human myometrial cells. J Nanoparticle Res. 2013;15:1776-1790.

151. Majoros J, Myc A, Thomas T, Mehta CB, Baker JR. PAMAM Dendrimer-Based Multifunctional Conjugate for Cancer Therapy : Synthesis , Characterization , and Functionality. Biomacromolecules 2006;7:572–579.

152. Karlsson I, Samuelsson K, Ponting DJ, Törnqvist M, Ilag LL, Nilsson U. Peptide Reactivity of Isothiocyanates – Implications for Skin Allergy. Nat Publ Gr 2016; 6:21203.

153. Barbero N, Barolo C, Viscardi G. Bovine Serum Albumin Bioconjugation with FITC. World J Chem Educ 2016;4:80–85.

154. Hoe Do J, An J, Seung Joun Y, June Chung D, Kim J-H. Cellular-uptake Behavior of Polymer Nanoparticles into Consideration of Biosafety. Macromol Res 2008;16:695–703.

155. Dougherty CA, Vaidyanathan S, Orr BG, Banaszak Holl MM. Fluorophore: Dendrimer ratio impacts cellular uptake and intracellular fluorescence lifetime. Bioconjug Chem 2015;26:304–315.

156. Yang Y, Sunoqrot S, Stowell C, Ji J, Lee C-W, Kim JW. Effect of Size, Surface Charge, and Hydrophobicity of Poly(amidoamine) Dendrimers on Their Skin Penetration. Biomacromolecules 2012;13:2154–2162.

157. Venuganti VV, Sahdev P, Hildreth M, Guan X, Perumal O. Structure-skin permeability relationship of dendrimers. Pharm Res 2011;28:2246–2260.

158. Verhaegh NAM, Van Blaaderen A. Dispersions of Rhodamine-Labeled Silica Spheres: Synthesis, Characterization, and Fluorescence Confocal Scanning Laser Microscopy. Langmuir 1994;10:1427-1438.

159. Zhu M, Nie G, Meng H, Xia T, Nel A, Zhao Y. Physicochemical properties determine nanomaterial cellular uptake, transport, and fate. Acc Chem Res 2013;46:622–631.

160. Martens TF, Remaut K, Demeester J, De Smedt SC, Braeckmans K. Intracellular delivery of nanomaterials: How to catch endosomal escape in the act. Nano Today 2014;9:344–364.

161. Beija M, Afonso C a M, Martinho JMG. Synthesis and applications of Rhodamine derivatives as fluorescent probes. Chem Soc Rev 2009;38:2410–2433.

162. Karpiuk J, Grabowski ZR, De Schryver FC. Photophysics of the Lactone Form of Rhodamine 101. J Phys Chem 1994;98:3247–3256.

163. Daly S, Kulesza A, Knight G, MacAleese L, Antoine R, Dugourd P. The Gas-Phase Photophysics of Eosin Y and its Maleimide Conjugate. J Phys Chem A 2016;120:3484–3490.

164. Lee C-M, Lee TK, Kim D-I, Kim Y-R, Kim M-K, Jeong H-J. Optical imaging of absorption and distribution of RITC-SiO2 nanoparticles after oral administration. Int J Nanomedicine 2014 2:243–250.

165. O'Brien J, Wilson I, Orton T, Pognan F. Investigation of the Alamar Blue (resazurin) fluorescent dye for the assessment of mammalian cell cytotoxicity. Eur J Biochem 2000;267:5421–5426.

166. John M. Walker. Mammalian Cell Viability, Methods and Protocol. Vol. 53, Journal of Chemical Information and Modeling. 2013. p.1689-1699.

167. Jevprasesphant R. The influence of surface modification on the cytotoxicity of PAMAM dendrimers. Int J Pharm 2003;252:263–266.

168. Zeng Y, Kurokawa Y, Win-Shwe T-T, Zeng Q, Hirano S, Zhang Z. Effects of PAMAM dendrimers with various surface functional groups and multiple generations on cytotoxicity and neuronal differentiation using human neural progenitor cells. The Journal of toxicological sciences 2016;41:351-370.

169. Wang W, Xiong W, Wan J, Sun X, Xu H, Yang X. The decrease of PAMAM dendrimer-induced cytotoxicity by PEGylation via attenuation of oxidative stress. Nanotechnology 2009;20:105103.

170. Mcmahon HT, Gallop JL. Membrane curvature and mechanisms of dynamic cell membrane remodelling. Nature 2005;438:590-596.

171. Shi Y, Massagué J. Mechanisms of TGF-β Signaling from Cell Membrane to the Nucleus. Cell 2003;113:685–700.

172. Pridgen EM, Alexis F, Farokhzad OC. Polymeric Nanoparticle Drug Delivery Technologies for Oral Delivery Applications. Expert Opin Drug Deliv 2015;12:1459–1473.

173. Treuel L, Ulrich Nienhaus G. Toward a molecular understanding of nanoparticle–protein interactions. Biophysical reviews 2012;4:137-147.

174. Treuel L, Jiang X, Nienhaus GU. New views on cellular uptake and trafficking of manufactured nanoparticles. J R Soc Interface 2013;10:20120939.

175. Goldberg DS, Vijayalakshmi N, Swaan PW, Ghandehari H. G3.5 PAMAM

Dendrimers Enhance Transepithelial Transport of SN38 while minimizing Gastrointestinal Toxicity. J Control Release 2011;30:318–325.

176. Corrado C, Raimondo S, Chiesi A, Ciccia F, De Leo G, Alessandro R. Exosomes as intercellular signaling organelles involved in health and disease: Basic science and clinical applications. Int J Mol Sci 2013;14:5338–5366.

177. Willms E, Johansson HJ, Mäger I, Lee Y, Emelie K, Blomberg M. Cells release subpopulations of exosomes with distinct molecular and biological properties. Nat Publ Gr 2016;6:22519

178. Johnstone RM. Exosomes biological significance: A concise review. Blood Cells, Molecules, and Diseases 2006;36:315-321.

179. Panyam J, Labhasetwar V. Dynamics of Endocytosis and Exocytosis of Poly(D,L-Lactide-co-Glycolide) Nanoparticles in Vascular Smooth Muscle Cells. Pharm Res 2003;20:212-220.

180. Buckmaster M, Lobraicojr D, Ferris A, Storrie B. Retention of pinocytized solute by cho cell lysosomes correlates with molecular weight. Cell Biol Int Rep 1987;11:501–507.

181. Swanson JA, Yirinec BD, Silverstein SC. Phorbol Esters and Horseradish Peroxidase Stimulate Pinocytosis and Redirect the Flow of Pinocytosed Fluid in Macrophages. The Journal of cell biology 1985;100:851-859.

182. Cartiera MS, Johnson KM, Rajendran V, Caplan MJ, Saltzman WM. The uptake and intracellular fate of PLGA nanoparticles in epithelial cells. Biomaterials 2009;30:2790–2798.

183. Sakhtianchi R, Minchin RF, Lee KB, Alkilany AM, Serpooshan V, Mahmoudi M. Exocytosis of nanoparticles from cells: Role in cellular retention and toxicity. Adv Colloid Interface Sci 2013;201:18–29.

184. Chou LYT, Ming K, Chan WCW. Strategies for the intracellular delivery of nanoparticles. Chem Soc Rev 2011;40:233–245.

185. Yezhelyev M V, Qi L, Regan RMO, Nie S. Yezhelyev. Proton-Sponge Coated Quantum Dots for siRNA Delivery and Intracellular Imaging. J Am Chem Soc 2008;130:9006-9012.

186. Fuller JE, Zugates GT, Ferreira LS, Ow HS, Nguyen NN, Wiesner UB. Intracellular delivery of core-shell fluorescent silica nanoparticles. Biomaterials 2008;29:1526–

1532.

187. Nel AE, Mädler L, Velegol D, Xia T, Hoek EM V, Somasundaran P. Understanding biophysicochemical interactions at the nano-bio interface. Nat Mater 2009;8:543–557.

188. Yameen B, Choi W Il, Vilos C, Swami A, Shi J, Farokhzad OC. Insight into nanoparticle cellular uptake and intracellular targeting. J Control Release 2014;190:485–499.

189. Greulich C, Diendorf J, Simon T, Eggeler G, Epple M, Köller M. Uptake and intracellular distribution of silver nanoparticles in human mesenchymal stem cells. Acta Biomater 2011;7:347-354.

Annexes

Contents

Annexes

A. Supplementary data regarding the characterization of PAMAM(NH_2)-RITC conjugates

A1. Supplementary characterization data of PAMAM(NH_2) G_4-RITC conjugates

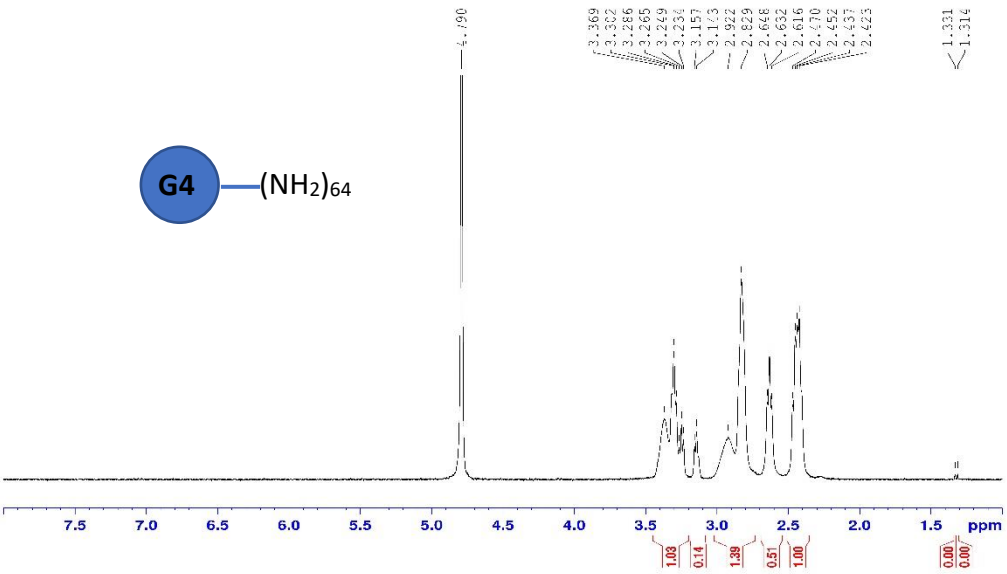

Figure A – I – Complete ^1H NMR spectrum of the PAMAM(NH_2) G_4 in D_2O at 400 MHz.

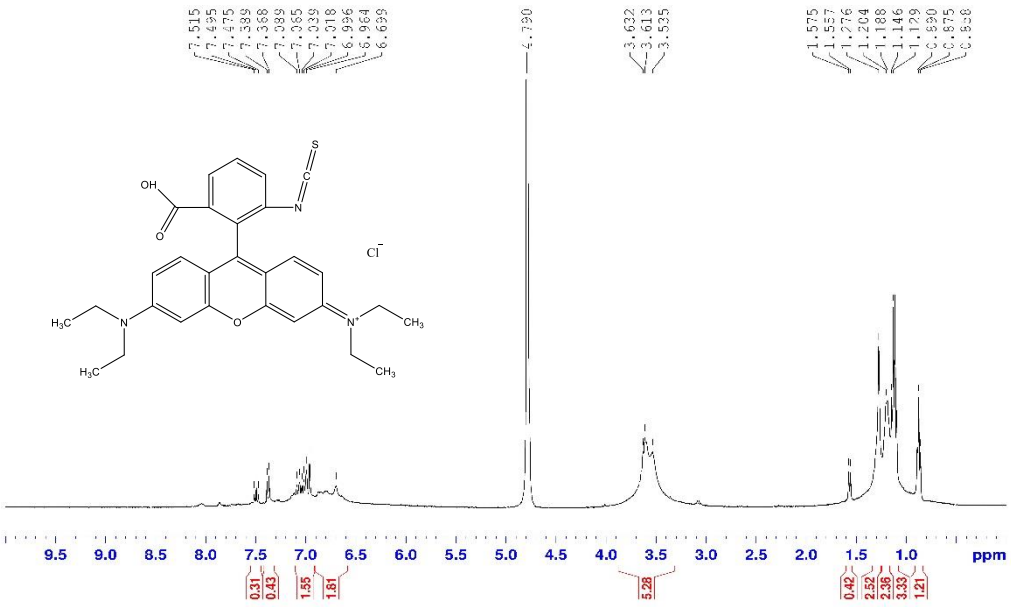

Figure A – II – Complete ^1H NMR spectrum of RITC in D_2O at 400 MHz.

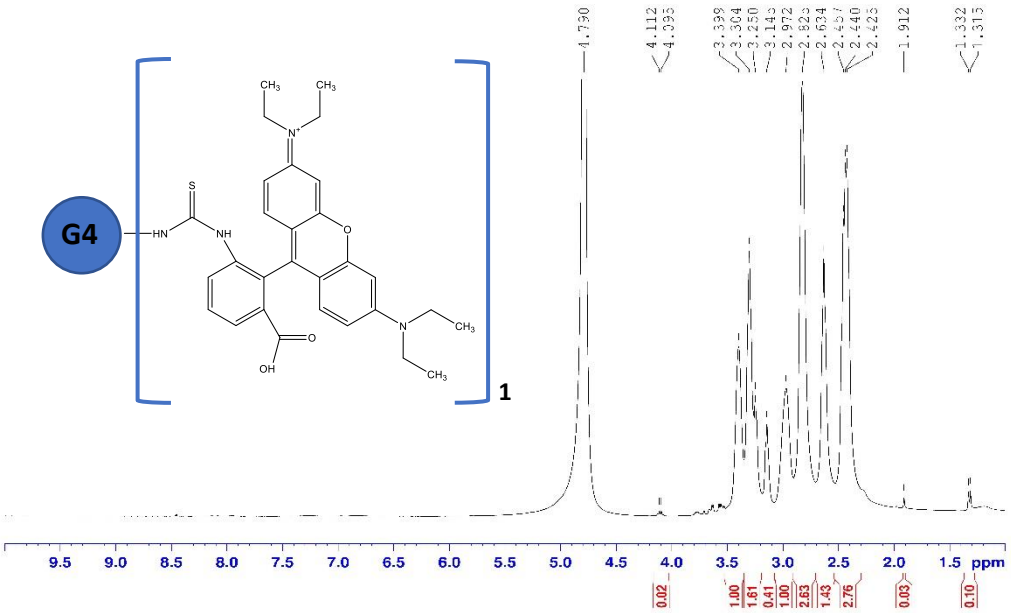

Figure A – III – Complete ^{1}H NMR spectrum of PAMAM(NH_2) G_4 - RITC in D_2O at 400 MHz.

B. Supplementary data regarding the exosome isolation and characterization from cell culture medium

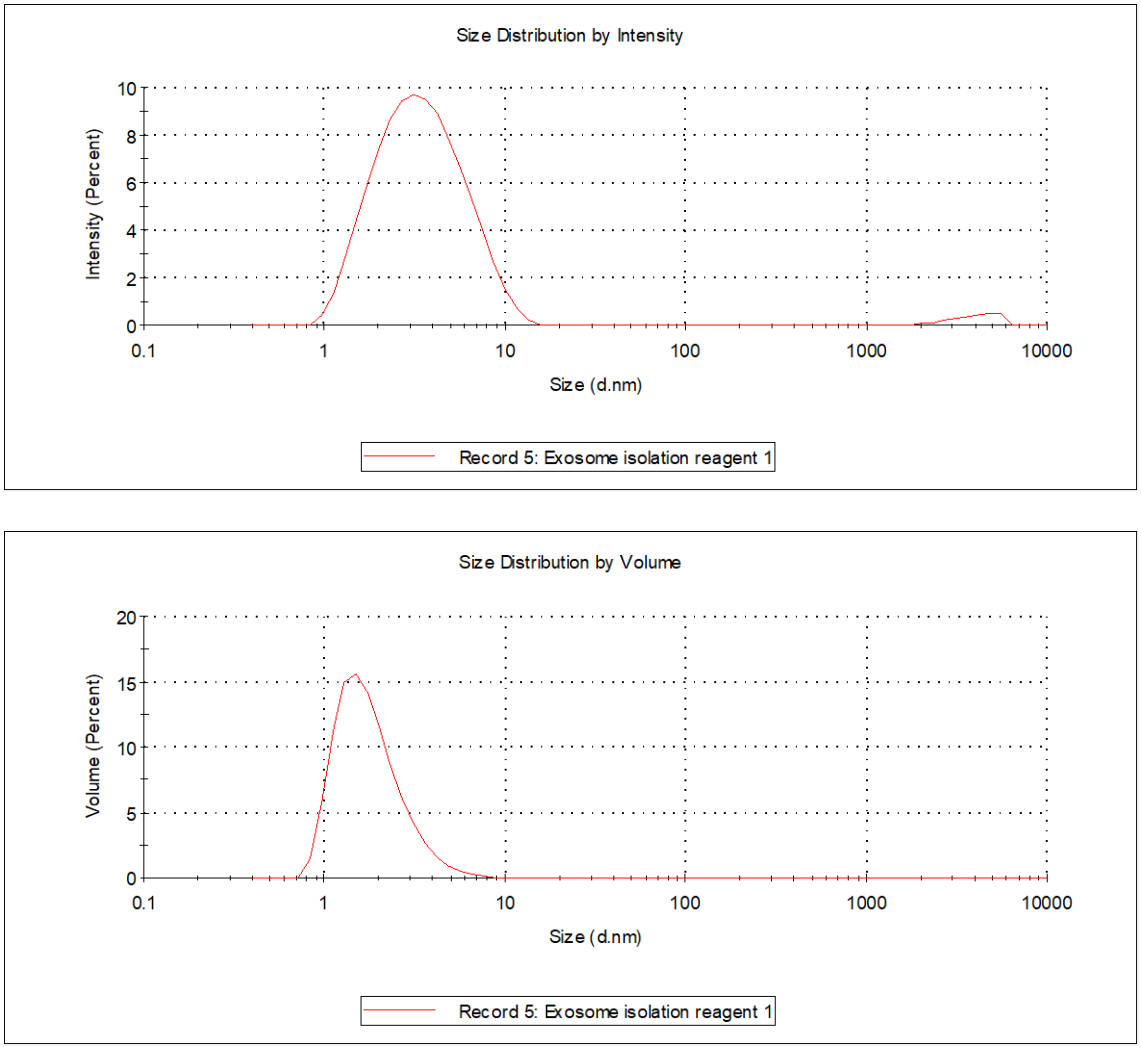

Figure B – I – Distribution of the hydrodynamic size of the Total Isolation Exosome Reagent. The top graphic represents the size distribution by intensity, and the bottom represents the size distribution by volume.

C. Certificate of the *Basics of Extracellular Vesicles* Course

D. Manufacturer instructions of the *Total Exosome Isolation Reagent*

invitrogen
by life technologies

Total Exosome Isolation (from cell culture media)

Publication No. MAN0006949 Rev. Date: 28 June 2012
Catalog Number: 4478359 Store at 2°C to 8°C

Product Description

Exosomes are small vesicles (30–120 nm) containing RNA and protein that are secreted by various types of cells in culture, and found in abundance in body fluids including blood, saliva, urine, and breast milk. Exosomes are thought to function as intercellular messengers, delivering their cargo of effector or signaling macromolecules between specific cells, however, their formation, the makeup of the cargo, and biological pathways in which they are involved remain incompletely understood.

The biological study of exosome function and trafficking requires the isolation of intact exosomes, but the current methods used are tedious, non-specific, and difficult. The Total Exosome Isolation (from cell culture media) reagent provides a simple and reliable method of concentrating intact exosomes from cell culture media samples. By tying up water molecules, the Total Exosome Isolation (from cell culture media) reagent forces less-soluble components (i.e. exosomes) out of solution, allowing them to be collected after brief, low-speed centrifugation.

Product Contents

Total Exosome Isolation (from cell culture media) reagent contains reagents sufficient for processing 100 mL of cell culture media.

Components	Amount	Storage
Total Exosome Isolation (from cell culture media)	50 mL	2°C to 8°C

General Guidelines

- To ensure that isolated exosomes originate from your cells of interest, culture the cells with exosome depleted fetal bovine serum (FBS), because normal FBS contains extremely high levels of exosomes that will contaminate the cell derived exosomes.

  If you cannot obtain exosome depleted FBS, certain cell lines can be grown for up to 12 hours in media without FBS.
- If you are isolating intact exosomes from serum, use the Total Exosome Isolation (from serum) reagent.
- After exosomes are isolated, total RNA and protein can be purified using the Total Exosome RNA and Protein Isolation Kit.
- To isolate exosomal proteins for immunoprecipitation, use Exosome Immunoprecipitation (Protein A) or Exosome Immunoprecipitation (Protein G).

Prepare Sample

1. Harvest cell culture media.
2. Centrifuge the cell media at 2000 × *g* for 30 minutes to remove cells and debris.
3. Transfer the supernatant containing the cell-free culture media to a new tube without disturbing the pellet.

Isolate Exosomes

1. Transfer the required volume of cell-free culture media to a new tube and add 0.5 volumes of the Total Exosome Isolation (from cell culture media) reagent.

Culture Media	Reagent
1 mL	500 µL
10 mL	5 mL

2. Mix the culture media/reagent mixture well by vortexing, or pipetting up and down until there is a homogenous solution.
3. Incubate samples at 2°C to 8°C overnight.
4. After incubation, centrifuge the samples at 10,000 × *g* for 1 hour at 2°C to 8°C.
5. Aspirate and discard the supernatant. Exosomes are contained in the pellet at the bottom of the tube (not visible in most cases).
6. Resuspend the pellet in a convenient volume of 1X PBS or similar buffer.

Starting Cell Culture Media Volume	Resuspension Volume
1 mL	25–100 µL
10 mL	100 µL–1 mL

7. Once the pellet is resuspended, the exosomes are ready for downstream analysis or further purification through affinity methods.

   Keep isolated exosomes at 2°C to 8°C for up to 1 week, or at ≤20°C for long-term storage.

Cofinanciado por: